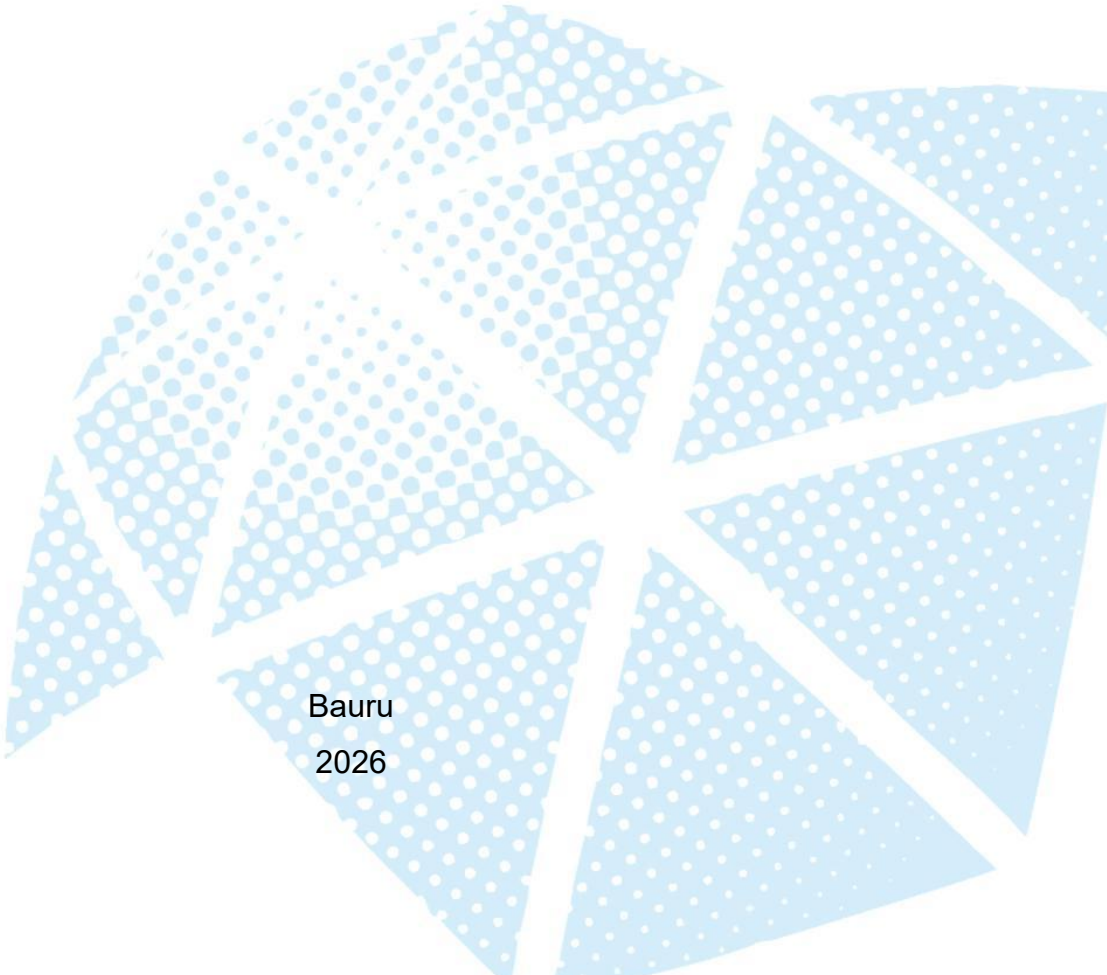
UNIVERSIDADE ESTADUAL PAULISTA (UNESP)
FACULDADE DE ENGENHARIA
CÂMPUS DE BAURU

NEYLAN LEAL DIAS

MODELOS DE INTELIGÊNCIA ARTIFICIAL APLICADOS À ESTIMAÇÃO DE ÂNGULO DE TENSÃO NODAL EM SISTEMAS ELÉTRICOS DE POTÊNCIA

Das Redes Neurais Artificiais aos Sistemas Neuro-Fuzzy Adaptativos



Bauru
2026

UNIVERSIDADE ESTADUAL PAULISTA (UNESP)

FACULDADE DE ENGENHARIA

CÂMPUS DE BAURU

NEYLAN LEAL DIAS

MODELOS DE INTELIGÊNCIA ARTIFICIAL APLICADOS À ESTIMAÇÃO DE ÂNGULO DE TENSÃO NODAL EM SISTEMAS ELÉTRICOS DE POTÊNCIA

Das Redes Neurais Artificiais aos Sistemas Neuro-Fuzzy Adaptativos

Tese apresentada à Faculdade de Engenharia de Bauru, Universidade Estadual Paulista (UNESP), como parte dos requisitos para obtenção do título de Doutor em Engenharia Elétrica.

Área de Concentração: Sistemas de Energia.

Orientador: Prof. Dr. Alfredo Bonini Neto

Coorientadora: Prof.ª Drª. Simone de Almeida Delphim Leal

Bauru

2026

Dias, Neylan Leal.
Modelos de inteligência artificial aplicados à estimação de ângulo de tensão nodal em sistemas elétricos de potência : das redes neurais artificiais aos sistemas neuro-fuzzy adaptativos / Neylan Leal Dias. – Bauru, 2026
120 f. : il.

Tese (Doutorado)–Universidade Estadual Paulista (Unesp), Faculdade de Engenharia, Bauru
Orientador: Alfredo Bonini

1. Sistemas elétricos de Potência. 2. Estimação de estado. 3. Ângulo de tensão nodal. 4. Inteligência artificial. 5. Redes neurais artificiais. 6. Sistemas de inferência neuro-fuzzy adaptativos (ANFIS). 7. Análise de sensibilidade. I. Universidade Estadual Paulista. Faculdade de Engenharia. II. Título.

ATA DA DEFESA PÚBLICA DA TESE DE DOUTORADO DE NEYLAN LEAL DIAS, DISCENTE DO PROGRAMA DE PÓS-GRADUAÇÃO EM ENGENHARIA ELÉTRICA, DA FACULDADE DE ENGENHARIA - CÂMPUS DE BAURU.

Aos 24 de setembro de 2026, às 8h, por meio de Videoconferência, realizou-se a defesa de TESE DE DOUTORADO de NEYLAN LEAL DIAS, intitulada "MODELOS DE INTELIGÊNCIA ARTIFICIAL APLICADOS À ESTIMAÇÃO DE ÂNGULO DE TENSÃO NODAL EM SISTEMAS ELÉTRICOS DE POTÊNCIA Das Redes Neurais Artificiais aos Sistemas Neuro-Fuzzy Adaptativos". A Comissão Examinadora foi constituída pelos seguintes membros: Prof. Dr. ALFREDO BONINI NETO (Orientador(a) - Participação Virtual) do(a) Departamento de Engenharia de Biossistemas / UNESP / Câmpus de Tupã - FCE, Prof. Dr. ENIO GARBELINI (Participação Virtual) do(a) Departamento de Matemática / UNIFADRA - Dracena, Profa. Dra. ANA CLAUDIA DE JESUS GOLZIO (Participação Virtual) do(a) Departamento de Engenharia de Biossistemas / UNESP / Câmpus de Tupã - FCE, Prof. Dr. RICARDO FONSECA BUZO (Participação Virtual) do(a) Departamento de Engenharia de Biossistemas / UNESP / Câmpus de Tupã - FCE, Prof. Dr. MESSIAS MENEGUETTE JUNIOR (Participação Virtual) do(a) Departamento de Matemática e Computação / Faculdade de Ciências e Tecnologia de Presidente Prudente - FCT/Unesp, Após a exposição pelo doutorando e arguição pelos membros da Comissão Examinadora que participaram do ato, de forma presencial e/ou virtual, o discente recebeu o conceito final:_ _ _ _ _ _ _ _ _ _ _ _ _ _ APROVADO _ _ _ _ . Nada mais havendo, foi lavrada a presente ata, que após lida e aprovada, foi assinada pelo(a) Presidente(a) da Comissão Examinadora.

gov.br Documento assinado digitalmente
ALFREDO BONINI NETO
Data: 28/09/2026 16:12:55-0300
Verifique em https://validar.iti.gov.br

Prof. Dr. ALFREDO BONINI NETO

IMPACTO POTENCIAL DESTA PESQUISA

A presente tese contribui diretamente para o avanço do monitoramento, controle e operação segura dos Sistemas Elétricos de Potência (SEP) ao introduzir abordagens de Inteligência Artificial — especificamente Redes Neurais Artificiais (RNA) e Sistemas de Inferência Neuro-Fuzzy Adaptativos (ANFIS) — para a estimação direta de ângulos de tensão nodal. Sob a perspectiva científica, técnica e inovadora, a pesquisa elimina a dependência de processos iterativos numéricos e soluções sucessivas de fluxo de carga durante a fase operacional, alcançando uma redução de cerca de 80% no esforço computacional com altíssimo nível de precisão ($R^2 > 0{,}99$), além de agregar valor metodológico por meio da análise de sensibilidade das variáveis de entrada e pré-processamento de dados.

Em termos econômicos e de inserção local, regional e nacional, a expressiva redução no tempo de processamento viabiliza o monitoramento em tempo real nos Centros de Operação do Sistema (como o ONS – Operação Nacional do Sistema Elétrico e concessionárias regionais de energia), aumentando a confiabilidade da rede, prevenindo falhas cascateadas ou desligamentos (*blackouts*) e otimizando custos operacionais do setor elétrico brasileiro. Adicionalmente, essa agilidade no processamento de múltiplos cenários operacionais impulsiona o desenvolvimento sustentável ao facilitar a integração segura de fontes renováveis e intermitentes (como eólica e solar), alinhando-se aos Objetivos de Desenvolvimento Sustentável da ONU para energia limpa e infraestrutura resiliente (ODS 7 e 9).

O alcance e a internacionalização do trabalho são assegurados pela validação das metodologias em sistemas-teste reconhecidos globalmente (IEEE 14, 30 e 57 barras) e pela disseminação dos resultados em periódicos científicos internacionais de alto impacto. Por fim, no âmbito educacional e cultural, a pesquisa fortalece a formação acadêmica de ponta na interseção entre Engenharia Elétrica e Ciência de Dados, estimulando a modernização tecnológica e a consolidação de uma cultura focada em redes elétricas inteligentes (*Smart Grids*) na academia e na indústria.

POTENTIAL IMPACT OF THIS RESEARCH

This thesis directly contributes to the advancement of monitoring, control, and secure operation of Electrical Power Systems (EPS) by introducing Artificial Intelligence approaches—specifically Artificial Neural Networks (ANN) and Adaptive Neuro-Fuzzy Inference Systems (ANFIS)—for the direct estimation of nodal voltage angles. From a scientific, technical, and innovative perspective, the research eliminates the dependence on iterative numerical processes and successive power flow solutions during the operational phase, achieving an expressive reduction of approximately 80% in computational effort with a high level of accuracy ($R^2 > 0.99$), while providing methodological value through the sensitivity analysis of input variables and data preprocessing.

In economic terms and regarding local, regional, and national integration, the expressive reduction in processing time enables real-time monitoring in System Operation Centers (such as the ONS - National Operation of the Electric Power System in Brazil and regional energy utilities), increasing grid reliability, preventing cascading failures or blackouts, and optimizing operational costs for the power sector. Additionally, this agility in processing multiple operating scenarios drives sustainable development by facilitating the safe integration of renewable and intermittent energy sources (such as wind and solar), aligning with the United Nations Sustainable Development Goals for affordable, clean energy and resilient infrastructure (SDGs 7 and 9).

The reach and internationalization of the work are ensured by the validation of the methodologies in globally recognized test systems (IEEE 14-, 30-, and 57-bus) and the dissemination of results in high-impact international scientific journals. Finally, in the educational and cultural spheres, this research strengthens high-level academic training at the intersection of Electrical Engineering and Data Science, fostering technological modernization and consolidating a culture focused on Smart Grids within both academia and industry.

NEYLAN LEAL DIAS

MODELOS DE INTELIGÊNCIA ARTIFICIAL APLICADOS À ESTIMAÇÃO DE ÂNGULO DE TENSÃO NODAL EM SISTEMAS ELÉTRICOS DE POTÊNCIA

Das Redes Neurais Artificiais aos Sistemas Neuro-Fuzzy Adaptativos

Tese apresentada à Universidade Estadual Paulista (UNESP), Faculdade de Engenharia (FEB), Bauru - SP, para obtenção do título de Doutor em Engenharia Elétrica.

Área de Concentração: Sistemas de Energia

Data da defesa: 24/09/2026

Banca Examinadora:

Documento assinado digitalmente
gov.br ALFREDO BONINI NETO
Data: 29/09/2026 21:42:03-0300
Verifique em https://validar.iti.gov.br

_____
Prof. Dr. Alfredo Bonini Neto
FCE/UNESP - Tupã

Documento assinado digitalmente
gov.br ENIO GARBELINI
Data: 29/09/2026 20:12:18-0300
Verifique em https://validar.iti.gov.br

_____
Prof. Dr. Enio Garbelini
UNIFAFRA – Dracena/SP

Documento assinado digitalmente
gov.br ANA CLAUDIA DE JESUS GOLZIO
Data: 28/09/2026 16:48:31-0300
Verifique em https://validar.iti.gov.br

_____
Profª. Dra. Ana Claudia de Jesus Golzio
FCE/UNESP – Tupã

Documento assinado digitalmente
gov.br RICARDO FONSECA BUZO
Data: 28/09/2026 16:59:12-0300
Verifique em https://validar.iti.gov.br

_____
Prof. Dr. Ricardo Fonseca Buzo
FCE/UNESP – Tupã

Documento assinado digitalmente
gov.br MESSIAS MENEGUETTE JUNIOR
Data: 26/09/2026 14:57:10-0300
Verifique em https://validar.iti.gov.br

_____
Prof. Dr. Messias Meneguette Jr
FCT/UNESP – Presidente Prudente

À minha avó Sabá (*in memoriam*),
À minha avó Lenita (*in memoriam*),
Ao meu avô Amauri (*in memoriam*),
À minha tia Isadoli (*in memoriam*),

Dedico.

AGRADECIMENTOS

Agradecimento e gratidão têm a mesma raiz etimológica, vindas do latim. Ambas derivam da palavra *gratus* (que significa grato ou agradecido) e de *gratia* (que significa graça), em síntese o ato de manifestar gratidão. Esse talvez seja a parte mais difícil dessa tese, pois eu me acho incapaz de manifestar a gratidão suficiente merecida para todos os envolvidos neste conquista que perdurou alguns anos (devido a felizes acontecimentos e troca de programa de Doutorado). Sempre fui uma pessoa que fez questão de manter próximo pessoas que me ajudaram em algo, mesmo que talvez aquela atitude estivesse implícita a sua atividade laboral, eu guardo cada atitude, palavra, gesto, olhar e vibração positiva para que eu enfim estivesse agora aonde estou neste exato momento.

Apesar de ser uma tese de doutorado, pra mim tudo começou em 2014 onde tomei a decisão de sair do meu estado Amapá para fazer mestrado, não tendo ideia do que me esperava pela frente, apenas com o sonho de me qualificar o suficiente para ser professor da Universidade na qual eu me formei, a Unifap, pois durante a graduação eu tive a certeza que era naquele ambiente científico com inúmeras oportunidade e possibilidade era o meu lugar. E sim ! hoje estou vivendo esse sonho, na verdade fazem 4 anos que vivo esse sonho como efetivo do lugar que me formou e que hoje eu tento retribuir a tudo que me foi oportunizado. Então o que há em meu coração é Gratidão ! gratidão por tudo, gratidão por me abrigarem, gratidão por me darem uma chance, e algumas vezes até duas... três ... Inclusive e especialmente a minha família, que nunca deixaram de acreditar, e nunca soltaram minha mão mesmo quando eu decepcionei em alguns momentos. Obrigado ! É por vocês, e pra vocês !

Esse agradecimento, diferente de todos os outros agradecimentos, não irei citar nomes ou pessoas, pois eu seria incapaz de lembrar de todos que participaram desde 2014 quando iniciei essa saída do estado. Á todos, que sabem o quanto me ajudaram, eu deixo a minha gratidão eterna ! e a cada dia estarei me dedicando o suficiente para que tudo o que a mim fizeram e oportunizaram seja multiplicado para outras pessoas.

Finalizo Agradecendo aquele que em todos os momentos, inclusive nos meus piores momentos, sempre esteve me fortalecendo e me lembrando que ele tinha tudo sob controle, e colocou todos vocês no meu caminho. Obrigado Deus por tudo !

“A mente que se abre a uma nova ideia

jamais voltará ao seu tamanho original.”

Albert Einstein

APRESENTAÇÃO

O presente trabalho teve como objetivo avaliar, por meio de modelos de inteligência artificial, a estimação direta de ângulos de tensão nodal em sistemas elétricos de potência submetidos a diferentes condições de carregamento. A pesquisa integra técnicas avançadas de aprendizado de máquina, com destaque para as Redes Neurais Artificiais do tipo Multilayer Perceptron com análise de sensibilidade e os Sistemas de Inferência Neuro-Fuzzy Adaptativos (ANFIS), visando a predição precisa e de baixo custo computacional de variáveis de estado associadas ao monitoramento e à operação segura de redes elétricas.

A tese está estruturada em dois estudos complementares. O primeiro "**ESTIMATION OF NODAL VOLTAGE ANGLES IN ELECTRICAL POWER SYSTEMS USINGARTIFICIAL NEURAL NETWORKS AND SENSITIVITY ANALYSIS OF INPUT VARIABLES**" aborda a aplicação de redes neurais artificiais na estimativa direta dos ângulos de tensão nodal a partir do algoritmo de *backpropagation*, sob diferentes condições de carregamento, em sistemas elétricos de potência (IEEE 14, 30 e 57 barras). Esse estudo busca identificar variáveis-chave e padrões de resposta do sistema por meio de análise de sensibilidade, reduzindo o esforço computacional em relação ao fluxo de potência tradicional sem comprometer a precisão na identificação do ponto de carregamento máximo.

O segundo estudo "**ADAPTIVE NEURO-FUZZY INFERENCE SYSTEM FOR ACCURATE VOLTAGE ANGLE STATE ESTIMATION IN ELECTRICAL POWER SYSTEMS: A TRAINING, VALIDATION, AND TESTING ANALYSIS**" concentra-se na estimativa direta dos ângulos de tensão nodal a partir do algoritmo *híbrido* (*backpropagation e least-squares*) do ANFIS, sob diferentes condições de carregamento do sistema IEEE 14 barras. Os resultados confirmam que a abordagem proposta baseada em ANFIS fornece uma solução precisa, confiável e computacionalmente eficiente, sendo competitivo quando comparado com modelos com eficácia já comprovada como as RNA's.

O trabalho busca avançar na estimativa direta de variáveis de estado em sistemas elétricos de potência, oferecendo subsídios científicos e computacionais para o monitoramento e a operação segura de redes elétricas. A combinação de redes neurais perceptron multicamadas e sistemas neuro-fuzzy adaptativos representa uma abordagem inovadora, de alta precisão e baixo custo computacional.

PRESENTATION

The objective of this study was to evaluate, using artificial intelligence models, the direct estimation of nodal voltage angles in electrical power systems subjected to different load conditions. The research integrates advanced machine learning techniques, with an emphasis on Multilayer Perceptron Artificial Neural Networks with sensitivity analysis and Adaptive Neuro-Fuzzy Inference Systems (ANFIS), aiming at the accurate and computationally efficient prediction of state variables associated with the monitoring and safe operation of power grids.

The thesis is structured into two complementary studies. The first, "**ESTIMATION OF NODAL VOLTAGE ANGLES IN ELECTRICAL POWER SYSTEMS USING ARTIFICIAL NEURAL NETWORKS AND SENSITIVITY ANALYSIS OF INPUT VARIABLES**," addresses the application of artificial neural networks in the direct estimation of nodal voltage angles using the *backpropagation* algorithm, under different load conditions in electrical power systems (IEEE 14, 30 and 57-bus systems). This study seeks to identify key variables and system response patterns through sensitivity analysis, reducing the computational effort compared to traditional power flow analysis without compromising the accuracy of identifying the point of maximum load.

The second study, "**ADAPTIVE NEURO-FUZZY INFERENCE SYSTEM FOR ACCURATE VOLTAGE ANGLE STATE ESTIMATION IN ELECTRICAL POWER SYSTEMS: A TRAINING, VALIDATION, AND TESTING ANALYSIS**," focuses on the direct estimation of nodal voltage angles using the ANFIS hybrid algorithm (*backpropagation and least squares*) under different load conditions of the IEEE 14-bus system. The results confirm that the proposed ANFIS-based approach provides an accurate, reliable, and computationally efficient solution, proving competitive when compared to models with proven effectiveness, such as RNA networks.

This work aims to advance the direct estimation of state variables in electrical power systems, providing scientific and computational support for the monitoring and safe operation of power grids. The combination of multilayer perceptron neural networks and adaptive neuro-fuzzy systems represents an innovative approach that offers high accuracy and low computational cost.

RESUMO

A estimação precisa de ângulos de tensão nodal é essencial para o monitoramento, controle e operação segura de sistemas elétricos de potência. Contudo, as abordagens tradicionais dependem de processos numéricos iterativos e da solução prévia do fluxo de potência, o que impõe limitações computacionais e elevado custo de processamento em cenários de tempo real ou de grande escala. Para superar esses gargalos, este trabalho investiga a estimação direta de variáveis de estado empregando técnicas de inteligência artificial aplicadas aos sistemas-teste IEEE 14, 30 e 57 barras. A pesquisa avalia duas abordagens complementares sob diferentes condições de carregamento: Redes Neurais Artificiais (RNA) do tipo *Multilayer Perceptron* treinadas pelo algoritmo *backpropagation* e associadas à análise de sensibilidade e normalização de dados; e Sistemas de Inferência Neuro-Fuzzy Adaptativos (ANFIS) baseados em agrupamento subtrativo e otimizados via algoritmo híbrido (*backpropagation* e mínimos quadrados). Ambas as metodologias demonstraram elevadíssima capacidade de generalização e precisão preditiva, alcançando coeficientes de determinação e correlação (R^2 e R) superiores a $0{,}99$ e erros quadráticos médios da ordem de 10^{-3} a 10^{-5} nas etapas de validação e teste. A abordagem via RNA permitiu obter as curvas $P-\theta$ e identificar o ponto de carregamento máximo com redução de cerca de 80% no esforço computacional em relação ao fluxo de potência convencional, enquanto a análise de sensibilidade mapeou as variáveis de maior impacto na resposta da rede. Por sua vez, o modelo ANFIS apresentou desempenho preditivo ligeiramente superior e competitivo quando comparado às RNAs. Os resultados confirmam que ambos os modelos representam soluções robustas, confiáveis e computacionalmente eficientes, com elevado potencial de aplicação no monitoramento e na estimação de estado em tempo real de redes elétricas.

Palavras-chave: Sistemas Elétricos de Potência; Estimação de Estado; Ângulos de Tensão Nodal; Inteligência Artificial; Redes Neurais Artificiais; Sistemas de Inferência Neuro-Fuzzy Adaptativos (ANFIS); Análise de Sensibilidade.

ABSTRACT

Accurate estimation of nodal voltage angles is essential for the monitoring, control, and secure operation of electrical power systems. However, traditional approaches rely on iterative numerical procedures and the prior solution of the power flow problem, imposing computational limitations and high processing costs in real-time or large-scale scenarios. To overcome these bottlenecks, this study investigates the direct estimation of state variables using artificial intelligence techniques applied to the IEEE 14-, 30-, and 57-bus test systems. The research evaluates two complementary approaches under various loading conditions: Multilayer Perceptron Artificial Neural Networks (ANN) trained with the backpropagation algorithm and integrated with sensitivity analysis and data normalization; and Adaptive Neuro-Fuzzy Inference Systems (ANFIS) based on subtractive clustering and optimized via a hybrid algorithm (backpropagation and least-squares). Both methodologies demonstrated exceptionally high generalization capability and predictive accuracy, achieving coefficients of determination and correlation (R^2 and R) above 0.99 and mean squared errors on the order of 10^{-3} to 10^{-5} during validation and testing phases. The ANN approach successfully generated $P-\theta$ curves and identified the maximum loading point with an approximate 80% reduction in computational effort compared to traditional power flow, while sensitivity analysis mapped the variables with the greatest impact on the network's response. In turn, the ANFIS model exhibited slightly superior predictive performance while remaining highly competitive with ANNs. The results confirm that both models provide robust, reliable, and computationally efficient solutions with significant potential for real-time state estimation and monitoring applications in power grids.

Keywords: Electrical Power Systems; State Estimation; Nodal Voltage Angles; Artificial Intelligence; Artificial Neural Networks; Adaptive Neuro-Fuzzy Inference System (ANFIS); Sensitivity Analysis.

LISTA DE FIGURAS

CAPÍTULO I

Figura 1 - Modelo Teórico de um neurônio Artificial 26
Figura 2 - Modelo de uma rede neural com mais de uma camada oculta. 27
Figura 3 - Arquitetura do sistema de inferência neuro-fuzzy adaptativo 29

CAPÍTULO II

Figure 1 - IEEE benchmark test systems considered in this study: (**a**) IEEE 14-bus system, (**b**) IEEE 30-bus system, and (**c**) IEEE 57-bus system 39
Figure 2 - MLP artificial neural network architecture used for nodal voltage angle estimation 40
Figure 3 - ANN performance for the IEEE 14-Bus System: (**a**) MSE curves for the training and validation phases; (**b**) histogram of the training and validation errors relative to zero error. 47
Figure 4 - Comparison between the target (Y_{des}) and estimated (Y_{ob}) values of the nodal voltage angle θ for each sample: (**a**) bus 3, (**b**) bus 6, (**c**) bus 13, and (**d**) bus 14 (critical bus). 48
Figure 5 - Nodal voltage angle values (θ) obtained from the CPF method (Y_{des}) and estimated by the ANN (Y_{ob}) as a function of the loading factor (λ), forming the P–θ curves: (**a**) bus 3, (**b**) bus 6, (**c**) bus 13, and (**d**) bus 14 (critical bus). 49
Figure 6 - Nodal voltage angle values (θ) obtained from the CPF method (Y_{des}) and estimated by the ANN (Y_{ob}) as a function of the loading factor (λ), forming the P–θ curves: (**a**) bus 3, (**b**) bus 6, (**c**) bus 13, and (**d**) bus 14 (critical bus).. 50
Figure 7 - P–θ curves of the IEEE 14-Bus System: (**a**) target values (Y_{des}) obtained from the CPF method; (**b**) ANN-estimated values (Y_{ob}). 51
Figure 8 - ANN performance for the IEEE 30-Bus System: (**a**) MSE curves for the training and validation phases; (**b**) histogram of the training and validation errors relative to zero error. 53
Figure 9 - Comparison between the target (Y_{des}) and ANN-estimated (Y_{ob}) nodal voltage angles (θ) for each sample: (**a**) bus 3, (**b**) bus 14, (**c**) bus 29, and (**d**) bus 30 54

Figure 10 - Comparison between the target (Y_{des}) and ANN-estimated (Y_{ob}) nodal voltage angles (θ) at the CP of the IEEE 30-Bus System 55
Figure 11 - Comparison between the target (Y_{des}) and ANN-estimated (Y_{ob}) nodal voltage angles (θ) as a function of the loading factor (λ) (P–θ curves): (**a**) bus 3, (**b**) bus 14, (**c**) bus 29, (**d**) bus 30 56
Figure 12 - P–θ curves of the IEEE 30-Bus System: (**a**) target output (Y_{des}) obtained from the CPF method and (**b**) ANN-estimated output (Y_{ob}) 57
Figure 13 - Performance evaluation of the proposed ANN: (**a**) training and validation MSE; (**b**) error histogram 58
Figure 14 - Comparison between CPF and ANN results for nodal voltage angle estimation: (**a**) critical bus angle (θ_{31}); (**b**) P-θ curve of the critical bus; (**c**) voltage angles of all buses at the maximum loading (critical) point of the system 59
Figure 15 - P-θ curves for all buses of the test system: (**a**) target P-θ curves obtained from CPF, (**b**) P-θ curves estimated by the proposed ANN 60
Figure 16 - Percentage contribution of the input variables to the ANN output, as determined by the Garson sensitivity analysis: (**a**) before normalization of $P_{g,8}$; (**b**) after normalization of $P_{g,8}$ 62
Figure 17 - Relative importance of input variables obtained by the Garson method: (**a**) IEEE 30-bus system without input normalization (R_7 and R_8); (**b**) IEEE 30-bus system with normalized inputs (R_7 and R_8); (**c**) IEEE 57-bus system without input normalization 70
Figure 18 - Comparative performance of ANN, MLR, and Regression Tree models for nodal voltage angle estimation at the critical bus (Bus 14) of the IEEE 14-bus system 79
Figure 19 - Comparative performance of ANN, MLR, and Regression Tree models for nodal voltage angle estimation at the critical bus (Bus 30) of the IEEE 30-bus system 80
Figure 20 – Comparative performance of ANN, MLR, and Regression Tree models for nodal voltage angle estimation at the critical bus (Bus 31) of the IEEE 57-bus system. 81

CAPÍTULO III

Figure 1 - Single-line diagram of the IEEE 14-bus test system, based on data from the Power Systems Test Case Archive (Christie, 1999). 92

Figure 2 - Architecture of the ANFIS model adopted for nodal voltage angle estimation, illustrating the six processing layers, including input normalization, fuzzification, fuzzy inference, firing-strength normalization, defuzzification, and final output generation 95

Figure 3 - Training performance of the ANN model: (a) mean squared error, (b) root mean squared error, and (c) error distribution for the training and validation datasets..... 99

Figure 4 - Evolution of the training and validation RMSE for the ANFIS models corresponding to buses (a) 3, (b) 6, (c) 13, and (d) 14. The markers indicate the minimum validation error used to select the final FIS... 100

Figure 5 - Error histograms of the ANFIS models for buses (a) 3, (b) 6, (c) 13, and (d) 14, considering the training and validation datasets 101

Figure 6 - Comparison of target, ANN-estimated, and ANFIS-estimated nodal voltage angles for buses 3, 6, 13, and 14. Left panels show voltage angles as a function of the operating-condition sample: (a) bus 3, (c) bus 6, (e) bus 13, and (g) bus 14. Right panels show the corresponding P−θ curves as a function of the loading parameter λ: (b) bus 3, (d) bus 6, (f) bus 13, and (h) bus 14. Markers identify the validation sample.....105

Figure 7 - Mean relative importance of the input variables obtained from the perturbation-based sensitivity analysis of the ANFIS models considering all 13 non-reference buses..... 107

LISTA DE TABELAS

CAPÍTULO II

Table 1 - First 10 samples of the input variables used for ANN training before normalization 63

Table 2 - First 10 samples of the input variables used for ANN training after normalization of $P_{g,8}$ 63

Table 3 - Synaptic weights of the connections between the input and hidden layers (14 × 7 weight matrix) before normalization of input variable R_7 ($P_{g,8}$). 64

Table 4 - Synaptic weights of the connections between the input and hidden layers (14 × 7 weight matrix) after normalization of input variable R_7 ($P_{g,8}$). ……64

Table 5 - Olden sensitivity analysis results before and after normalization of the input variable R_7 ($P_{g,8}$) for the IEEE 14-Bus System..... 66

Table 6 - Garson and Olden sensitivity analysis results before and after normalization of the input variable R_7 ($P_{g,11}$) and R_8 ($P_{g,13}$) for the IEEE 30-Bus System. 68

Table 7 - Garson and Olden sensitivity analysis results for the IEEE 57-Bus System 72

Table 8 - CPU time for obtaining nodal voltage angles in the validation phase (validation samples) 74

CAPÍTULO III

Table 1 - Performance metrics of the ANN and ANFIS models for the representative buses during training and validation 103

Table 2 - Computational performance of the ANN and ANFIS models..... 104

LISTA DE ABREVIATURAS E SÍMBOLOS

Abreviaturas

ANN – Artificial Neural Network

ANFIS – Adaptive Neuro-Fuzzy Inference System

CPF – Continuation Power Flow

CPU – Central Processing Unit

FIS – Fuzzy Inference System

IEEE – Institute of Electrical and Electronics Engineers

IA – Inteligência Artificial

MLP – Multilayer Perceptron

MLR – Multiple Linear Regression

MSE – Mean Squared Error

ONS – Operação Nacional do Sistema Elétrico

RMSE – Root Mean Squared Error

RNA – Rede Neural Artificial

SEP – Sistema Elétrico de Potência

Símbolos

λ – Fator/parâmetro de carregamento do sistema

θ – Ângulo de tensão nodal

θ_k – Ângulo de tensão nodal da barra k

P – Potência ativa

Q – Potência reativa

P_g – Potência ativa gerada

Q_g – Potência reativa gerada

P_g^{slack} – Potência ativa gerada na barra de referência (slack)

Q_g^{slack} – Potência reativa gerada na barra de referência (slack)

$P_{g,k}$ – Potência ativa gerada na barra k

Y_{des} – Valor desejado/alvo (target)

Y_{ob} – Valor obtido/estimado pelo modelo

R^2 – Coeficiente de determinação

R – Coeficiente de correlação

μ – Grau/função de pertinência fuzzy

σ – Parâmetro de largura da função de pertinência

ω – Força de ativação (firing strength) de uma regra fuzzy

$\overline{\omega}$ – Força de ativação normalizada

x_i – i-ésima variável de entrada

c_{ij} – Centro da função de pertinência

σ_{ij} – Largura da função de pertinência

R_j – j-ésima regra fuzzy

m – Número total de regras fuzzy

SUMÁRIO

SUMÁRIO....20
1 CAPÍTULO I....22
1.1 INTRODUÇÃO GERAL....22
1.2 OBJETIVOS....23
1.2.1 Objetivo geral....23
1.2.2 Objetivos específicos....23
1.3 HIPÓTESE....24
1.4 MATERIAL E MÉTODOS....24
1.4.1 Arquiteturas de Inteligência Artificial....26
1.4.1.1 Redes Neurais Artificiais (RNA's)....26
1.4.1.1.1 Forward Pass....28
1.4.1.1.2 Backward Pass....28
1.4.1.2 Adaptative Neuro-Fuzzy (ANFIS)....28
1.4.2 Implementação Computacional....30
REFERÊNCIAS....30
2 CAPÍTULO II - Estimation of Nodal Voltage Angles in Electrical Power Systems Using Artificial Neural Networks and Sensitivity Analysis of Input Variables....34
2.1 INTRODUCTION....35
2.2 MATERIALS AND METHODS....38
2.3 SENSITIVITY ANALYSIS OF INPUT VARIABLES....43
2.4 RESULTS....45
2.4.1 IEEE 14-Bus System....46
2.4.2 IEEE 30-Bus System....51
2.4.3 IEEE 57-Bus System....57
2.4.4 Sensitivity Analysis Results for The Input Variables....60
2.4.5 Computational Time For Nodal Voltage Angle Estimation....73
2.4.6 Cross-Validation Analysis And Comparative Evaluation Of Ann, Multiple Linear Regression, And Tree Models....77
2.5 CONCLUSIONS....82
REFERENCES....83
3 CAPÍTULO III - ADAPTIVE NEURO-FUZZY INFERENCE SYSTEM FOR ACCURATE VOLTAGE ANGLE STATE ESTIMATION IN ELECTRICAL POWER SYSTEMS: A TRAINING, AND VALIDATION ANALYSIS....87
ABSTRACT....87
3.1 INTRODUCTION....88
3.2 MATERIALS AND METHODS....91
3.2.1 Dataset....91

3.2.2 Architecture of the Adaptive Neuro-Fuzzy Inference System (ANFIS) 93
3.2.3 Mathematical formulation of the ANFIS model 95
3.2.4 Model Performance Evaluation 97
3.2.5 Perturbation-Based Sensitivity Analysis 97
3.3 RESULTS AND DISCUSSION 98
3.3.1 Training and Convergence Performance 98
3.3.2 Predictive Performance and Comparison between ANN and ANFIS 102
3.3.3 Voltage-Angle Estimation and P−θ Characteristics 104
3.3.4 Input-Variable Sensitivity Analysis 106
3.5 CONCLUSION 108
REFERENCES 109
4 CONCLUSÃO GERAL 114
APÊNDICE A - PRODUÇÃO ACADÊMICA DESENVOLVIDA DURANTE O DOUTORADO 116

1 CAPÍTULO I

1.1 INTRODUÇÃO GERAL

A operação segura, confiável e eficiente dos sistemas elétricos de potência modernos depende diretamente do monitoramento contínuo do estado de operação da rede (Zhao et al., 2025; Anthony e Arunachalam, 2025). Entre as variáveis de estado, as magnitudes e os ângulos de fase da tensão nodal são fundamentais para analisar a distribuição do fluxo de potência, avaliar a estabilidade de tensão estática e determinar a proximidade de limites operacionais críticos, como o ponto de carregamento máximo (Malik et al., 2024; dos Santos et al., 2023). Contudo, a contínua expansão das redes elétricas, aliada à crescente penetração de fontes renováveis intermitentes, geração distribuída e cargas não lineares, aumentou significativamente a dinâmica e a complexidade operacional dos sistemas (Molla et al., 2024; Anthony e Arunachalam, 2025).

Tradicionalmente, a estimação de estado e as avaliações de estabilidade de tensão, como a construção das curvas P–V e P–θ, dependem de técnicas numéricas iterativas, como o método de Newton–Raphson ou algoritmos de Fluxo de Potência Continuado (CPF) (Tostado-Véliz et al., 2020; Kim et al., 2024). Embora bem estabelecidos, esses procedimentos impõem um elevado esforço computacional e são suscetíveis a falhas de convergência, matrizes mal condicionadas e limitações de processamento em tempo real (da Silva et al., 2026). Para superar esses gargalos, abordagens baseadas em inteligência artificial e *soft computing* têm se destacado como alternativas promissoras, capazes de modelar relações não lineares complexas e aprender diretamente a partir de dados operacionais (Oladipo et al., 2025; Safari et al., 2024).

Nesse contexto, as Redes Neurais Artificiais (RNA) e os Sistemas de Inferência Neuro-Fuzzy Adaptativos (ANFIS) têm demonstrado alta precisão e eficiência computacional em tarefas de predição e monitoramento em sistemas de potência (Aydin e Gümüş, 2020; Siddikov e Porubay, 2022). As RNAs, especialmente do tipo *Multilayer Perceptron* (MLP) treinadas por *backpropagation*, destacam-se pela capacidade de generalização e estimação rápida, reduzindo drasticamente o tempo de processamento ao eliminar a necessidade de soluções iterativas de fluxo de potência na fase de aplicação (da Silva et al., 2026). Para complementar esse poder

preditivo, métodos de análise de sensibilidade (como os propostos por Garson, 1991, e Olden e Jackson, 2002) são empregados para avaliar a importância das variáveis de entrada e aumentar a interpretabilidade do modelo (Gevrey et al., 2003). Paralelamente, estruturas híbridas como o ANFIS integram a capacidade de aprendizado adaptativo das redes neurais com a interpretabilidade baseada em regras dos sistemas *fuzzy*, oferecendo uma modelagem do tipo "*gray-box*" mais transparente (Ayoubi e Isermann, 1997; Babuška e Verbruggen, 2003; Jang, 1993).

Apesar do avanço do uso de aprendizado de máquina em sistemas elétricos, estudos comparativos abrangentes que avaliem tanto modelos de RNA (associados à análise de sensibilidade) quanto o ANFIS especificamente para a estimação direta de ângulos de tensão nodal em sistemas-teste reconhecidos (como os sistemas IEEE 14, 30 e 57 barras) ainda são escassos. Portanto, esta pesquisa propõe e avalia metodologias avançadas baseadas em dados para estimar diretamente os ângulos de tensão nodal sob diferentes condições de carregamento, visando fornecer ferramentas precisas, confiáveis e computacionalmente eficientes para o monitoramento e a avaliação da segurança de redes elétricas em tempo real.

1.2 OBJETIVOS

1.2.1 Objetivo geral

Avaliar, por meio de modelos de inteligência artificial (RNAs do tipo *Multilayer Perceptron* e sistemas ANFIS), a estimação direta de ângulos de tensão nodal em sistemas elétricos de potência submetidos a diferentes condições de carregamento, visando a predição precisa e de baixo custo computacional para o monitoramento e a operação segura de redes elétricas.

1.2.2 Objetivos específicos

- Desenvolver e implementar arquiteturas de inteligência artificial (RNA do tipo *Multilayer Perceptron* e modelos ANFIS) para a estimação direta dos ângulos de tensão nodal em sistemas elétricos de potência, eliminando a dependência de processos numéricos iterativos complexos na fase de aplicação.
- Validar a robustez e a capacidade de generalização das metodologias propostas utilizando os sistemas de teste padrão IEEE de 14, 30 e 57 barras,

sob diversas condições de carregamento, desde a operação base até o limite de estabilidade.

- Construir curvas de ângulo de tensão versus fator de carga (curvas P–θ) para identificar com precisão o Ponto de Carregamento Máximo (ponto crítico) e avaliar as margens de estabilidade de tensão dos sistemas analisados.
- Aprimorar a interpretabilidade dos modelos através da hibridização neuro-fuzzy, permitindo a extração de regras linguísticas (IF–THEN) que descrevam o comportamento do sistema.
- Avaliar, pelos métodos de Garson e Olden, a influência e a direção do impacto das variáveis de entrada (como fator de carga e potências) nos ângulos de tensão.
- Executar uma análise comparativa de desempenho entre as RNA's e ANFIS avaliando através de métricas de erro como MSE, RMSE e coeficientes de correlação (R).
- Investigar a eficiência computacional das soluções propostas, visando uma o tempo de processamento em comparação ao método tradicional de Fluxo de Potência Continuado (CPF), destacando o potencial para aplicações em tempo real.

1.3 HIPÓTESE

As hipóteses desta pesquisa fundamentam-se na premissa de que modelos de inteligência artificial, especificamente as Redes Neurais Artificiais (RNA) e os sistemas ANFIS, podem estimar os ângulos de tensão nodal com precisão estatística equivalente aos métodos numéricos tradicionais, como o Fluxo de Potência Continuado (CPF). Além disso, espera-se uma redução no esforço computacional, identificação de variáveis governantes e a tradução de padrões complexos em regras linguísticas interpretáveis, consolidando uma base robusta para o monitoramento e o controle de redes elétricas modernas em tempo real.

1.4 MATERIAL E MÉTODOS

O Fluxo de Carga Continuado (FCC) permite traçar a curva P-V completa de um sistema elétrico a partir de um caso base até o Ponto de Máximo Carregamento

(PMC), avaliando o comportamento das tensões nodais $\mathbf{V}$ e dos ângulos de fase $\boldsymbol{\theta}$. O sistema de equações do fluxo de carga é representado na forma:

$$G(\mathbf{V}, \boldsymbol{\theta}, \lambda) = 0$$

em que $\mathbf{V}$ é o vetor das magnitudes de tensões nodais, $\boldsymbol{\theta}$ é o vetor dos ângulos de fase nodais (excetuando o da barra de referência), λ é o fator de carregamento, e G é um vetor composto pelas equações dos balanços de potência ativa e reativa nodais. Essa equação pode ser reescrita como:

$$\Delta\mathbf{P} = \mathbf{P}^{\mathbf{esp}}(\lambda) - \mathbf{P}(\boldsymbol{\theta}, \mathbf{V}) = \mathbf{0}$$
$$\Delta\mathbf{Q} = \mathbf{Q}^{\mathbf{esp}}(\lambda) - \mathbf{Q}(\boldsymbol{\theta}, \mathbf{V}) = \mathbf{0}$$

$$\mathbf{P}^{\mathbf{esp}}(\lambda) = \mathbf{P}_{\mathbf{ger}}(\lambda) - \mathbf{P}_{\mathbf{carga}}(\lambda) \quad \text{e} \quad \mathbf{Q}^{\mathbf{esp}}(\lambda) = \mathbf{Q}_{\mathbf{ger}} - \mathbf{Q}_{\mathbf{carga}}(\lambda)$$

em que as potências ativas e reativas das barras PQ, e ativas das barras PV, têm seus valores especificados no caso base ($\lambda = 1$), e os parâmetros k_{pg}, k_{pc} e k_{qc} são valores prefixados usados para caracterizar um cenário de carga específico. Usualmente, adota-se $k_{pg} = k_{pc} = k_{qc} = 1$ para manter o fator de potência constante por ser a condição operacional mais segura. A inclusão do fator de carregamento λ expande a dimensão do sistema de $n = 2n_{pq} + n_{pv}$ para n equações e $n + 1$ incógnitas, permitindo definir qualquer uma delas como parâmetro de continuação. No entanto, no fluxo de carga convencional, o valor de λ é incrementado gradualmente até o algoritmo divergir, o que ocorre no PMC devido à singularidade da matriz Jacobiana $\mathbf{J}$, exigindo as técnicas de parametrization do método de continuação para determinar com precisão o ponto de colapso de tensão.

Com base nesse equacionamento, por meio do FCC foram obtidas as amostras que compõem o banco de dados utilizado nas metodologias aqui empregadas em sistemas de teste do IEEE 14, 30 e 57 barras. Essa abordagem permite a obtenção de pontos de operação ao longo de toda a margem de carregamento do sistema, desde a condição de carga leve até o ponto crítico de estabilidade. Assim, as amostras coletadas englobam variáveis de entrada como o fator de carregamento (λ), as potências ativas e reativas na barra slack, e as injeções de potência ativa nas barras

de geração, tendo como variável de saída em todos os modelos os ângulos de tensão nodal ($\boldsymbol{\theta}$), expressos em radianos.

1.4.1 Arquiteturas de Inteligência Artificial

As arquiteturas de Inteligência Artificial (IA) são projetadas para capacitar computadores a realizar tarefas complexas, como o reconhecimento de padrões, inspirando-se originalmente no funcionamento do cérebro humano (OLDEN; JOY; DEATH, 2004). Essas estruturas variam amplamente em complexidade e funcionamento, dependendo do problema estatístico ou preditivo que visam resolver (HTUN, 2026).

1.4.1.1 Redes Neurais Artificiais (RNA's)

O neurônio artificial, mostrado na Figura 01, é a unidade fundamental de processamento em redes neurais, operando através da recepção de sinais de entrada ($x_0, x_1, \dots, x_n$) multiplicados por pesos sinápticos ($w_0, w_1, \dots, w_n$) que definem a importância de cada informação. Na etapa de combinação linear, o neurônio realiza a soma ponderada desses valores com o viés/bias ($b = x_0.w_0$), enviando o resultado para a função de ativação, que normaliza a resposta e introduz a não-linearidade necessária ao sistema. Organizados em rede, esses elementos se conectam em camadas de entrada, ocultas e de saída, atuando em sequência para converter dados brutos em estimativas finais.

Figura 1 – Modelo Teórico de um neurônio Artificial



Fonte: Adaptado de FAUSETT (1994), aprimorada pelo autor utilizando o Google Gemini (2026).
Legenda: Representação esquemática do modelo matemático de um neurônio artificial, indicando a ponderação das entradas, a combinação linear e a aplicação da função de ativação com limiar.

O neurônio calcula o valor intermediário net multiplicando cada sinal de entrada pelo seu peso associado e somando os produtos:

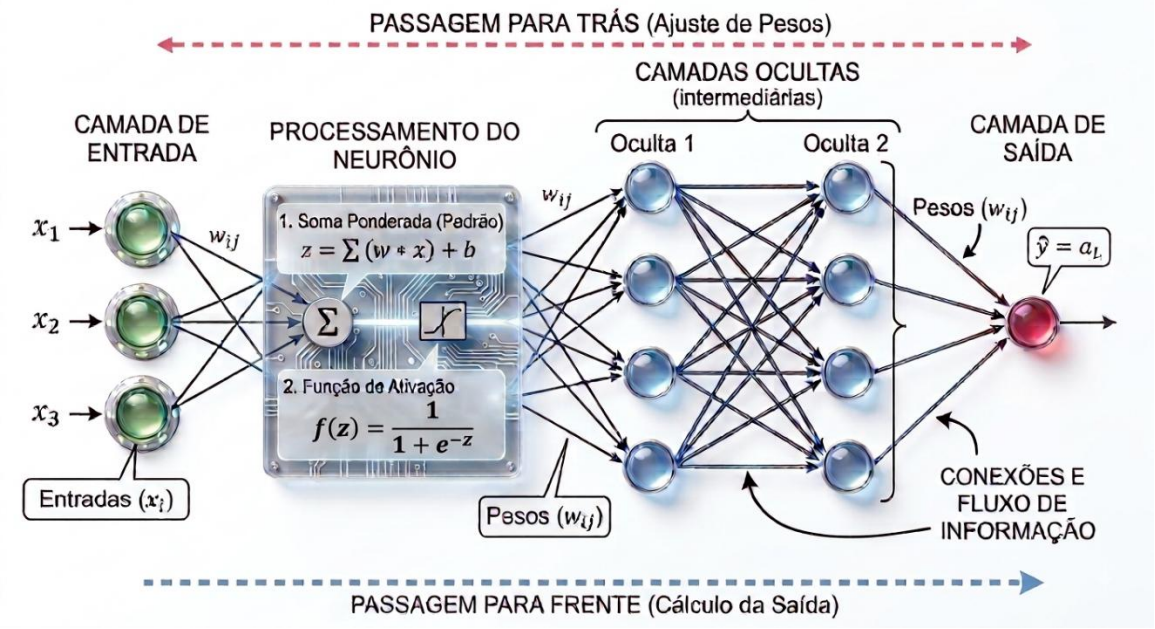
$$net = \sum w_i \cdot x_i = w_1 x_1 + w_2 x_2 + \cdots + w_0 x_0$$

O valor net é submetido à função de ativação. A função compara o resultado da combinação linear com o limiar μ (neste caso, função sigmoide):

$$y = f(net) = \begin{cases} 1, & \text{se } net \geq \mu \\ 0, & \text{se } net < \mu \end{cases}$$

A saída y assume um valor discreto (como 0 ou 1), representando uma decisão direta de classificação binária baseada no cumprimento do limiar de ativação.

Figura 2 – Modelo de uma rede neural com mais de uma camada oculta (MutiLeyer Perceptron - MLP).



Fonte: Elaborado pelo autor utilizando o Google Gemini (2026).
Legenda: Arquitetura de uma rede neural MLP, destacando o fluxo de propagação direta (feedforward) com soma ponderada (*z*) e uma função de ativação sigmoide *f(z)*, além da retropropagação do erro (backpropagation) para ajustes dos pesos sinápticos (w_{ij}).

1.4.1.1.1 Forward Pass

Na passagem para frente (*forward pass*), os dados percorrem a rede da entrada até a saída para gerar o resultado e calcular a taxa de erro em comparação com a resposta esperada.

Cada neurônio multiplica os sinais recebidos por seus respectivos pesos, soma os resultados e adiciona um viés (b):

$$z = \sum (w \cdot x) + b$$

O valor z passa pela função sigmóide, introduzindo não-linearidade e normalizando a saída em um intervalo entre 0 e 1:

$$f(z) = \frac{1}{1 + e^{-z}}$$

A saída ativada é enviada aos neurônios da camada posterior (Camadas Ocultas 1 e 2) até alcançar a camada de saída para gerar o valor previsto ($\hat{y}$).

1.4.1.1.2 Backward Pass

Em seguida, na passagem para trás (*backward pass*), o algoritmo de retropropagação (*backpropagation*) distribui esse erro no sentido inverso. O sistema compara o valor previsto ($\hat{y}$) com o valor real esperado através de uma função de custo/perda. Os Algoritmos de otimização utilizam cálculos de gradiente para recalibrar os pesos sinápticos e os vieses, reduzindo o erro progressivamente a cada iteração do treinamento. Dessa forma, recalibram os pesos (w_{ij}) e os vieses (b), reduzindo a margem de erro para as próximas execuções.

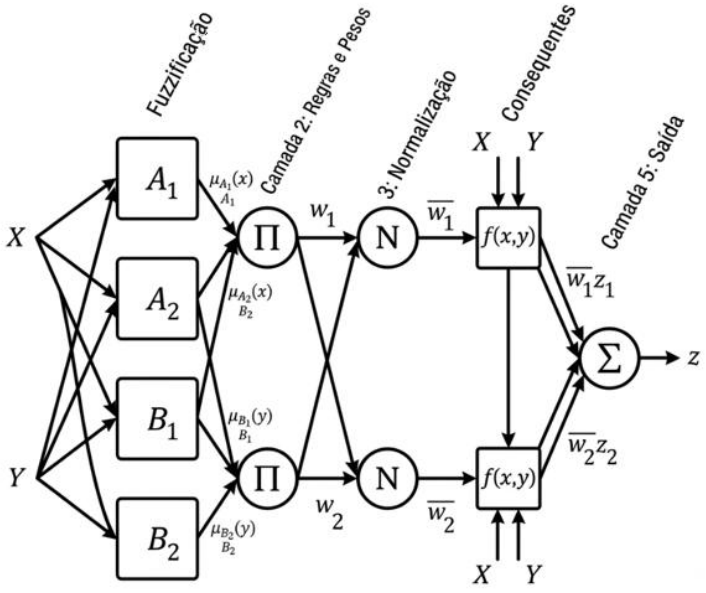
1.4.1.2 Adaptative Neuro-Fuzzy (ANFIS)

O Sistema de Inferência Neuro-Fuzzy Adaptativo (ANFIS) combina a capacidade de aprendizado adaptativo das redes neurais artificiais com a representação baseada em regras dos sistemas de inferência *fuzzy* (Jang, 1993; Babuška e Verbruggen, 2003). Ao contrário dos modelos convencionais de "caixa-

preta", o ANFIS representa as relações não lineares aprendidas por meio de regras *fuzzy* do tipo SE-ENTÃO (*IF-THEN*), proporcionando uma estrutura potencialmente mais interpretável para aplicações em sistemas de energia.

O desempenho e a complexidade dos modelos ANFIS são fortemente influenciados pela construção do sistema de inferência *fuzzy* inicial. O agrupamento subtrativo (*subtractive clustering*) oferece uma estratégia eficiente, baseada em dados, para identificar agrupamentos no espaço de entrada e saída e gerar automaticamente funções de pertinência e regras *fuzzy*, sem a necessidade de definir previamente o número delas (Chiu, 1994).

Figura 3 – Arquitetura do sistema de inferência neuro-fuzzy adaptativo (ANFIS)



Fonte: Autoria própria.
Legenda: Fluxo de processamento e estrutura em camadas de um modelo ANFIS, detalhando as etapas desde a fuzzificação das entradas até a defuzzificação e obtenção da saída final *z*.

Na camada 01 cada nó recebe as entradas e calcula o grau de pertinência às variáveis linguísticas (ex: "frio", "médio", "quente") através de funções gaussianas ou triangulares. Já a camada 02 realiza a multiplicação (Π) dos graus de entrada para determinar a força de disparo de cada regra *Se-Então*. Na camada seguinte, é calculada a razão entre a força de uma regra específica e a soma da força de todas as regras (N). A penúltima camada aplica os parâmetros de saída das regras (funções lineares de Takagi-Sugeno) e a última soma (Σ) os resultados ponderados de todas as regras para gerar a saída numérica final (z).

1.4.2 Implementação Computacional

O Matlab® versão 2025b (MathWorks, 2026), foi utilizado para a implementação, o treinamento e a validação da RNA e ANFIS, bem como para a geração dos resultados.

REFERÊNCIAS

ANTHONY, K.; ARUNACHALAM, V. Voltage stability monitoring and improvement in a renewable energy dominated deregulated power system: a review. **e-Prime - Advances in Electrical Engineering, Electronics and Energy**, v. 11, p. 100893, mar. 2025. DOI: https://doi.org/10.1016/j.prime.2024.100893

AYDIN, F.; GÜMÜŞ, B. Study of different ANN algorithms for voltage stability analysis. In: INNOVATIONS IN INTELLIGENT SYSTEMS AND APPLICATIONS CONFERENCE (ASYU), 2020, Istanbul. **Proceedings [...]**. Istanbul: IEEE, 2020. p. 1–5. DOI: https://doi.org/10.1109/ASYU50717.2020.9259817

AYOUBI, M.; ISERMANN, R. Neuro-fuzzy systems for diagnosis. **Fuzzy Sets and Systems**, v. 89, n. 3, p. 289–307, 1997. DOI: https://doi.org/10.1016/S0165-0114(97)00011-0

BABUŠKA, R.; VERBRUGGEN, H. Neuro-fuzzy methods for nonlinear system identification. **Annual Reviews in Control**, v. 27, n. 1, p. 73–85, 2003. DOI: https://doi.org/10.1016/S1367-5788(03)00009-9

CHIU, S. L. Fuzzy model identification based on cluster estimation. **Journal of Intelligent & Fuzzy Systems**, v. 2, n. 3, p. 267–278, 1994. DOI: https://doi.org/10.3233/IFS-1994-2306

DA SILVA, G. G.; ROQUE, R. F. M.; ARREGUÍN SÁMANO, M.; DIAS, N. L.; GOLZIO, A. C. DE J.; BONINI NETO, A. Multilayer perceptron, radial basis function, and generalized regression networks applied to the estimation of total power losses in electrical systems. **Machine Learning and Knowledge Extraction**, v. 8, n. 1, p. 4, 2026. DOI: https://doi.org/10.3390/make8010004

DOS SANTOS, W. P. L.; BONINI NETO, A.; GABRIEL FILHO, L. R. A. Post-contingency loading margin through plane change in the continuation power flow. **Energies**, v. 16, n. 22, p. 7583, 2023. DOI: https://doi.org/10.3390/en16227583

GARSON, G. D. Interpreting neural-network connection weights. **AI Expert**, v. 6, n. 4, p. 47–51, abr. 1991.

GEVREY, M.; DIMOPOULOS, I.; LEK, S. Review and comparison of methods to study the contribution of variables in artificial neural network models. **Ecological Modelling**, v. 160, n. 3, p. 249–264, 2003. DOI: https://doi.org/10.1016/S0304-3800(02)00257-0

HTUN, N. M.; OWARI, T.; SUZUKI, S. N.; DENG, S.; KOBAYASHI, T.; ASATO, S.; OSHIMA, A.; HIRAMA, M.; TAKAHASHI, K.; ISOZAKI, Y. et al. A multi-sensor machine learning framework integrating UAV multispectral imagery and LiDAR data for living biomass carbon stock estimation in silviculturally treated forests. **Sensors**, v. 26, n. 14, p. 4496, 2026. DOI: https://doi.org/10.3390/s26144496

JANG, J.-S. R. ANFIS: adaptive-network-based fuzzy inference system. **IEEE Transactions on Systems, Man, and Cybernetics**, v. 23, n. 3, p. 665–685, maio/jun. 1993. DOI: https://doi.org/10.1109/21.256541

KIM, H.; WOO, H.; YOON, Y.; KIM, H.-T.; KIM, Y. J.; KANG, M.; ZHANG, X.; CHOI, S. An enhanced continuation power flow method using hybrid parameterization. **Sustainability**, v. 16, n. 17, p. 7595, 2024. DOI: https://doi.org/10.3390/su16177595

MALIK, F. H.; KHAN, M. W.; RAHMAN, T. U.; EHTISHAM, M.; FAHEEM, M.; HAIDER, Z. M.; LEHTONEN, M. A comprehensive review on voltage stability in wind-integrated power systems. **Energies**, v. 17, n. 3, p. 644, 2024. DOI: https://doi.org/10.3390/en17030644

MATHWORKS. **MATLAB: version 2025b (R2025b)**. Natick: The MathWorks Inc., 2026.

MOLLA, S.; FARROK, O.; ALAM, M. J. Electrical energy and the environment: prospects and upcoming challenges of the world's top leading countries. **Renewable**

and Sustainable Energy Reviews, v. 191, p. 114177, mar. 2024. DOI: https://doi.org/10.1016/j.rser.2023.114177

OLADIPO, S.; SUN, Y.; ADEGOKE, S. A. Application of soft computing techniques to load frequency control system of electric power systems: a brief survey. **Cogent Engineering**, v. 12, n. 1, p. 2572297, 2025. DOI: https://doi.org/10.1080/23311916.2025.2572297

OLDEN, J. D.; JACKSON, D. A. Illuminating the “black box”: a randomization approach for understanding variable contributions in artificial neural networks. **Ecological Modelling**, v. 154, n. 1–2, p. 135–150, 2002. DOI: https://doi.org/10.1016/S0304-3800(02)00064-9

OLDEN, J. D.; JOY, M. K.; DEATH, R. G. An accurate comparison of methods for quantifying variable importance in artificial neural networks using simulated data. **Ecological Modelling**, v. 178, n. 3–4, p. 389–397, 2004. DOI: https://doi.org/10.1016/j.ecolmodel.2004.03.013

SAFARI, A.; DANESHVAR, M.; ANVARI-MOGHADDAM, A. Energy intelligence: a systematic review of artificial intelligence for energy management. **Applied Sciences**, v. 14, n. 23, p. 11112, 2024. DOI: https://doi.org/10.3390/app142311112

SIDDIKOV, I. K.; PORUBAY, O. V. Neuro-fuzzy system for regulating the processes of power flows in electric power facilities. **AIP Conference Proceedings**, v. 2432, n. 1, p. 020010, 2022. DOI: https://doi.org/10.1063/5.0089473

TOSTADO-VÉLIZ, M.; KAMEL, S.; JURADO, F. Development and comparison of efficient Newton-like methods for voltage stability assessment. **Electric Power Components and Systems**, v. 48, n. 16–17, p. 1798–1813, 2020. DOI: https://doi.org/10.1080/15325008.2021.1908452

ZHAO, J.; SRIVASTAVA, A.; GUO, Y.; CETENOVIC, D.; LIN, Y.; LEVI, V.; YIN, G.; HUANG, M.; ZHANG, T.; LI, Z.; CHEN, Y.; EXPOSITO, A. G.; ZHANG, W.; ZHENG, W.; CHAKRABARTI, S.; LI, Y.; SHARMA, A.; KAMWA, I.; GUO, Q.; TERZIJA, V.; MILI, L. State estimation for integrated energy systems: motivations, advances, and future

work. **IEEE Transactions on Power Systems**, v. 40, n. 3, p. 3057–3073, maio 2025. DOI: https://doi.org/10.1109/TPWRS.2024.3524323

2 CAPÍTULO II - Estimation of Nodal Voltage Angles in Electrical Power Systems Using Artificial Neural Networks and Sensitivity Analysis of Input Variables

Neylan Leal Dias [1,2], Alexandre de Queiroz [1], Ana Claudia de Jesus Golzio [3], Ricardo Fonseca Buzo [3], Simone de Almeida Delphin Leal [2], Gabriel Henrique Doi [3] and Alfredo Bonini Neto [2].

Abstract

The estimation of nodal voltage angles is essential for the efficient and secure operation of electrical power systems. Traditionally, this estimation depends on the prior solution of the power flow problem, a procedure that may become computationally expensive in studies involving multiple operating scenarios. The present research demonstrates relevant potential impact by employing artificial neural networks for the direct estimation of nodal voltage angles. Although the power flow is used during the database generation stage, it is no longer required during the model application phase, resulting in a significant reduction in computational effort of approximately 80%. The proposed model was trained using the error backpropagation algorithm, achieving a mean squared error (MSE) on the order of 10^{-3} in only four iterations, with a training time of approximately 3 s and a correlation coefficient (R) of 0.99. Validation using unseen samples (10% of the samples) also demonstrated high accuracy, with an error on the order of 10^{-3} between the estimated and expected values. Furthermore, the P–θ curves were successfully obtained for the IEEE 14-, 30-, and 57-bus systems, enabling the identification of the maximum loading point with low estimation error. These results confirm the neural network's ability to generalize and operate as a reliable estimator under different system loading conditions. Another relevant aspect of this work was the sensitivity analysis of the input variables, which made it possible to identify the variables that exerted the greatest influence on the neural network response. In addition, a normalization step was proposed to overcome distortions associated with the

[1] School of Engineering, São Paulo State University (Unesp), Bauru 17033-360, Brazil; neylan.dias@unesp.br; alexandre.queiroz@unesp.br.
[2] Department of Exact and Technological Sciences, Federal University of Amapá, Macapá 68903-419, Brazil; neylan@unifap.br; leal@unifap.br.
[3] School of Sciences and Engineering, São Paulo State University (Unesp), Tupã 17602-496, Brazil; a.golzio@unesp.br; ricardo.f.buzo@unesp.br; abriel.doi@unesp.br; alfredo.bonini@unesp.br.

magnitudes of the input data, demonstrating the efficiency and robustness of the proposed method.

Keywords: artificial neural networks; nodal voltage angles; electrical power systems; state estimation; power flow

2.1 INTRODUCTION

The dispatch of electrical energy has become increasingly complex in recent years, mainly due to the expansion of electrical networks, the integration of intermittent renewable energy sources, and long-distance power transmission (Molla; Farrok; Alam, 2024). These developments have intensified the challenges associated with power system stability, resulting in a higher risk of voltage instability and voltage collapse events. In particular, the increasing penetration of renewable energy sources, especially wind power, has introduced additional variability and operational uncertainties that can adversely affect voltage stability and overall system reliability (Malik *et al.*, 2024; Anthony; Arunachalam, 2025). Moreover, the transition toward deregulated power systems and the growing share of non-dispatchable renewable generation have increased the need for advanced voltage stability monitoring, assessment, and control techniques to ensure secure and reliable system operation (Anthony; Arunachalam, 2025; Werkie; Nyakoe; Wekesa, 2025). Such challenges may lead to significant economic losses, service interruptions, and social impacts, highlighting the importance of accurate voltage stability analysis and prediction methodologies.

To analyze static voltage stability in electrical power systems, P–V curves are widely employed to represent the relationship between bus voltage magnitude and system loading, providing valuable insights into stability margins and the proximity to voltage collapse (Tostado-Véliz; Kamel; Jurado, 2020; Santos; Bonini Neto; Gabriel Filho, 2023; Kim *et al.*, 2024). These graphical representations are fundamental for determining power transfer capabilities between different system areas, establishing secure operating margins, monitoring voltage profiles at critical buses, and supporting planning decisions related to network expansion and reinforcement. In addition, they enable the assessment of system behavior under varying loading levels and contingency conditions (Tostado-Véliz; Kamel; Jurado, 2020; Santos; Bonini Neto; Gabriel

Filho, 2023; Kim *et al.*, 2024). Consequently, the construction of P–V curves is recognized as one of the most effective approaches for evaluating voltage security and identifying the maximum loading point, also known as the critical point (CP) (Santos; Bonini Neto; Gabriel Filho, 2023; Bento, 2024).

Traditionally, these curves are obtained through conventional power flow analysis based on the Newton–Raphson method. The solution process is performed iteratively, with successive increases in system loading, until convergence can no longer be achieved, typically due to the singularity of the Jacobian matrix. This operating condition is generally interpreted as the maximum loading limit of the system.

Currently, the Continuation Power Flow (CPF) method is the most widely used technique for static voltage stability analysis (Kim *et al.*, 2024; Ruan *et al.*, 2018). CPF is performed in four main stages: prediction, in which an initial estimate of the solution is obtained; step-size control, responsible for defining the process increments; parameterization, which identifies the control variable required to ensure convergence; and correction, responsible for adjusting the solution until the desired accuracy is achieved. In addition to the P–V curve, the voltage angle versus loading factor curve (P–θ curve) represents a complementary approach for loading margin analysis, since variations in voltage angles provide valuable information regarding system stress levels and proximity to voltage instability (Santos; Bonini Neto; Gabriel Filho, 2023; Lopez *et al.*, 2022). This curve makes it possible to evaluate how nodal voltage angles vary with respect to the loading factor, providing additional information for identifying the stability margin. The CP identified in this curve also represents an important indicator of the system stability limit.

Given the increasing complexity and the challenges associated with voltage stability, power companies have sought tools capable of improving the operation of electrical power systems. In this context, Artificial Neural Networks (ANNs) have emerged as a promising approach due to their learning capability, generalization capacity, and ability to model complex nonlinear systems (Silva *et al.*, 2026; Simonič; Ficko; Klančnik, 2025; Safari; Daneshvar; Anvari-Moghaddam, 2024). Recent studies have demonstrated satisfactory results using machine learning techniques for voltage stability margin prediction. One example is the Extreme Learning Machine (ELM), which achieved a mean percentage error of only 3.32% and a mean error of 0.0495 in voltage stability margin prediction, values considered suitable for practical applications (Zhang *et al.*,

2013).

Other studies have also demonstrated that ANNs can reproduce voltage stability assessment results with high accuracy and computational efficiency, comparable to conventional methods. By evaluating different input variables and training algorithms, suitable ANN configurations were identified for predicting the loading parameter and the Voltage Stability Margin Index, showing promising results for voltage stability analysis (Aydin; Gümüş, 2020).

ANN applications are not limited to electrical power systems. In other contexts, such as predictive biomarker identification for diffuse large B-cell lymphoma and geometric prediction of finished products, Multilayer Perceptron (MLP) and Radial Basis Function Network (RBF) models have also demonstrated high accuracy, achieving accuracy rates above 92% (Carreras *et al.*, 2021; Ke; Huang, 2020). These results reinforce the potential of ANNs in different areas of engineering and applied science.

ANNs have been widely applied to the modeling and analysis of complex nonlinear systems due to their ability to learn patterns and generalize solutions from data. Among the most commonly used training approaches, the backpropagation algorithm has demonstrated high efficiency in solving nonlinear engineering problems and modeling complex systems. However, despite their strong predictive capability, ANNs are often regarded as “black-box” models because of the difficulty in interpreting the influence of input variables on network outputs (Garson, 1991; Goh, 1995; Olden; Jackson, 2002).

To address this limitation, several studies have proposed methodologies for interpreting synaptic weights and evaluating the relative importance of input variables in neural networks. One of the pioneering approaches was introduced by Garson (1991), who proposed a method based on synaptic weights to quantify the contribution of each input variable to the network response. Subsequently, Olden and Jackson (2002) developed a randomization-based approach to improve the interpretation of variable contributions in ANNs, while Olden, Joy and Death (2004) compared different methodologies for quantifying variable importance, demonstrating that some techniques provide more accurate interpretations than traditional approaches. In addition, Yoon, Guimaraes and Swales (1994) discussed the integration of neural networks with rule-based expert systems to improve explanation capabilities and decision-support processes in intelligent systems.

These studies demonstrate that sensitivity analysis and variable importance evaluation are essential for improving the transparency, reliability, and interpretability of ANN-based models (Garson, 1991; Olden; Jackson, 2002; Gevrey; Dimopoulos; Lek, 2003). In particular, Gevrey, Dimopoulos and Lek (2003) performed a comprehensive comparison of sensitivity analysis techniques and concluded that methods based on partial derivatives may provide a more detailed assessment of input variable contributions than conventional weight-based approaches, although the latter remain attractive due to their simplicity and ease of implementation. In the context of electrical power systems, such analyses are particularly relevant because they enable the identification of the variables that most strongly influence system behavior and voltage stability conditions. Consequently, sensitivity analysis not only enhances the interpretability of ANN models but also increases confidence in their application to power system studies and decision-making processes.

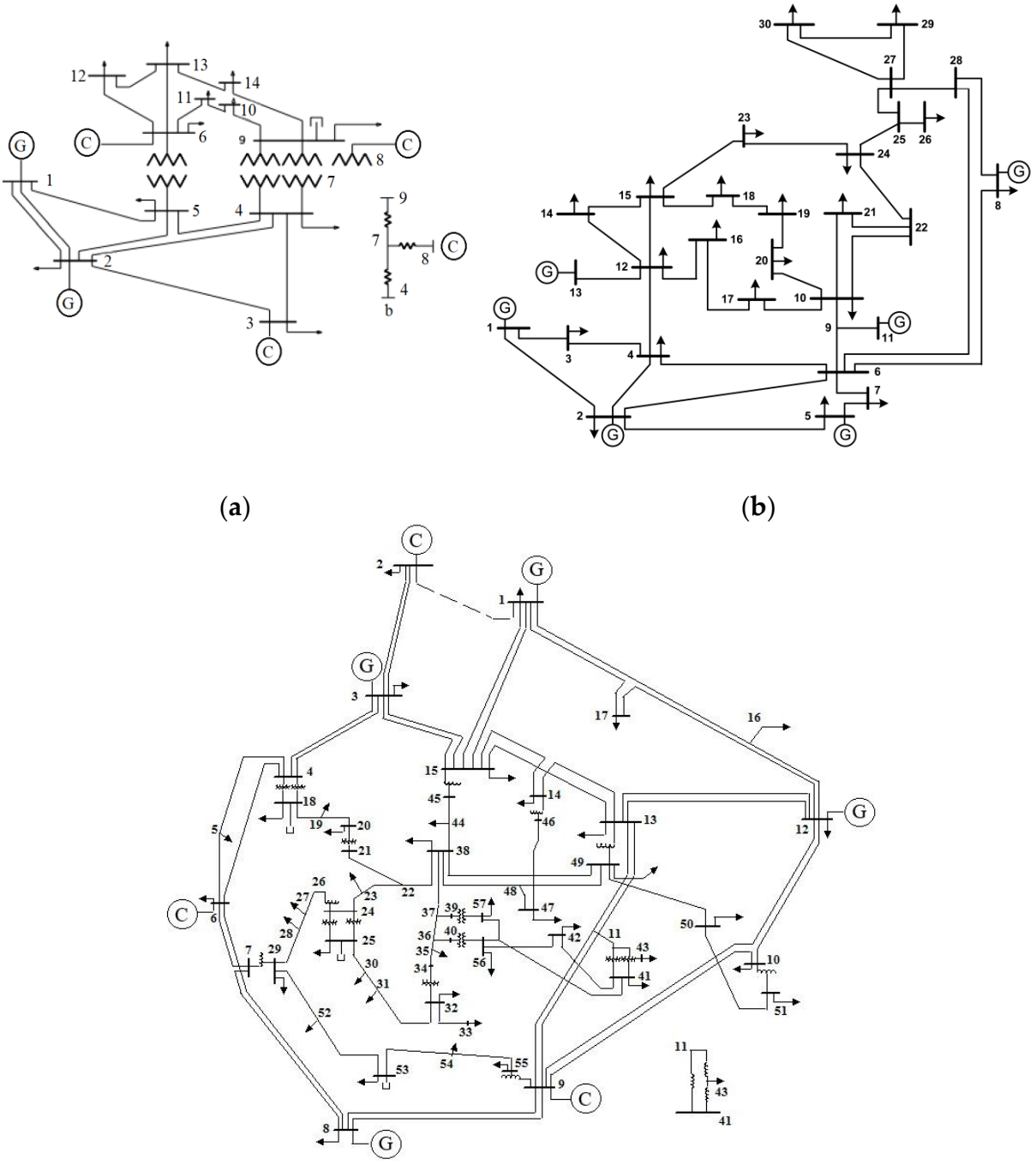
The main contributions of this work are fourfold. First, an ANN-based methodology is proposed to directly estimate nodal voltage angles and construct P–θ curves without requiring CPF calculations during the application stage. Second, the proposed model is validated using the IEEE 14-, 30-, and 57-bus benchmark systems under different loading conditions. Third, a comprehensive sensitivity analysis based on the Garson and Olden methods is performed to investigate the relative importance of the input variables. Finally, a normalization strategy is proposed to eliminate distortions caused by input variables with extremely small numerical magnitudes, resulting in a more reliable and physically meaningful sensitivity analysis while preserving the predictive accuracy of the ANN. In addition, the proposed approach reduces the computational time required for nodal voltage angle estimation by approximately 88% compared with the conventional CPF method.

2.2 MATERIALS AND METHODS

The system analyzed in this work corresponds to the IEEE 14-bus, 30-bus, and 57-bus test systems, presented in Figure 1a, 1b, and 1c, respectively. The IEEE 14-bus system consists of 1 slack bus, 4 generation buses, 9 load buses, and 20 transmission lines. The IEEE 30-bus system comprises 1 slack bus, 5 generation buses, 24 load buses, and 41 transmission lines. The IEEE 57-bus system includes 1 slack bus, 6 generation buses, 50 load buses, and 80 transmission lines, and is widely used in

studies involving the analysis and validation of methodologies applied to electric power systems.

Figure 1 – IEEE benchmark test systems considered in this study: (**a**) IEEE 14-bus system, (**b**) IEEE 30-bus system, and (**c**) IEEE 57-bus system.

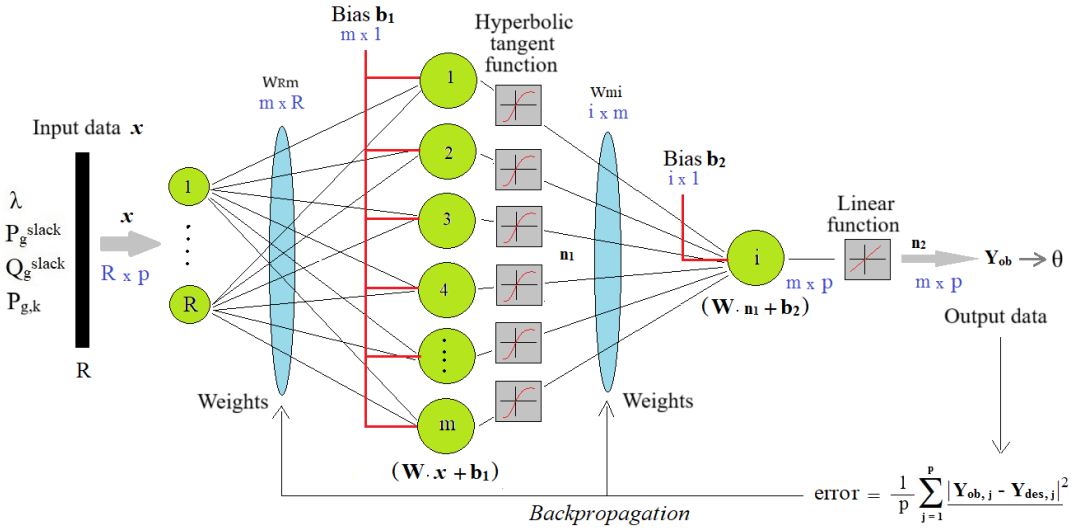


Source: Christie (1999)

The Artificial Neural Network (ANN) employed in this work is an MLP trained

using the backpropagation learning algorithm. The adopted architecture consists of three layers, as illustrated in Figure 2. The hidden layer was configured with a number of neurons equal to the largest dimension between the input and output vectors. For the IEEE 14-bus system, the input layer contains 7 neurons and the output layer 14 contains neurons, resulting in a hidden layer with 14 neurons. For the IEEE 30-bus system, the input layer consists of 8 neurons, while both the hidden and output layers contain 30 neurons. Similarly, for the IEEE 57-bus system, the input layer contains 9 neurons, whereas the hidden and output layers are composed of 57 neurons each. This variation in the ANN architecture is associated with the total number of buses in the system and the number of generation buses, which directly affect the dimensions of the input and output vectors. Matlab® version 2025b (MathWorks, 2026) was used for ANN implementation, training, validation, and result generation.

Figure 2 – MLP artificial neural network architecture used for nodal voltage angle estimation.



Source: Elaborated by the author

The ANN architecture was not selected empirically. Instead, the optimal configuration was determined using the algorithm proposed by Da Silva et al. (2026). The training procedure was repeatedly executed while systematically varying the number of hidden layers, the number of neurons in each hidden layer (in increments of one neuron), and the proportion of samples allocated for training and validation. For each

configuration, multiple training runs were performed because different random initializations of the synaptic weights may lead to different solutions. The network configuration that achieved the best validation performance was selected, and its corresponding synaptic weights were stored to ensure the reproducibility of the proposed methodology. Following this optimization procedure, the best-performing architecture consisted of a single hidden layer with 14, 30, and 57 neurons for the IEEE 14-, 30-, and 57-bus systems, respectively, using 90% of the available samples for training and 10% for validation. Increasing the number of hidden neurons beyond these values did not produce significant improvements in validation performance, whereas smaller networks resulted in lower prediction accuracy.

A total of 302 samples were used, including 107 samples from the IEEE 14-bus system, 93 samples from the IEEE 30-bus system, and 102 samples from the IEEE 57-bus system. These samples were obtained using the parameterized CPF method (Dos Santos; Bonini Neto; Gabriel Filho, 2023). The CPF database was generated by progressively varying the loading factor (λ) using a fixed step size of 0.02. The continuation process produced operating points covering the entire loading margin of each IEEE test system, including the base operating condition, the maximum loading point (critical point), and the lower branch of the P--θ curve. Consequently, the generated dataset comprises operating conditions ranging from light loading to critical and post-critical conditions, providing a diverse set of nonlinear operating scenarios for ANN training and validation. Each sample consists of a set of input variables and the corresponding desired outputs. The input variables include the loading factor (λ), the real ($P_{g\text{slack}}$) and reactive ($Q_{g\text{slack}}$) power generated at the slack bus, as well as the specified real power injections at the generation buses ($P_{g,k}$). The ANN outputs correspond to the nodal voltage angles (θ), expressed in radians.

In Figure 2, x is the input vector, R is the number of input variables in each sample, and p is the total number of samples. W represents the synaptic weights connecting the input layer to the hidden layer and the hidden layer to the output layer, while b denotes the bias terms. The parameter m corresponds to the number of neurons in the hidden layer, and i represents the number of neurons in the output layer. The hyperbolic tangent function was employed as the activation function in the hidden layer, as defined by Equation (1). A linear activation function was used in the output layer, as described by Equation (2).

$$n_1 = f(W.x + b_1) = \frac{(1 - e^{t(W.x + b_1)})}{(1 + e^{t(W.x + b_1)})} \quad (1)$$

In Equation (1), t denotes the gain parameter of the hyperbolic tangent activation function. This parameter controls the steepness of the activation curve and, consequently, the sensitivity of the neuron output to variations in the input signal. In this work, t = 1 was adopted, resulting in the standard hyperbolic tangent function used in the hidden layer of the ANN.

$$n_2 = f(W.n_1 + b_2) = W.n_1 + b_2 \quad (2)$$

The performance of the ANN is evaluated using the Mean Squared Error (MSE), calculated according to Equation (3), where Y_{ob} denotes the output values predicted by the ANN and Y_{des} represents the corresponding target values obtained from the CPF method.

$$MSE = \frac{1}{p} \sum_{j=1}^{p} (Y_{ob,j} - Y_{des,j})^2 \quad (3)$$

The MSE is a fundamental metric for evaluating ANN performance, as it quantifies the discrepancy between the predicted outputs (Y_{ob}) and the target values (Y_{des}). The closer the predicted values are to the desired outputs, the lower the error, indicating a more accurate adjustment of the network synaptic weights during the training process. Consequently, minimizing the MSE is a primary objective in model optimization, as it directly contributes to improving prediction accuracy and enhancing the network's ability to capture the underlying patterns present in the data.

Unlike a random classification experiment, the CPF method is based on a set of nonlinear equations whose solution is obtained by progressively varying the loading factor parameter. For each loading level, the corresponding nodal voltage angles (θ) at all system buses are determined through an iterative solution process. Since these values are directly derived from the power flow equations, they provide a reliable and physically consistent dataset for training ANNs, particularly MLP networks, which have demonstrated strong capabilities in approximating nonlinear relationships.

However, the main challenge lies in the ANN's generalization capability, that is, its ability to accurately predict system states under different operating conditions and network configurations. To achieve this objective, the input dataset must contain variables that effectively represent the changes occurring in the system, enabling the network to learn robust patterns and maintain high prediction accuracy under a wide range

of scenarios. Once properly trained, the ANN can estimate the nodal voltage angles directly, eliminating the need for the iterative solution process traditionally required by the CPF method.

To further assess the robustness and generalization capability of the proposed ANN, an additional 10-fold cross-validation procedure was performed (Kohavi, 1995; Özesmi; Tan; Özesmi, 2006; Wong, 2015). The available dataset was randomly partitioned into ten approximately equal subsets. At each iteration, one subset was reserved for external validation, while the remaining nine subsets were used for model development. Within each training fold, 90% of the samples were used for network training and 10% for internal validation (early stopping). This procedure was repeated until each subset had been used once as the external validation set. The predictive performance was evaluated using the average MSE, Root Mean Squared Error (RMSE), and correlation coefficient (R) obtained over the ten folds, providing a more robust assessment of the proposed model than a single train–validation split (Kohavi, 1995; Özesmi; Tan; Özesmi, 2006; Wong, 2015).

To provide a benchmark for the proposed ANN, two additional supervised learning methods were implemented using the same training and validation datasets.
Multiple Linear Regression (MLR): MLR was employed as a baseline linear model to estimate nodal voltage angles from the input variables. The model assumes a linear relationship between the predictor variables and the output, allowing a direct comparison with the nonlinear ANN approach (Montgomery; Peck; Vining, 2012; Htun et al., 2026).

Regression Tree: A regression tree model was also implemented to estimate nodal voltage angles. This method recursively partitions the input space into homogeneous regions according to decision rules, generating a tree-based predictive model. The Regression Tree was included as an interpretable machine learning approach for comparison with the proposed ANN (Breiman et al., 2017; Boyaci; Tumbek, 2026).
For both methods, the same input variables, output variables, and training/validation partitions adopted for the ANN were used to ensure a fair performance comparison.

2.3 SENSITIVITY ANALYSIS OF INPUT VARIABLES

To enhance the interpretability of the ANN model, a sensitivity analysis of the input variables was performed using the synaptic weights obtained after the network

training process. Two widely adopted methodologies were employed: the Garson method (Garson, 1991), including the modification proposed in Goh (1995), and the Olden technique (Olden; Jackson, 2002). These approaches enable the evaluation of the relative contribution of each input variable to the estimation of the nodal voltage angles (θ), providing additional insights into the relationships learned by the ANN during training.

The Garson method (Garson, 1991) determines the relative importance of input variables by decomposing the connection weights between the input, hidden, and output layers. By considering the absolute values of the synaptic weights, the method estimates the contribution of each variable to the model output and expresses the results as normalized percentage values. Consequently, this procedure quantifies the relative influence of each input variable on the network response, regardless of whether its effect is positive or negative.

The relative importance index obtained using the Garson method (Garson, 1991) can be calculated according to Equation (4):

$$RI_R = \frac{\sum_{m=1}^{M} \left(\frac{\left| W_{Rm} . W_{mi} \right|}{\sum_{R=1}^{N} \left| W_{Rm} \right|} \right)}{\sum_{R=1}^{N} \sum_{m=1}^{M} \left(\frac{\left| W_{Rm} . W_{mi} \right|}{\sum_{R=1}^{N} \left| W_{Rm} \right|} \right)} \quad (4)$$

In this formulation, the relative importance value associated with each predictor variable is obtained from the combination of the connection weights between neurons across the network layers. The terms related to the input-to-hidden and hidden-to-output connections represent the contribution propagated through the ANN structure. The total number of hidden neurons is represented by M, whereas N indicates the number of input parameters considered in the model.

To complement the interpretability analysis, the method proposed by Olden (Olden; Jackson, 2002) was also applied. Unlike the Garson approach, which considers only the absolute magnitude of the synaptic weights, the Olden technique preserves the algebraic sign of the network connections. This allows the identification of whether each input variable exerts a positive or negative influence on the estimation of the nodal voltage angles (θ), while also quantifying the intensity of this contribution.

Previous studies have indicated that the Olden method may provide a more reliable representation of variable influence in neural network models when compared with conventional weight-decomposition techniques (Olden; Joy; Death, 2004). The importance values obtained through the Olden method (Olden; Jackson, 2002) were determined using Equation (5):

$$I_R = \sum_{m=1}^{M} (W_{Rm} . W_{mi}) \quad (5)$$

In (5), the importance associated with each predictor variable is obtained from the interaction between the connection weights linking the input layer to the hidden neurons and those connecting the hidden layer to the output neuron. These synaptic weights describe how information propagates throughout the ANN structure and contributes to the final prediction. The variable importance analysis was carried out using the optimized ANN configuration adopted in this work, which consisted of a single hidden layer with 14, 30, and 57 neurons. After the training stage, the connection weights of the network were extracted and analyzed in Matlab® version 2025b (MathWorks, 2026). This procedure enabled the evaluation of both the relative contribution and the influence direction of the input variables on the estimation of the nodal voltage angles (θ) in the electrical power system.

The Olden method was employed to evaluate the relative importance of the input variables based on the synaptic weights of the trained ANN. Unlike the Garson approach, the Olden algorithm preserves the sign of the connection weights and computes the contribution of each input variable as the product of the weights connecting the input-hidden and hidden-output layers. Consequently, the resulting importance values are expressed as relative influence indices rather than percentages.

The sign of the importance index provides information about the direction of the relationship between the input and output variables. Positive values indicate that an increase in the input variable tends to increase the estimated nodal voltage angle magnitude (θ), whereas negative values indicate an inverse relationship. Furthermore, the absolute value of the index reflects the strength of the contribution, with larger magnitudes corresponding to greater influence on the network output.

2.4 RESULTS

Among the available samples, 90% were randomly selected for training the ANN, while the remaining 10% were reserved for model validation. The validation stage aims to assess the network's generalization capability when exposed to unseen input data, evaluating the consistency, accuracy, and reliability of the obtained estimates. This procedure ensures that the trained model can effectively generalize its learned relationships beyond the training dataset. Consequently, the proposed ANN is capable of directly estimating the voltage angles of all system buses without requiring conventional iterative solution procedures.

2.4.1 IEEE 14-Bus System

A total of 107 samples were used for the IEEE 14-Bus System, of which 96 were allocated for ANN training and 11 were reserved for model validation. Figure 3a presents the training and validation performance curves in terms of the MSE. It can be observed that the predefined convergence criterion (MSE ≤ 0.001) was achieved after only four training iterations, resulting in MSE values of 0.0008325 and 0.0010755 for the training and validation datasets, respectively. These results demonstrate the efficiency, fast convergence, and learning capability of the proposed ANN model. Similar applications of artificial intelligence for power loss estimation and management in electrical power systems have been widely reported in the literature (Niste et al., 2025), demonstrating the capability of ANN-based models to accurately predict system operating variables.

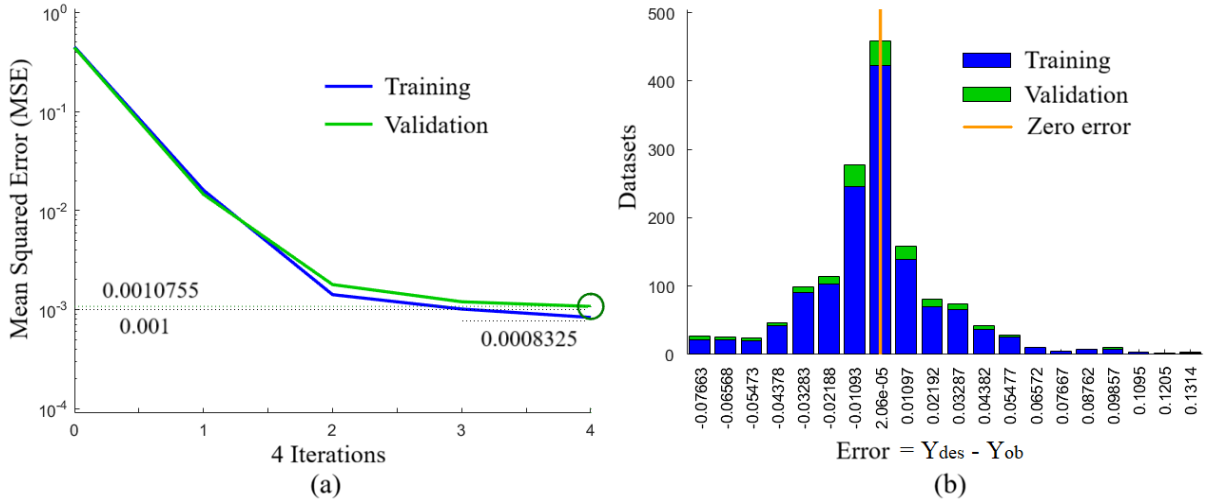
Figure 3b presents the histogram of the absolute errors ($|Y_{\text{ob}} - Y_{\text{des}}|$) for both the training and validation datasets. It can be observed that most errors are concentrated near zero, indicating the high accuracy of the proposed ANN model during both phases.

Furthermore, the total processing time was approximately 3 s, highlighting the computational efficiency of the proposed methodology. These results demonstrate the model's ability to rapidly learn and accurately generalize the underlying patterns contained in the dataset.

The obtained results also reveal high correlation coefficient (R) values, reaching 0.99567 for the training dataset and 0.99502 for the validation dataset. Such values indicate a very strong agreement between the ANN-predicted outputs (Y_{ob}) and the target values (Y_{des}), confirming that the network successfully captured the nonlinear

relationships present in the data while maintaining excellent generalization capability when applied to previously unseen samples.

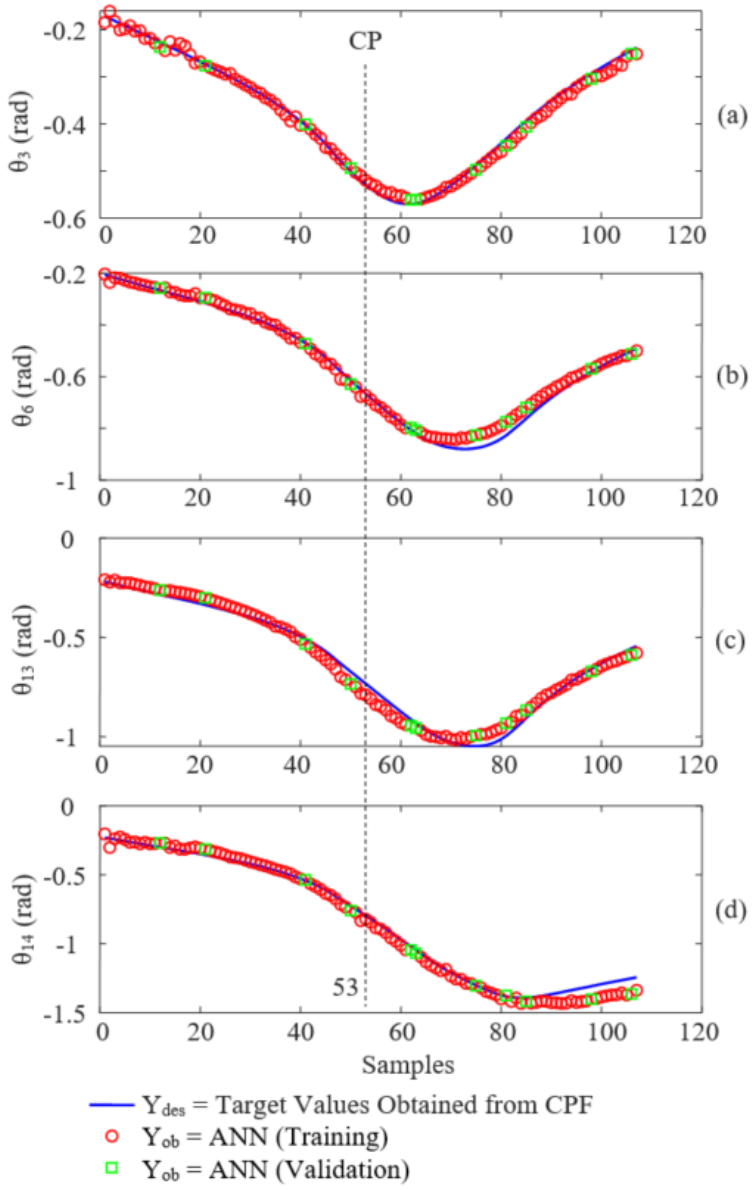
Figure 3 – ANN performance for the IEEE 14-Bus System: (**a**) MSE curves for the training and validation phases; (**b**) histogram of the training and validation errors relative to zero error.



Source: Elaborated by the author

Figure 4a–d compares the target values (Y_{des}) of the nodal voltage angles (θ), obtained from the CPF method, with the values estimated by the ANN (Y_{ob}) during the training and validation phases for buses 3, 6, 13, and the critical bus 14, which were selected for illustrative purposes. The results demonstrate the ANN's ability to accurately reproduce the behavior of the voltage angles across the entire range of operating conditions, including regions near the CP or Maximum Loading Point.

Figure 4 – Comparison between the target (Y_{des}) and estimated (Y_{ob}) values of the nodal voltage angle θ for each sample: (**a**) bus 3, (**b**) bus 6, (**c**) bus 13, and (**d**) bus 14 (critical bus).



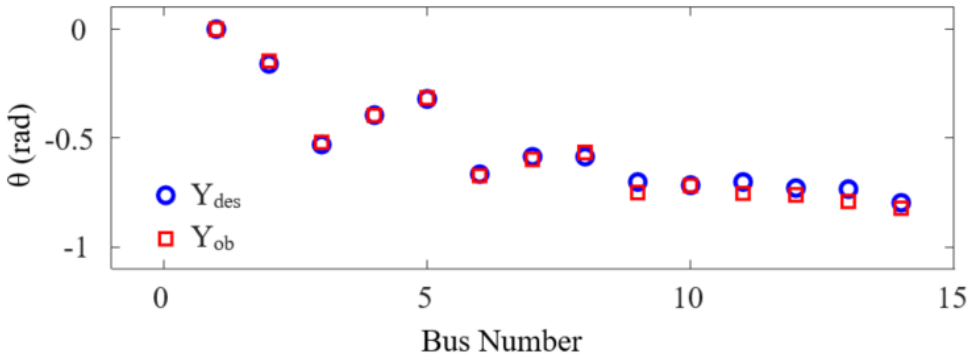
Source: Elaborated by the author

For ANN development, 90% of the available samples (96 samples) were randomly selected for training, while the remaining 10% (11 samples) were reserved for model validation. The validation samples, represented by the green square markers in Figure 4, were not used during the training process. This procedure enables a rigorous assessment of the network's generalization capability, demonstrating its ability to provide accurate estimates for previously unseen operating conditions.

Figure 5 presents a comparison between the target values (Y_{des}, blue circles) and the values estimated by the ANN (Y_{ob}, red squares) at the CP for each bus of the IEEE 14-Bus System. The horizontal axis represents the system buses (1–14), while the vertical axis shows the corresponding nodal voltage angles (θ) expressed in radians.

It can be observed that the ANN-predicted values closely match the target values for all buses, demonstrating the high accuracy of the proposed model in estimating nodal voltage angles under critical operating conditions. The excellent agreement between Y_{des} and Y_{ob} confirms the ability of the ANN to accurately capture the system behavior near the voltage stability limit.

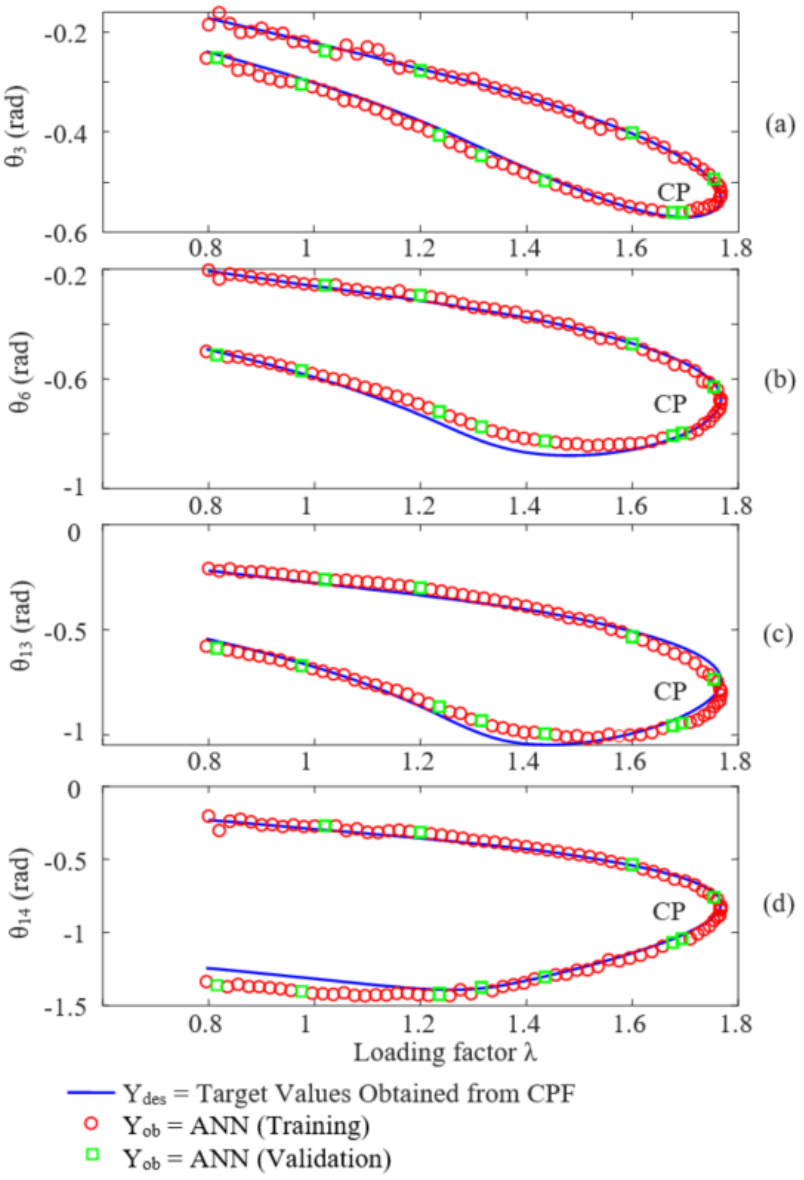
Figure 5 – Comparison between the target (Y_{des}) and ANN-estimated (Y_{ob}) nodal voltage angles at the CP of the IEEE 14-Bus System.



Source: Elaborated by the author

Figure 6a–d presents the P–θ curves for the selected buses, including the critical bus. These curves illustrate the relationship between the loading factor (λ), which represents the system real power loading level, and the nodal voltage angles (θ), providing a clear visualization of the voltage angle behavior throughout the loading process. The curves also enable the identification of the loading margin up to the CP, which corresponds to the voltage stability limit of the system.

Figure 6 – Nodal voltage angle values (θ) obtained from the CPF method (Y_{des}) and estimated by the ANN (Y_{ob}) as a function of the loading factor (λ), forming the P–θ curves: (**a**) bus 3, (**b**) bus 6, (**c**) bus 13, and (**d**) bus 14 (critical bus).



Source: Elaborated by the author

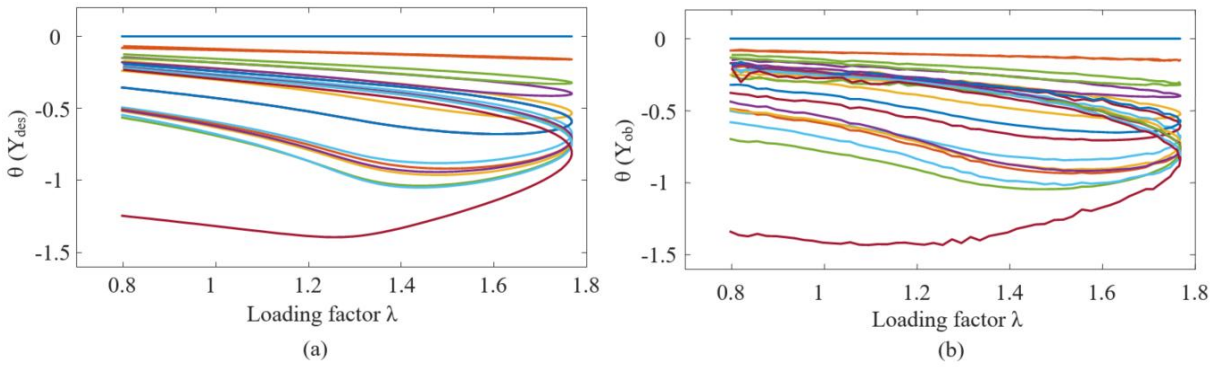
A strong agreement can be observed between the target values (Y_{des}), obtained from the CPF method, and the values estimated by the ANN (Y_{ob}) over the entire loading range. Training samples are represented by blue markers, whereas validation samples are represented by green markers. It is important to note that the validation samples were not included in the ANN training process; nevertheless, the estimated values

remained very close to the target values. These results demonstrate the excellent generalization capability of the proposed ANN and confirm its ability to accurately capture the nonlinear behavior of nodal voltage angles under different loading conditions, including operating points close to the voltage stability limit.

Figure 7 presents the P–θ curves, relating the loading factor (λ) to the nodal voltage angles (θ), for all buses of the IEEE 14-Bus System. Therefore, these curves provide a comprehensive representation of the system behavior under varying loading conditions, allowing the visualization of voltage angle evolution from the base operating point up to the CP.

Figure 7a shows the target P–θ curves (Y_{des}) obtained through the parameterized CPF method, whereas Figure 7b presents the corresponding curves estimated by the ANN (Y_{ob}). The comparison between the two sets of curves reveals a high degree of agreement, demonstrating the ANN's ability to accurately reproduce the behavior of nodal voltage angles throughout the entire loading range. These results further confirm the effectiveness of the proposed model in capturing the nonlinear characteristics of the power system and accurately representing its behavior near the voltage stability limit.

Figure 7 – P–θ curves of the IEEE 14-Bus System: (**a**) target values (Y_{des}) obtained from the CPF method; (**b**) ANN-estimated values (Y_{ob}).



Source: Elaborated by the author

2.4.2 IEEE 30-Bus System

Similar results were obtained for the IEEE 30-Bus System. A total of 93 samples were used, of which 84 were randomly selected for ANN training and the remaining 9

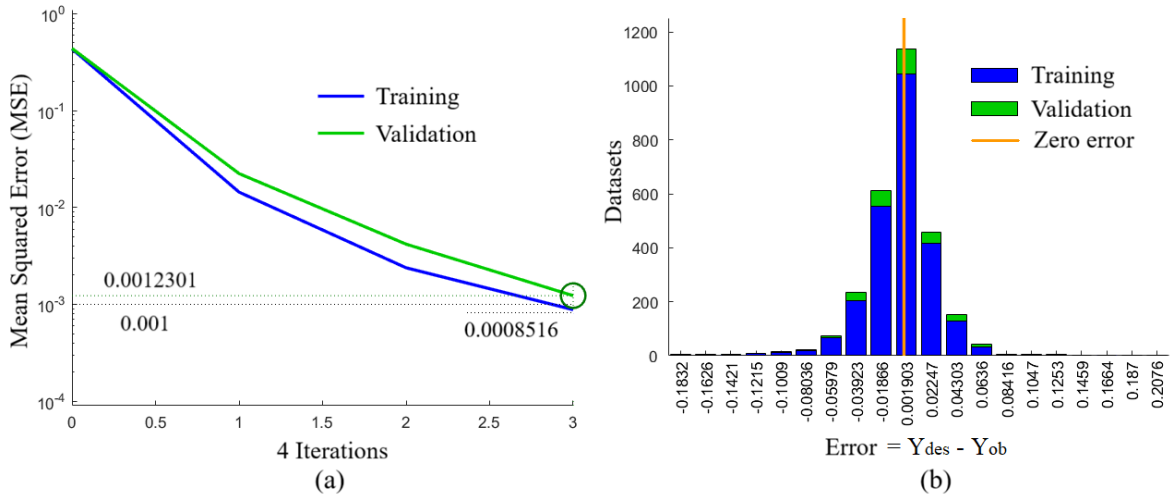
samples were reserved for model validation. Figure 8a presents the training and validation performance curves in terms of the MSE. It can be observed that the network converged rapidly, reaching the predefined stopping criterion (MSE ≤ 0.001) after only three iterations and approximately 3 s of computational time. The final MSE values were 0.0008516 for the training set and 0.0012301 for the validation set, indicating a high level of accuracy and good generalization capability.

Figure 8b shows the histogram of the prediction errors ($Y_{des} - Y_{ob}$) for both the training and validation datasets. Most of the errors are concentrated around zero, demonstrating that the estimated nodal voltage angles are in close agreement with the target values obtained from the CPF method. Furthermore, the error distributions for the training and validation sets exhibit similar behavior, suggesting that the ANN successfully learned the underlying nonlinear relationships without evidence of overfitting.

The correlation coefficients obtained were R = 0.98971 for the training phase and R = 0.98856 for the validation phase. These values indicate an excellent agreement between the target outputs (Y_{des}) and the ANN predictions (Y_{ob}), confirming the effectiveness of the proposed model for estimating nodal voltage angles in the IEEE 30-Bus System.

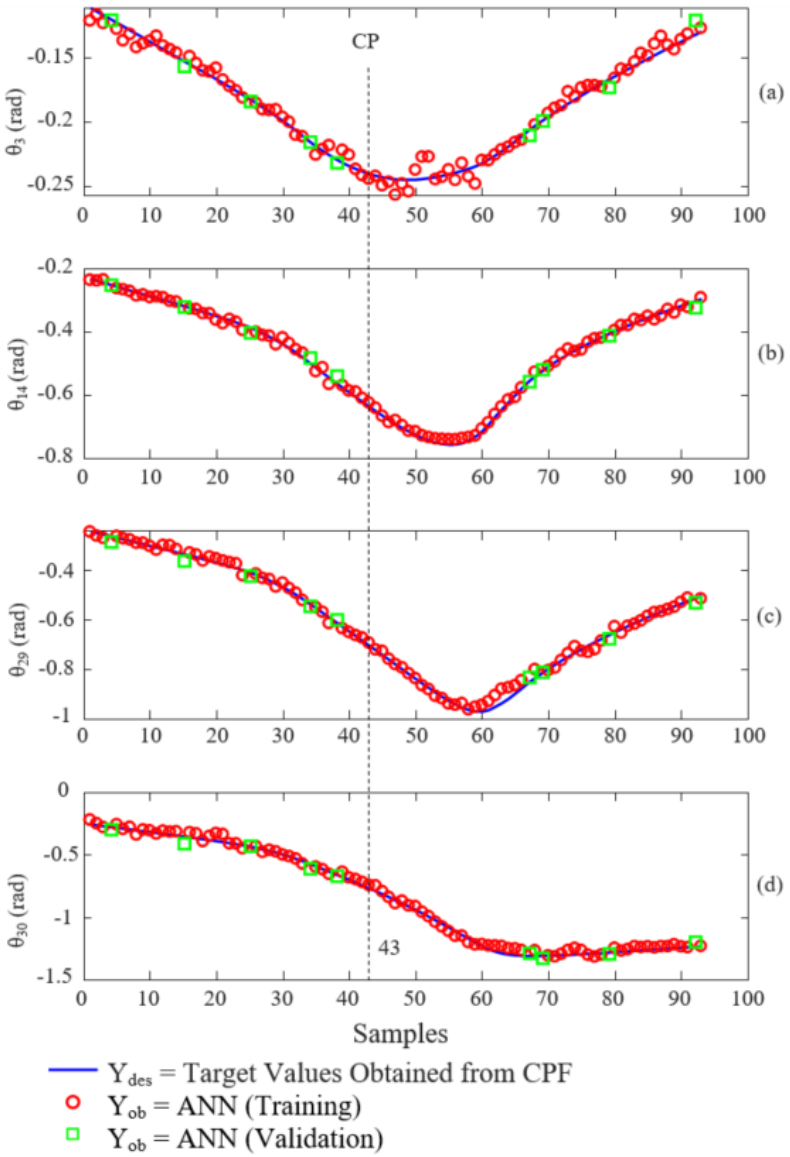
Figure 9 presents the nodal voltage angles (θ) for a set of randomly selected buses. Both the target values (Y_{des}), obtained from the CPF method, and the values estimated by the ANN (Y_{ob}) during the training and validation stages are shown. Figure 9a–d correspond to buses 3, 14, 29, and the critical bus 30, respectively. The CP, corresponding to the maximum loading condition of the system, occurs at sample 43. It can be observed that the ANN predictions closely follow the target values over the entire loading range, including the vicinity of the CP, demonstrating the ability of the proposed model to accurately reproduce the nonlinear behavior of the nodal voltage angles.

Figure 8 – ANN performance for the IEEE 30-Bus System: (**a**) MSE curves for the training and validation phases; (**b**) histogram of the training and validation errors relative to zero error.



Source: Elaborated by the author

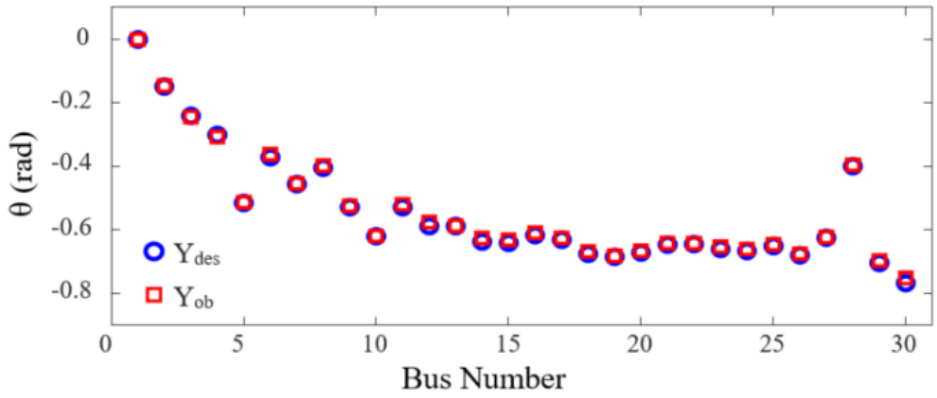
Figure 9 – Comparison between the target (Y_{des}) and ANN-estimated (Y_{ob}) nodal voltage angles (θ) for each sample: (**a**) bus 3, (**b**) bus 14, (**c**) bus 29, and (**d**) bus 30.



Source: Elaborated by the author

Figure 10 compares the target values (Y_{des}), represented by blue circles, with the ANN estimates (Y_{ob}), represented by red squares, at the CP for all buses of the IEEE 30-Bus System. The horizontal axis identifies the system buses (1–30), while the vertical axis represents the nodal voltage angles in radians. A strong agreement between the target and estimated values can be observed for all buses, confirming the high accuracy of the ANN in reproducing the system operating condition at the voltage stability limit.

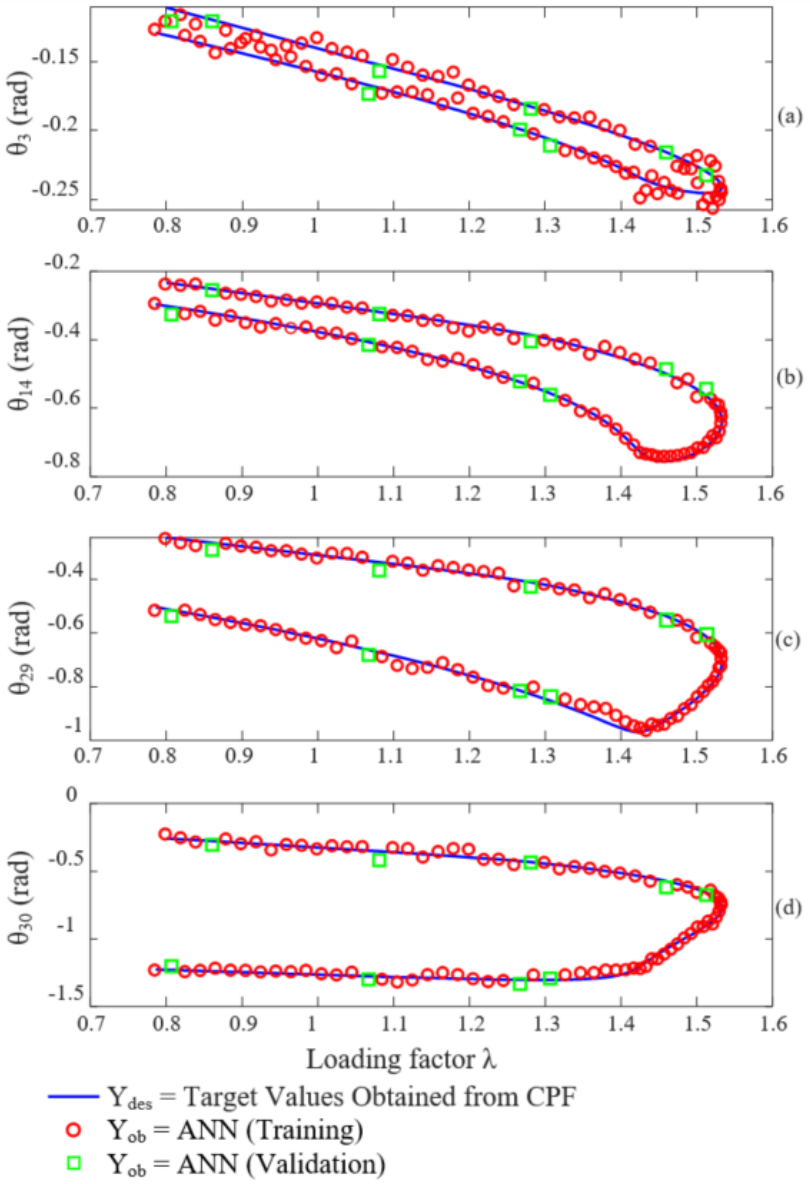
Figure 10 – Comparison between the target (Y_{des}) and ANN-estimated (Y_{ob}) nodal voltage angles (θ) at the CP of the IEEE 30-Bus System.



Source: Elaborated by the author

Figure 11 illustrates the P–θ curves obtained for buses 3, 14, 29, and the critical bus 30, as shown in Figure 11a–d. The nodal voltage angles obtained from the CPF method (blue line) are compared with the ANN predictions for the training samples (red circles) and validation samples (green squares) over the entire loading factor range (λ). The curves exhibit an almost perfect overlap, including in the vicinity of the CP (λ = 1.5335), indicating that the ANN accurately reproduces the P–θ trajectory and maintains excellent generalization capability, even under highly stressed operating conditions near voltage collapse.

Figure 11 – Comparison between the target (Y_{des}) and ANN-estimated (Y_{ob}) nodal voltage angles (θ) as a function of the loading factor (λ) (P–θ curves): (**a**) bus 3, (**b**) bus 14, (**c**) bus 29, (**d**) bus 30.

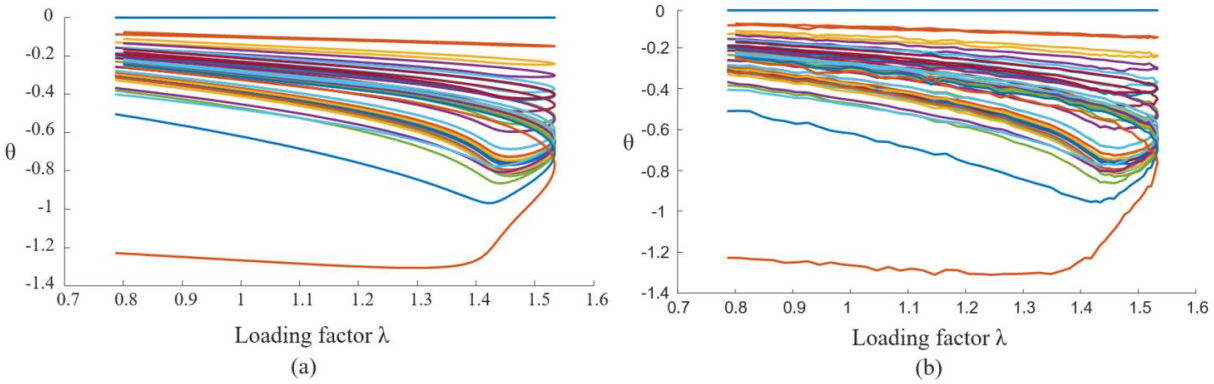


Source: Elaborated by the author

Finally, Figure 12 presents the complete set of P–θ curves for all buses of the IEEE 30-Bus System, relating the loading factor (λ) to the nodal voltage angles (θ). These results provide a comprehensive representation of the system behavior under increasing loading conditions and further demonstrate the capability of the proposed

ANN model to accurately estimate nodal voltage angles throughout the entire operating range.

Figure 12 – P–θ curves of the IEEE 30-Bus System: (**a**) target output (Y_{des}) obtained from the CPF method and (**b**) ANN-estimated output (Y_{ob}).



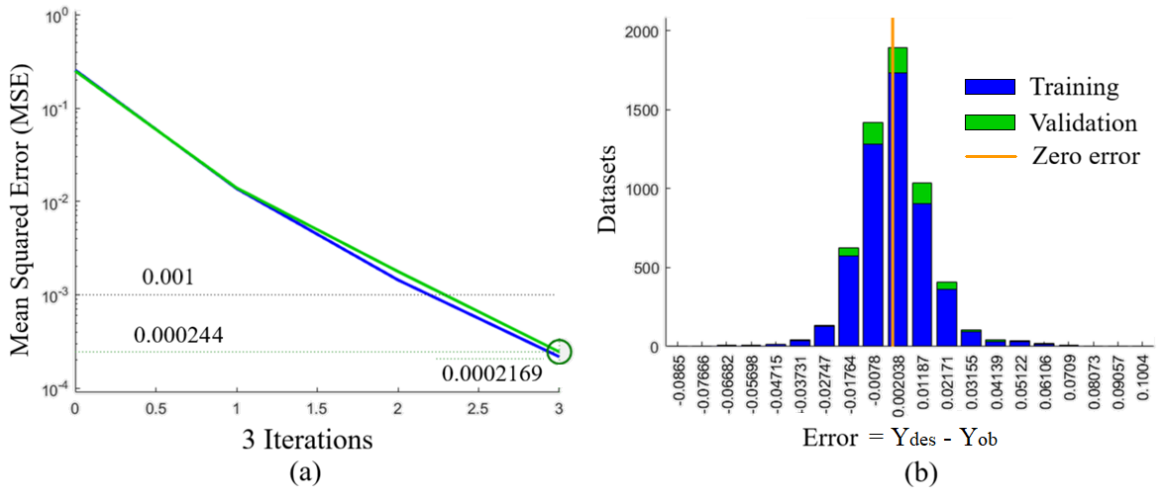
Source: Elaborated by the author

2.4.3 IEEE 57-Bus System

The dataset consisted of 102 samples, randomly divided into 92 samples used for ANN training and 10 samples reserved exclusively for model validation. Figure 13a presents the training and validation performance of the artificial neural network in terms of MSE over the training epochs. Both curves exhibit a similar decreasing trend, indicating a consistent learning process without evidence of overfitting. The training process required approximately 3 s of computational time, demonstrating the efficiency of the proposed model. The best validation performance was achieved at epoch 3, with an MSE of 2.44×10^{-4}, demonstrating the network's ability to accurately approximate the target values. The close agreement between the training and validation curves suggests good generalization capability and adequate model convergence.

Figure 13b shows the error histogram obtained for the training and validation datasets. Most prediction errors are concentrated around zero, indicating that the network outputs closely match the target values. The approximately symmetric distribution and the absence of significant outliers suggest that the prediction errors are small and randomly distributed. These results confirm the robustness of the trained model and reinforce its suitability for the proposed estimation task.

Figure 13 – Performance evaluation of the proposed ANN: (**a**) training and validation MSE; (**b**) error histogram.



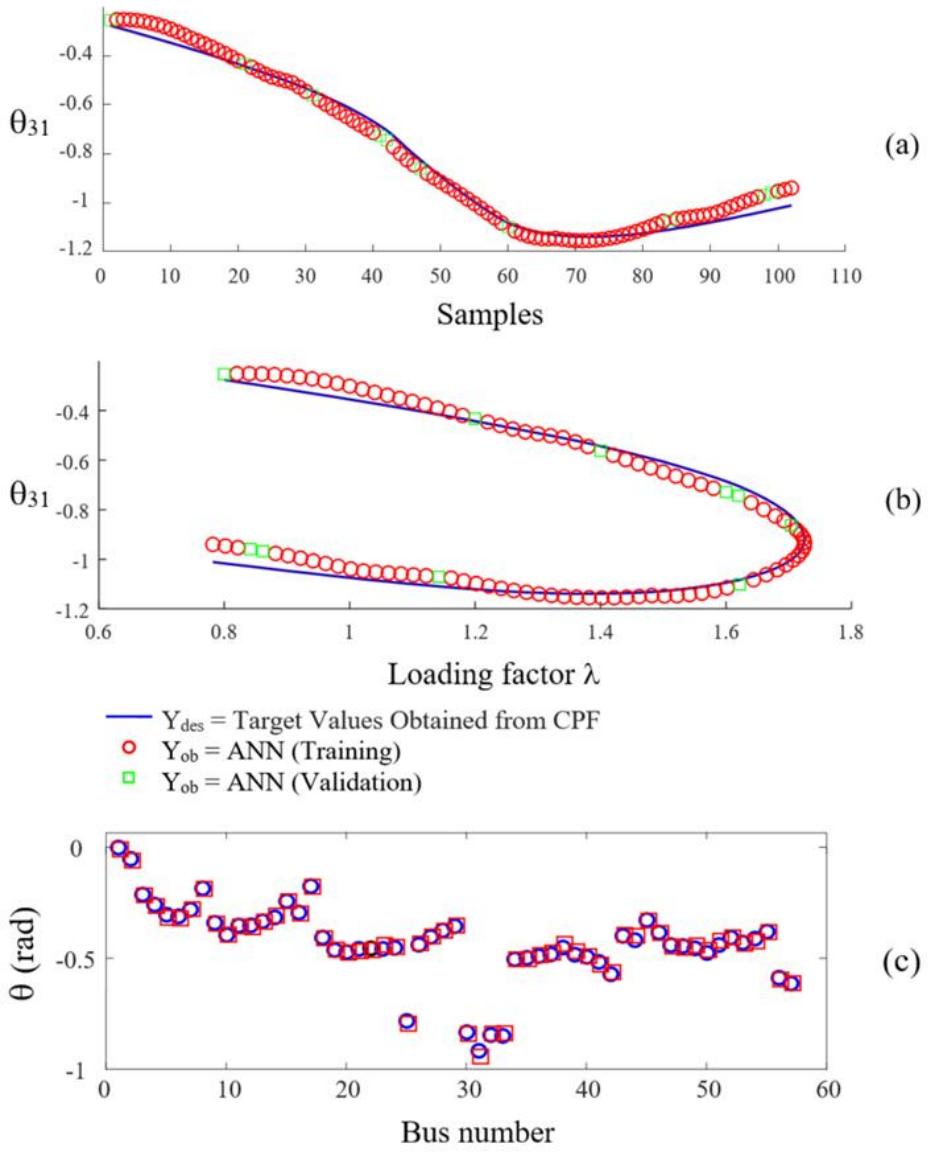
Source: Elaborated by the author

Figure 14a presents the comparison between the ANN outputs and the target values obtained from the CPF for the critical bus angle (θ_{31}) as a function of the 102 samples considered in the study. The blue line represents the target values, while the red circles and green squares correspond to the ANN estimates for the training and validation datasets, respectively. The close overlap between the estimated and target values demonstrates the high accuracy of the proposed ANN in predicting the nodal voltage angle at the critical bus. Similar results were obtained for the remaining buses. Figure 15a,b present the corresponding P-θ curves, comparing the target values obtained from CPF and the estimates provided by the ANN for all buses of the test system. The strong agreement between both sets of curves further confirms the ability of the proposed ANN to accurately capture the nonlinear relationship between the loading factor and the nodal voltage angles over the entire operating range.

Figure 14b illustrates the P-θ curve associated with the critical bus (θ_{31}). The results show that the ANN accurately reproduces the nonlinear relationship between the loading factor λ and the corresponding voltage angle, closely matching the CPF solutions throughout the entire operating range, including the vicinity of the maximum loading condition.

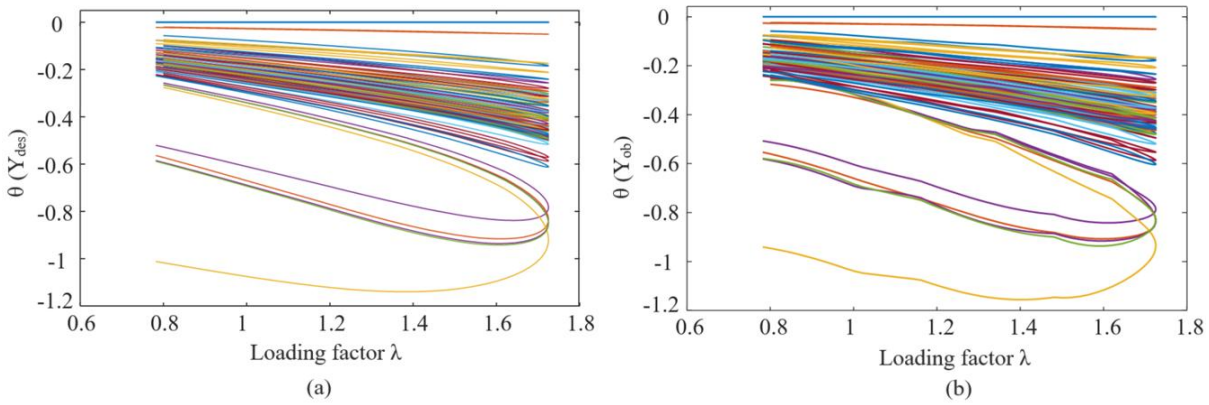
Figure 14c compares the target and ANN-estimated voltage angles for all 57 buses of the test system. It can be observed that the ANN predictions closely follow the reference values obtained from CPF for every bus, indicating excellent generalization capability. Furthermore, the lowest voltage angle magnitude occurs at bus 31, confirming its identification as the critical bus of the system and demonstrating the ability of the proposed ANN to accurately estimate the most critical operating conditions.

Figure 14 – Comparison between CPF and ANN results for nodal voltage angle estimation: (**a**) critical bus angle (θ_{31}); (**b**) P-θ curve of the critical bus; (**c**) voltage angles of all buses at the maximum loading (critical) point of the system.



Source: Elaborated by the author

Figure 15 – P-θ curves for all buses of the test system: (**a**) target P-θ curves obtained from CPF, (**b**) P-θ curves estimated by the proposed ANN.



Source: Elaborated by the author

2.4.4 Sensitivity Analysis Results for The Input Variables

When the Garson algorithm was applied to the input variables λ, P_g^{slack}, Q_g^{slack}, $P_{g,2}$, $P_{g,3}$, $P_{g,6}$ and $P_{g,8}$ for the IEEE 14-bus system, discrepant results were observed. The analysis revealed that the last input variable ($P_{g,8}$) exhibited the highest contribution to the estimation of the nodal voltage angles (θ), accounting for 100% of the influence on the network output, as illustrated in Figure 16a. In other words, the ANN indicated that $P_{g,8}$ was virtually the sole variable responsible for estimating the nodal voltage angles. Such a result is inappropriate for CPF studies, as it neglects the effective contribution of the remaining variables that characterize the operating condition of the electrical power system.

To investigate this behavior, a detailed analysis of the input data used during ANN training was performed. It was found that the last input variable ($P_{g,8}$) assumed numerical values very close to zero (10^{-15}), as shown in Table 1. This characteristic affected the magnitude of the synaptic weights adjusted during training and directly influenced the application of the Garson algorithm for determining input variable relevance.

To overcome this limitation, the variable $P_{g,8}$ was normalized according to Equation (6). Table 2 presents the input variables after the normalization procedure. Subsequently, the ANN was trained under two different conditions: using the original da-

taset and using the normalized dataset. In both cases, very similar results were obtained for the estimation of the nodal voltage angles, demonstrating that the ANN performance was not adversely affected by the normalization process.

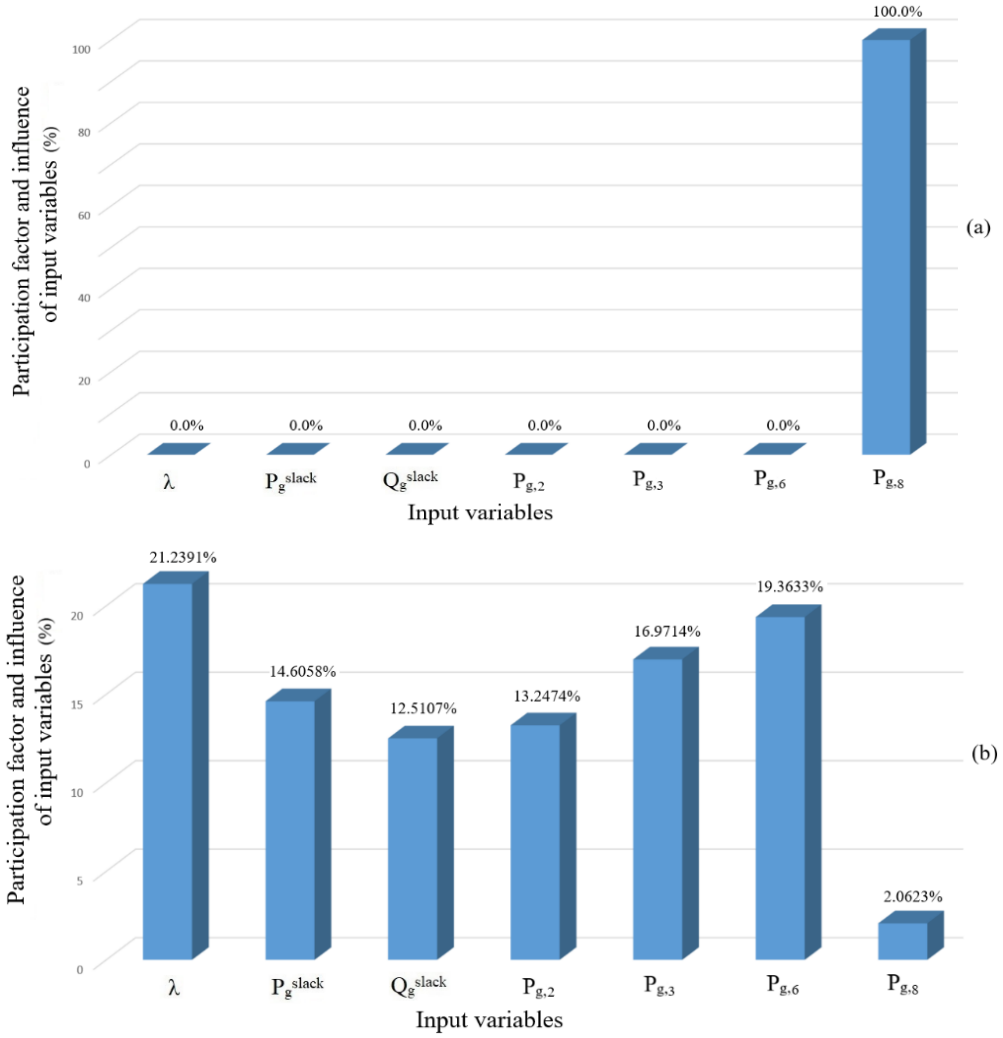
$$R_{7,\text{norm}}(i) = \frac{R_7(i)}{\max(|R_7|)} \tag{6}$$

The normalization procedure was applied only to the input variables exhibiting extremely small numerical magnitudes. Specifically, the affected input variables were rescaled before retraining the ANN, and the resulting synaptic weights were subsequently used in the sensitivity analysis. This procedure was not intended to improve the predictive performance of the ANN, but rather to avoid numerical distortions in the Garson and Olden weight-based sensitivity indices.

The normalization rescales the importance indices by the maximum absolute value, resulting in values within the interval [−1, 1] while preserving both the relative importance ranking and the sign of each variable. Its purpose is to reduce the influence of large differences in synaptic weight magnitudes by providing a common scale for comparison, thereby allowing the Garson and Olden methods to produce a more balanced and physically interpretable representation of the relative contribution of each input variable. From a physical perspective, the normalized importance index expresses the contribution of each input variable relative to the most influential variable, whose normalized importance is equal to ±1, reflecting the influence of each input on the network output rather than the numerical scale of the corresponding synaptic weights.

Furthermore, the MSE values obtained during the training and validation stages remained close to those obtained with the original dataset, indicating that the ANN maintained its generalization capability. Therefore, although the normalization procedure did not significantly modify the quality of the network predictions, it proved essential for obtaining a more meaningful and physically coherent interpretation of the results provided by the Garson algorithm.

Figure 16 – Percentage contribution of the input variables to the ANN output, as determined by the Garson sensitivity analysis: (**a**) before normalization of $P_{g,8}$; (**b**) after normalization of $P_{g,8}$.



Source: Elaborated by the author

Table 1. First 10 samples of the input variables used for ANN training before normalization of $P_{g,8}$.

	First 10 Samples									
	S_1	S_2	S_3	S_4	S_5	S_6	S_7	S_8	S_9	S_{10}
Input data	$R_1 = \lambda$	0.8000	0.8200	0.8400	0.8600	0.8800	0.9000	0.9200	0.9400	0.9600	0.9800
	$R_2 = P_g^{slack}$	1.8373	1.8854	1.9336	1.9820	2.0305	2.0791	2.1279	2.1768	2.2259	2.2751
	$R_3 = Q_g^{slack}$	−0.1550	−0.1601	−0.1651	−0.1699	−0.1746	−0.1791	−0.1835	−0.1877	−0.1918	−0.1957
	$R_4 = P_{g,2}$	0.1464	0.1501	0.1537	0.1574	0.1610	0.1647	0.1684	0.1720	0.1757	0.1793
	$R_5 = P_{g,3}$	−0.7536	−0.7724	−0.7913	−0.8101	−0.8290	−0.8478	−0.8666	−0.8855	−0.9043	−0.9232
	$R_6 = P_{g,6}$	−0.0896	−0.0918	−0.0941	−0.0963	−0.0986	−0.1008	−0.1030	−0.1053	−0.1075	−0.1098
	$R_7 = P_{g,8}$	* 0.2220	* −0.6453	* −0.0833	* 0.2082	* −0.0347	* −0.2082	* −0.0694	* −0.1735	* −0.0278	* −0.0763

* $\times 10^{-15}$

Source: Elaborated by the author

Table 2. First 10 samples of the input variables used for ANN training after normalization of $P_{g,8}$.

	First 10 Samples with Normalization									
	S_1	S_2	S_3	S_4	S_5	S_6	S_7	S_8	S_9	S_{10}
Input data	$R_1 = \lambda$	0.8000	0.8200	0.8400	0.8600	0.8800	0.9000	0.9200	0.9400	0.9600	0.9800
	$R_2 = P_g^{slack}$	1.8373	1.8854	1.9336	1.9820	2.0305	2.0791	2.1279	2.1768	2.2259	2.2751
	$R_3 = Q_g^{slack}$	−0.1550	−0.1601	−0.1651	−0.1699	−0.1746	−0.1791	−0.1835	−0.1877	−0.1918	−0.1957
	$R_4 = P_{g,2}$	0.1464	0.1501	0.1537	0.1574	0.1610	0.1647	0.1684	0.1720	0.1757	0.1793
	$R_5 = P_{g,3}$	−0.7536	−0.7724	−0.7913	−0.8101	−0.8290	−0.8478	−0.8666	−0.8855	−0.9043	−0.9232
	$R_6 = P_{g,6}$	−0.0896	−0.0918	−0.0941	−0.0963	−0.0986	−0.1008	−0.1030	−0.1053	−0.1075	−0.1098
	$R_7 = P_{g,8}$	0.4571	−1.3286	−0.1714	0.4286	−0.0714	−0.4286	−0.1429	−0.3571	−0.0571	−0.1571

Source: Elaborated by the author

Table 3. Synaptic weights of the connections between the input and hidden layers (14 × 7 weight matrix) before normalization of input variable R_7 ($P_{g,8}$).

	Neurons in the Input Layer						
Neurons in the hidden layer	R_1	R_2	R_3	R_4	R_5	R_6	R_7
m_1	−0.9399	−0.1434	−0.3361	1.3251	−0.759	0.798	* −0.7232
m_2	−0.9608	−0.5948	0.728	0.5886	0.8901	−0.5701	* −0.4440
m_3	−0.1664	−0.3494	0.9395	−1.126	−0.6434	0.3243	* −1.6970
m_4	0.2143	0.3025	0.3102	−0.8799	−0.8419	−0.8433	* 1.3440
m_5	0.4601	−0.8578	0.5875	0.0448	−0.599	−0.4291	* −0.2567
m_6	0.2948	−0.0799	0.7322	−0.0608	0.6026	0.7116	* −1.7435
m_7	−0.8227	−0.2594	0.4863	−0.7555	0.2389	−1.0183	* 0.7309
m_8	−0.3428	0.7508	0.7553	−0.0015	0.6847	0.8475	* 0.0331
m_9	0.3257	0.9717	0.891	−1.1874	0.4802	−0.3875	* −0.7229
m_{10}	0.716	0.5412	−0.7023	0.7507	0.9756	0.549	* 0.9714
m_{11}	−0.8683	−0.4937	−0.2279	0.6231	−0.7038	−0.6636	* 1.0831
m_{12}	0.1055	−0.4369	0.6634	−1.5269	−0.4255	0.6631	* −1.1297
m_{13}	0.8831	−0.2712	−0.6717	0.1913	−0.6033	0.4231	* 0.1960
m_{14}	0.4259	−0.0489	−1.3345	0.6374	−0.2324	0.9438	* −0.2285

* ×1015

Source: Elaborated by the author

Table 4. Synaptic weights of the connections between the input and hidden layers (14 × 7 weight matrix) after normalization of input variable R_7 ($P_{g,8}$).

	Neurons in the Input Layer						
Neurons in the hidden layer	R_1	R_2	R_3	R_4	R_5	R_6	R_7
m_1	−0.4445	0.8273	−0.0573	0.5491	−0.5884	−0.8051	−0.9429
m_2	−0.9743	0.9498	0.6986	0.6972	0.7046	0.6618	0.1534
m_3	0.1589	−0.0683	0.1781	−0.9934	0.1580	−1.1241	−1.0736
m_4	−0.2461	−0.7264	0.6062	0.5026	−0.9468	−0.3381	−0.6302
m_5	0.3464	−1.0797	0.9552	0.2885	−0.7067	−0.9449	0.1043
m_6	0.6352	0.1834	0.6705	−1.2512	0.5123	0.1162	−0.0908
m_7	0.3779	1.1036	−0.7082	0.2162	0.1203	1.0537	−0.0268
m_8	−1.3456	−0.2380	0.5405	−0.2282	−1.2287	0.0174	0.2096
m_9	−1.0578	−0.9105	−0.4081	1.0473	−0.4084	−0.1982	0.0377
m_{10}	−0.2848	−0.6011	0.4141	−1.2874	0.0549	0.1716	−0.1619
m_{11}	0.2030	−1.2549	0.3970	−0.0505	−1.2308	0.4583	0.4327
m_{12}	0.3375	−0.6727	−0.5655	−0.4451	0.9988	0.7967	−0.2767
m_{13}	−0.4454	−0.1559	−0.4790	−0.2380	−0.9144	0.6142	0.9593
m_{14}	0.9012	0.2118	−0.5370	0.7827	0.8537	0.9198	0.7528

Source: Elaborated by the author

The same issue observed with the Garson algorithm was also identified when applying the Olden method. When the original input variables were used, without normalization of variable R_7, the analysis indicated that R_7 accounted for virtually 100% of the influence on the network output, preventing a meaningful interpretation of the relative contributions of the remaining input variables.

After normalizing R_7, this limitation was successfully overcome, resulting in a more balanced distribution of synaptic weights and enabling a reliable application of the Olden algorithm. Consequently, the influence of all input variables could be properly assessed, providing a more realistic interpretation of their contributions to the estimation of the nodal voltage angles (θ). The results obtained before and after the normalization procedure are presented in Table 5.

Table 5. Olden sensitivity analysis results before and after normalization of the input variable R_7 ($P_{g,8}$) for the IEEE 14-Bus System.

	$R_1 = \lambda$	$R_2 = P_g^{slack}$	$R_3 = Q_g^{slack}$	$R_4 = P_{g,2}$	$R_5 = P_{g,3}$	$R_6 = P_{g,6}$	$R_7 = P_{g,8}$
R_7	0.0	0.0	0.0	0.0	0.0	0.0	−100
$R_7/\max(R_7)$	29.56	−26.67	7.10	−7.02	11.13	10.40	−8.13

Source: Elaborated by the author

The sensitivity analysis performed using the Olden method provided additional information regarding both the magnitude and direction of the influence of each input variable on the estimation of the nodal voltage angles (θ). Unlike the Garson method, which only quantifies the relative importance of the inputs, the Olden approach preserves the sign of the synaptic weights, allowing the identification of positive and negative effects on the network output.

The results indicated that the loading factor (λ) was the most influential variable, presenting the highest positive contribution (29.56), followed by the active power generation at the slack bus (P_g^{slack}), which exhibited the strongest negative contribution (−26.67). The variables $P_{g,3}$ (11.13) and $P_{g,6}$ (10.40) also showed significant positive influences, whereas $P_{g,2}$ (−7.02) and $P_{g,8}$ (−8.13) contributed negatively to the ANN output. These findings suggest that λ and P_g^{slack} are the dominant factors affecting the

estimation of nodal voltage angles, while the remaining variables exert secondary but still relevant contributions.

Overall, the Olden analysis corroborates the results obtained with the Garson method, identifying the loading factor (λ) as one of the most important variables in the ANN model. However, by preserving the sign of the contributions, the Olden method provides a more comprehensive interpretation of the relationships learned by the neural network.

The results obtained in this study are consistent with the findings reported by Goh (1995), Haykin (2009), and Gevrey et al. (2003), who emphasized the importance of input data normalization in ANN applications. Proper normalization improves numerical stability during training, prevents disproportionate synaptic weight magnitudes, and contributes to a more reliable interpretation of variable importance when applying weight-based sensitivity analysis methods such as those proposed by Garson and Olden.

Haykin (2009) highlighted that input normalization is often necessary to improve network training and avoid excessive weight adjustments caused by variables with significantly different numerical scales. Similarly, Goh (1995) emphasized that appropriate scaling of input variables is an essential step in ANN modeling because differences in variable magnitudes may affect both the learning process and the resulting synaptic weights. Furthermore, Gevrey et al. (2003) pointed out that weight-based sensitivity analysis methods can be strongly influenced by the magnitude of synaptic weights, potentially leading to misleading interpretations of variable importance. The normalization procedure adopted in this work successfully mitigated these effects, resulting in more balanced synaptic weights and a more physically meaningful sensitivity analysis.

Similar results were obtained for the IEEE 30-Bus System, further validating the findings and methodology proposed in this work. The main difference was that two of the eight input variables, namely $P_{g,11}$ and $P_{g,13}$ (corresponding to input variables R_7 and R_8), exhibited values very close to zero, also on the order of 10^{-15}. As observed in the IEEE 14-Bus System, this characteristic caused both the Garson and Olden methods to attribute nearly all the variable importance to these inputs, leading to distorted sensitivity analysis results.

To address this issue, the input variables R_7 ($P_{g,11}$) and R_8 ($P_{g,13}$) were normalized according to Equation (6). After the normalization procedure, it became possible

to obtain a more balanced and physically meaningful assessment of the contribution of each input variable to the estimation of the nodal voltage angles. The predictive performance of the ANN remained practically unchanged, indicating that the normalization process did not affect the quality of the estimates.

Table 6 presents the sensitivity analysis results obtained using the Garson and Olden methods before and after normalization of the input variables R_7 ($P_{g,11}$) and R_8 ($P_{g,13}$). Table 6 confirms that the same sensitivity analysis issue observed in the IEEE 14-Bus System was also present in the IEEE 30-Bus System. Before normalization, the Garson method attributed 53.88% and 46.12% of the total importance to variables R_7 ($P_{g,11}$) and R_8 ($P_{g,13}$), respectively, while all remaining input variables exhibited zero contribution, as illustrated in Figure 17a. Similarly, the Olden method indicated that these two variables dominated the sensitivity analysis, preventing a meaningful interpretation of the influence of the other inputs.

Table 6. Garson and Olden sensitivity analysis results before and after normalization of the input variable R_7 ($P_{g,11}$) and R_8 ($P_{g,13}$) for the IEEE 30-Bus System.

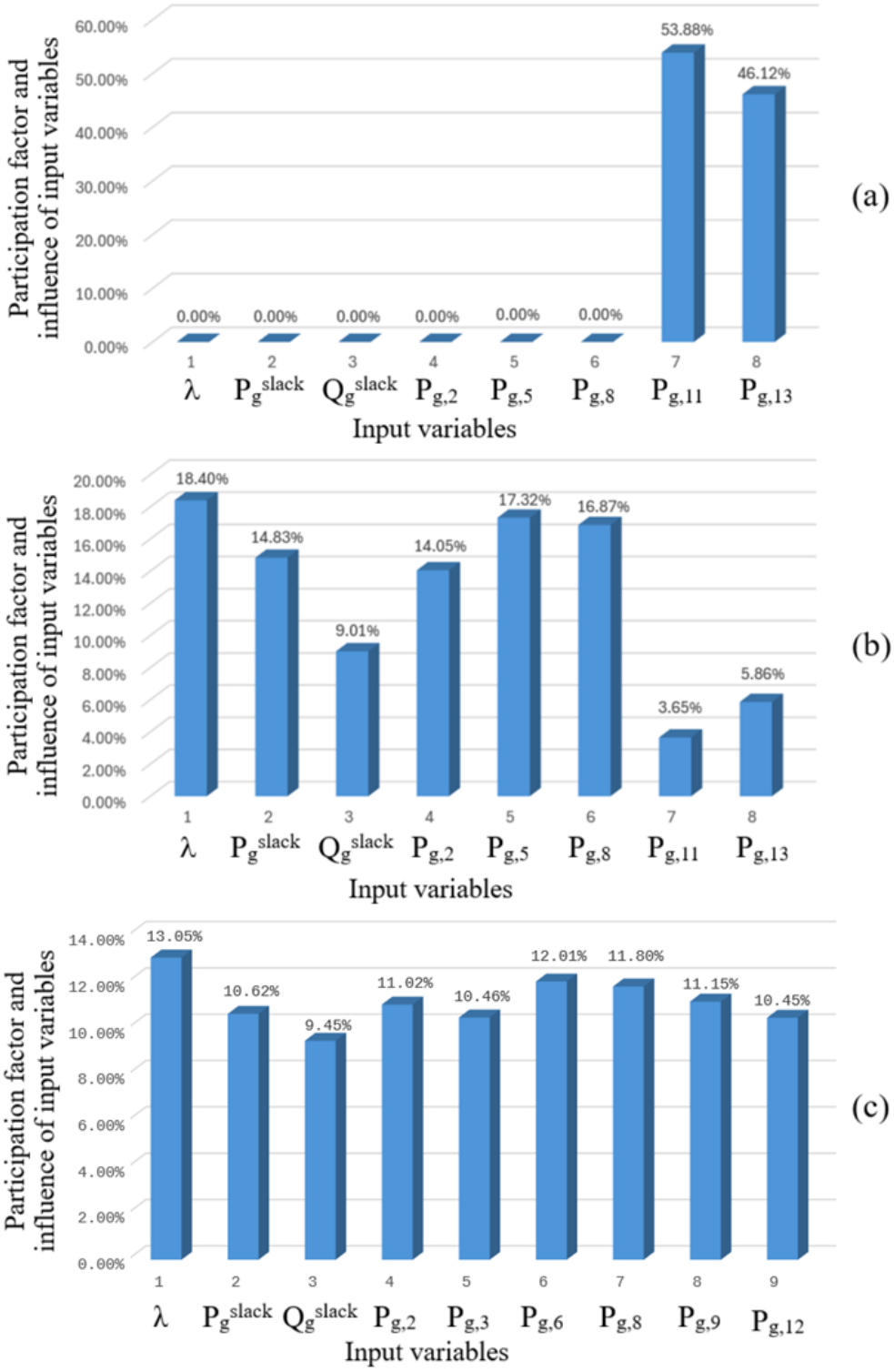
		$R_1 = \lambda$	$R_2 = P_g^{slack}$	$R_3 = Q_g^{slack}$	$R_4 = P_{g,2}$	$R_5 = P_{g,5}$	$R_6 = P_{g,8}$	$R_7 = P_{g,11}$	$R_8 = P_{g,13}$
Garson	$R_{7,8}$	0.0%	0.0%	0.0%	0.0%	0.0%	0.0%	53.88%	46.12%
	$R_{7,8}/\max(R_{7,8})$	18.40%	14.83%	9.01%	14.05%	17.32%	16.87%	3.65%	5.86%
Olden	$R_{7,8}$	0.0	0.0	0.0	0.0	0.0	0.0	−62.92	−37.08
	$R_{7,8}/\max(R_{7,8})$	−26.37	−19.57	−1.99	−12.31	−5.26	−22.49	−4.72	−7.30

Source: Elaborated by the author

After normalization of R_7 and R_8 according to Equation (6), both the Garson (Figure 17b) and Olden methods produced more balanced and physically consistent results. The loading factor (λ) and the real power generation variables became the most influential inputs, while the contributions of $P_{g,11}$ and $P_{g,13}$ were significantly reduced. These findings reinforce the importance of proper input normalization when applying weight-based sensitivity analysis methods, ensuring a more reliable interpretation of variable importance in ANN models.

For the IEEE 57-Bus System, no normalization procedure was required because none of the input variables exhibited values close to zero, as presented in Figure 17c. Consequently, no distortions associated with excessively large synaptic weights were observed, allowing the sensitivity analysis to be performed directly using the original dataset. Table 7 presents the variable importance results obtained using the Garson and Olden methods for the nine input variables considered in the ANN model.

Figure 17 – Relative importance of input variables obtained by the Garson method: (**a**) IEEE 30-bus system without input normalization (R_7 and R_8); (**b**) IEEE 30-bus system with normalized inputs (R_7 and R_8); (**c**) IEEE 57-bus system without input normalization.



Source: Elaborated by the author

Table 7 shows that the Garson and Olden methods produced balanced and physically meaningful sensitivity results for the IEEE 57-Bus System. The Garson method indicated that the loading factor (λ) was the most influential variable (13.05%), although the remaining inputs also presented significant contributions, demonstrating that the estimation of nodal voltage angles depends on multiple operating variables. The Olden method complemented this analysis by identifying both the magnitude and direction of the influence of each variable, highlighting λ and P_g^{slack} as the strongest negative contributors and $P_{g,8}$ and $P_{g,12}$ as the most influential positive contributors. These results confirm the robustness of the ANN model and the consistency of the proposed sensitivity analysis approach.

Table 7. Garson and Olden sensitivity analysis results for the IEEE 57-Bus System.

	$R_1 = \lambda$	$R_2 = P_g^{slack}$	$R_3 = Q_g^{slack}$	$R_4 = P_{g,2}$	$R_5 = P_{g,3}$	$R_6 = P_{g,6}$	$R_7 = P_{g,8}$	$R_8 = P_{g,9}$	$R_9 = P_{g,12}$
Garson	13.05%	10.62%	9.45%	11.02%	10.46%	12.01%	11.80%	11.15%	10.45%
Olden	−17.47	−15.75	−8.40	7.65	11.29	1.00	20.41	−0.60	17.43

Source: Elaborated by the author

2.4.5 Computational Time For Nodal Voltage Angle Estimation

A computational time analysis was performed using the validation samples (10% of the dataset not used during the ANN training phase) for each test system. These validation samples were processed using both the CPF method and the proposed ANN model to estimate the nodal voltage angles (θ). The simulations were carried out on a computer equipped with an Intel® Core™ i7-8750H CPU (2.20 GHz), 16 GB of RAM, and running a 64-bit Windows operating system. The models were implemented in MATLAB® version 2025b, and the computational times were obtained using CPU execution. It is important to emphasize that the computational time comparison was performed after the ANN training stage. Therefore, the reported ANN processing times correspond exclusively to the inference (validation) phase and do not include the network training time. Once trained, the ANN is capable of directly estimating the nodal voltage angles for different loading conditions without requiring additional power flow calculations. In contrast, the CPF method must repeatedly solve the power flow equations for each new operating condition in order to obtain updated nodal voltage angles. For a fair comparison, both approaches were evaluated using the same convergence tolerance of 10^{-3}.

Table 8 presents the CPU time required by each methodology for the estimation of nodal voltage angles in the validation phase. The results demonstrate that the ANN significantly reduces the computational effort when compared with CPF. For the IEEE 14-bus system, the average computational time reduction achieved by the ANN was 87.63%. Similar results were obtained for the IEEE 30-bus and IEEE 57-bus systems, with average time savings of 87.55% and 88.30%, respectively.

These results indicate that the proposed ANN model is capable of accurately estimating nodal voltage angles while requiring substantially less computational time than the CPF method. The average reduction of approximately 88% in processing time highlights the potential of ANN-based approaches for real-time applications and online security assessment in power systems, where fast computation is essential.

Table 8. CPU time for obtaining nodal voltage angles in the validation phase (validation samples).

System	CPU Time										
14-Bus	Validation samples	12	21	41	50	62	63	75	81	85	98	106
	CPF	0.0441	0.0549	0.0572	0.0540	0.0659	0.0587	0.0571	0.0569	0.0542	0.0344	0.0386
	ANN	0.0057	0.0058	0.0064	0.0058	0.0060	0.0062	0.0057	0.0066	0.0059	0.0062	0.0072
	Time saved (%)	87%	89%	89%	89%	91%	89%	90%	88%	89%	82%	81%
	Mean time saved (%)	87.63%										
30-Bus	Validation samples	4	15	25	34	38	67	69	79	92		
	CPF	0.0459	0.0509	0.0550	0.0627	0.0620	0.0625	0.0545	0.0523	0.0424		
	ANN	0.0072	0.0062	0.0064	0.0066	0.0063	0.0062	0.0063	0.0065	0.0070		
	Time saved (%)	84%	88%	88%	89%	90%	90%	88%	88%	83%		
	Mean time saved (%)	87.55%										
57-Bus	Validation samples	1	21	31	41	42	47	60	84	98	99	
	CPF	0.0488	0.0590	0.0630	0.0737	0.0750	0.0752	0.0788	0.0556	0.0482	0.0499	
	ANN	0.0074	0.0065	0.0069	0.0066	0.0062	0.0070	0.0064	0.0087	0.0068	0.0081	
	Time saved (%)	85%	89%	89%	91%	92%	91%	92%	84%	86%	84%	
	Mean time saved (%)	88.30%										

Source: Elaborated by the author

Additionally, the computational-time analysis was improved by performing multiple evaluations using all validation samples. The results are now presented as mean values ± standard deviation, providing information about the variability of the execution times. The revised results are summarized in Table 9. The variability of the computational times among the validation samples was also analyzed. The ANN exhibited a more stable execution time compared with CPF, with standard deviations below 0.001 s for all test systems, whereas CPF presented larger variations due to the iterative nature of the power flow solution.

Table 9 presents the statistical summary of the CPU time required by each methodology for estimating nodal voltage angles during the validation phase. The results are expressed as mean values ± standard deviation, calculated from all validation samples presented in Table 8. For the IEEE 14-bus system, the CPF method required 0.0525 ± 0.0100 s, whereas the ANN inference stage required only 0.0061 ± 0.0005 s, resulting in an average computational time reduction of 87.63%. Similar behavior was observed for the IEEE 30-bus and IEEE 57-bus systems.

Table 9. Comparison of computational time reduction obtained using ANN inference instead of CPF for nodal voltage angle estimation.

System	CPF Time (s) (Mean ± SD)	ANN Inference Time (s) (Mean ± SD)	Reduction (%)
IEEE 14-Bus	0.0525 ± 0.0100	0.0061 ± 0.0005	87.63
IEEE 30-Bus	0.0548 ± 0.0071	0.0066 ± 0.0003	87.55
IEEE 57-Bus	0.0626 ± 0.0115	0.0070 ± 0.0008	88.30

Source: Elaborated by the author

The low standard deviation observed for the ANN inference times confirms the computational stability of the proposed approach, while the higher variability observed for the CPF method is associated with the iterative nature of the power flow solution, whose computational effort depends on the operating condition.

2.4.6 Cross-Validation Analysis And Comparative Evaluation Of Ann, Multiple Linear Regression, And Tree Models

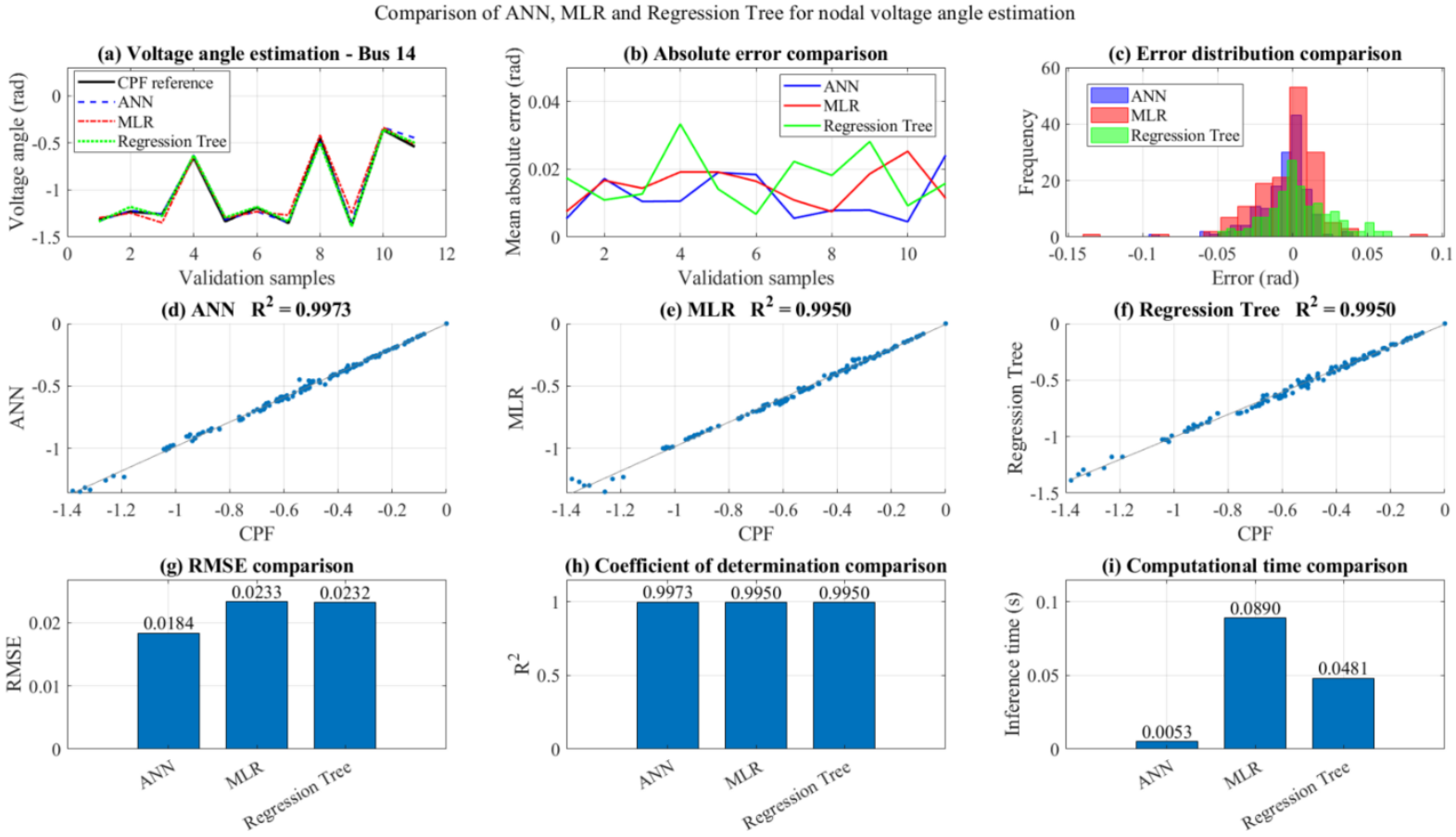
To further assess the robustness and generalization capability of the proposed ANN, a 10-fold cross-validation procedure was performed for the IEEE 14-, 30-, and 57-bus systems. Considering the average performance across the three benchmark systems, the proposed model achieved a training MSE of 3.11×10^{-5} and a validation MSE of 6.41×10^{-5}, corresponding to average RMSE values of 5.44×10^{-3} and 7.15×10^{-3}, respectively. The average MAE values were 3.61×10^{-3} during training and 4.47×10^{-3} during validation, while the average maximum absolute errors were 4.59×10^{-2} and 4.27×10^{-2}, respectively. In addition, the average correlation coefficient (R) reached 0.99971 during training and 0.99941 during validation, corresponding to average coefficients of determination (R^2) of 0.99943 and 0.99883. These results, together with the low variability observed among the folds, demonstrate that the proposed ANN provides stable and highly accurate predictions, confirming its robustness and excellent generalization capability across all IEEE benchmark systems.

Figures 18–20 compare the performance of the ANN, MLR, and Regression Tree models for nodal voltage angle estimation in the IEEE 14-, 30-, and 57-bus systems, respectively. Overall, the ANN consistently provided the best compromise between prediction accuracy and computational efficiency, yielding the lowest RMSE values for the IEEE 14- and 30-bus systems (Figures 18g and 19g), while maintaining the shortest inference time in all cases (Figures 18i–20i). Although the MLR achieved slightly better statistical indicators for the IEEE 57-bus system (Figure 20), the ANN exhibited more consistent performance across the three benchmark systems, accurately reproducing the CPF reference values with error distributions concentrated around zero (Figures 18c–20c). In contrast, the Regression Tree generally presented larger prediction errors and lower accuracy, particularly for the IEEE 57-bus system,

indicating greater difficulty in representing the nonlinear behavior of nodal voltage angles under different loading conditions.

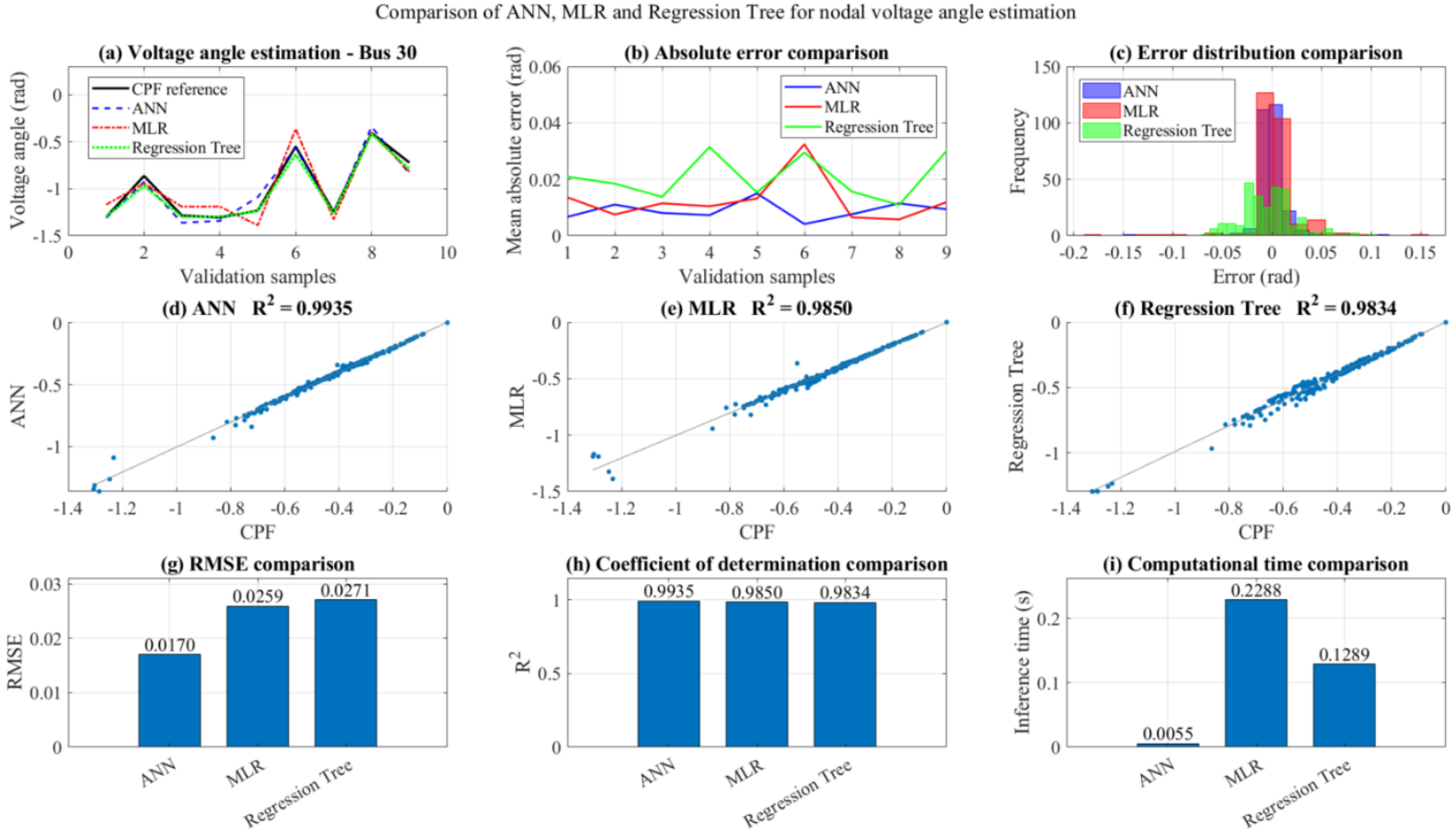
Although the proposed ANN demonstrated excellent predictive performance under the benchmark operating conditions considered in this study, practical electrical power systems are also influenced by factors that were beyond the scope of the present work, including network topology changes, transmission line outages, contingency events, renewable generation variability, load uncertainty, and measurement noise associated with Phasor Measurement Units (PMUs). These factors may affect the predictive performance of data-driven models and should therefore be considered when extending the proposed methodology to real-world applications. Nevertheless, the proposed framework is sufficiently flexible to incorporate these practical operating conditions by retraining the ANN using representative datasets that include such scenarios. Therefore, the present methodology constitutes a promising foundation for future applications involving online voltage stability assessment under realistic operating conditions.

Figure 18 – Comparative performance of ANN, MLR, and Regression Tree models for nodal voltage angle estimation at the critical bus (Bus 14) of the IEEE 14-bus system. Source: Elaborated by the author.



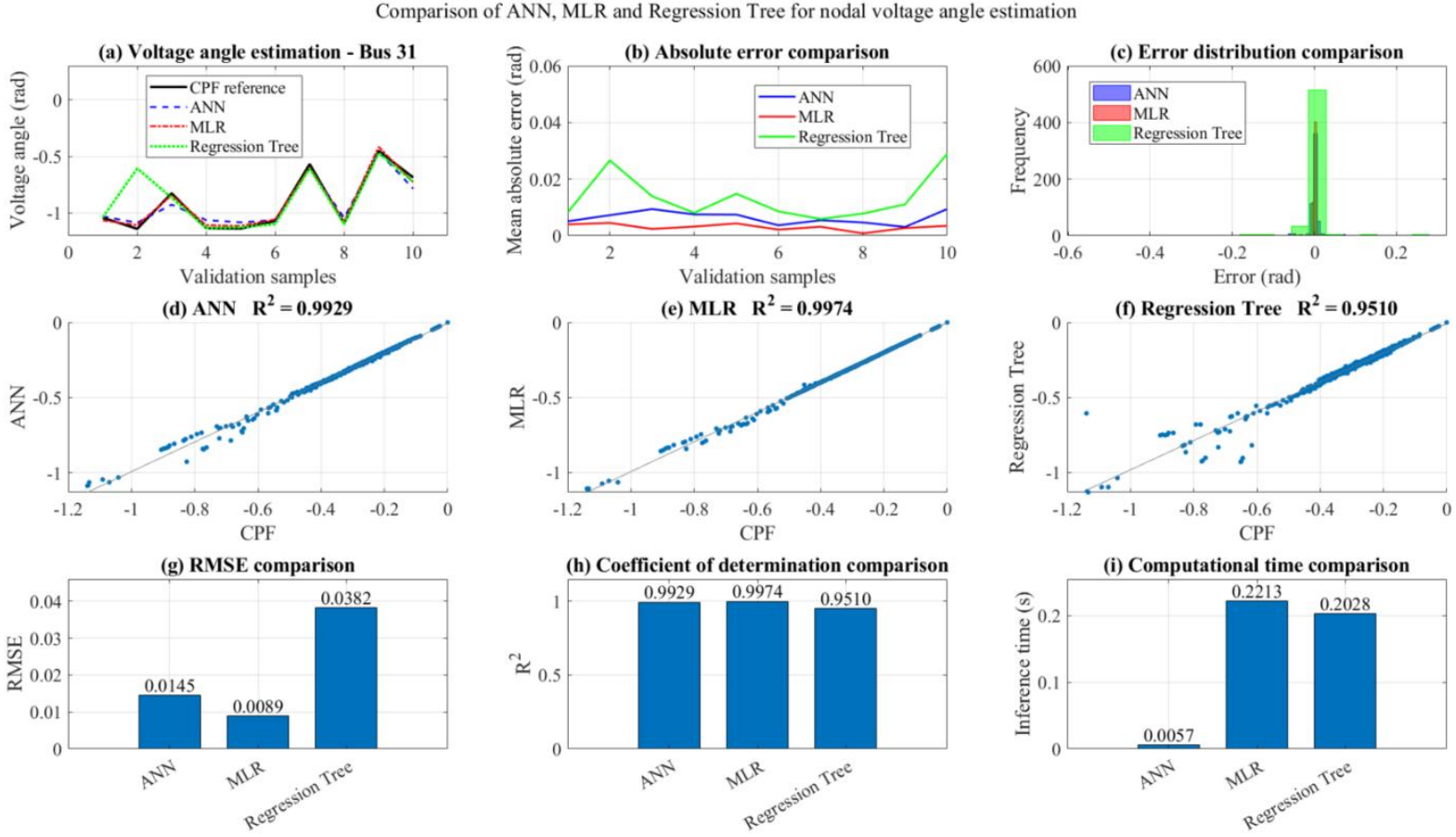
	MSE	RMSE	R2
ANN	0.00033741	0.018369	0.9973
MLR	0.00054402	0.023324	0.99503
Regression Tree	0.00053961	0.023229	0.99496

Figure 19 – Comparative performance of ANN, MLR, and Regression Tree models for nodal voltage angle estimation at the critical bus (Bus 30) of the IEEE 30-bus system. Source: Elaborated by the author.



	MSE	RMSE	R2
ANN	0.00028929	0.017008	0.9935
MLR	0.00067245	0.025932	0.98497
Regression Tree	0.00073251	0.027065	0.98343

Figure 20 – Comparative performance of ANN, MLR, and Regression Tree models for nodal voltage angle estimation at the critical bus (Bus 31) of the IEEE 57-bus system. Source: Elaborated by the author.



	MSE	RMSE	R2
ANN	0.00020939	0.01447	0.99294
MLR	7.9117e-05	0.0088947	0.99735
Regression Tree	0.0014605	0.038216	0.95096

2.5 CONCLUSIONS

This study presented an ANN-based approach for the direct estimation of nodal voltage angles and the construction of P–θ curves in electrical power systems. The proposed methodology was evaluated using the IEEE 14-, 30-, and 57-bus test systems, demonstrating high accuracy, fast convergence, and excellent generalization capability under different loading conditions.

The results showed that the MLP trained with the backpropagation algorithm was able to accurately reproduce the nodal voltage angles obtained from the CPF method. The trained networks achieved MSE values on the order of 10^{-3} or lower and correlation coefficients close to 0.99 for both training and validation datasets. Furthermore, the ANN successfully estimated the P–θ curves and accurately identified the maximum loading condition of the systems, including operating points near the voltage stability limit. The 10-fold cross-validation further confirmed the robustness of the proposed model, yielding consistently high prediction accuracy and excellent generalization across all benchmark systems. In addition, comparative analyses demonstrated that the ANN provided the best overall balance between predictive accuracy and computational efficiency when compared with MLR and Regression Tree models.

An important contribution of this work was the sensitivity analysis of the input variables using the Garson and Olden methodologies. The analysis revealed that variables with numerical values close to zero may produce disproportionately large synaptic weights, leading to misleading interpretations of variable importance. To address this issue, a normalization procedure was proposed and applied to the affected variables. Although the normalization had a negligible impact on the predictive performance of the ANN, it significantly improved the reliability and physical consistency of the sensitivity analysis results. After normalization, both methods identified the loading factor (λ) as one of the most influential variables in the estimation of nodal voltage angles, while also allowing the contribution of the remaining operating variables to be properly assessed.

The computational time analysis demonstrated another relevant advantage of the proposed methodology. When compared with the CPF method, the ANN reduced the computational effort by approximately 87% on average while maintaining high estimation accuracy. This reduction is particularly attractive for applications requiring

rapid assessment of multiple operating scenarios, such as online security analysis, contingency evaluation, and real-time decision support in power system operation. Overall, the results confirm that the proposed ANN model constitutes an efficient, accurate, and computationally attractive alternative for nodal voltage angle estimation and P–θ curve construction. The cross-validation results and the comparison with alternative machine learning techniques further reinforce the reliability and applicability of the proposed approach for voltage stability assessment in electrical power systems. In addition, the study highlights the importance of proper input data normalization when applying weight-based sensitivity analysis methods in neural networks. Future work may investigate the application of the proposed methodology to larger-scale power systems, contingency scenarios, renewable energy integration studies, and other machine learning architectures aimed at further improving prediction accuracy and model interpretability.

Author Contributions: N.L.D.: writing—original draft, writing—review and editing, investigation, methodology; A.d.Q.: formal analysis, visualization; A.C.d.J.G.: data curation, visualization, validation; R.F.B.: visualization, investigation, validation; S.d.A.D.L.: formal analysis, visualization; G.H.D.: formal analysis, visualization; A.B.N.: writing—original draft, methodology, writing—review and editing, supervision. All authors have read and agreed to the published version of the manuscript.

Funding: This research is funded by Conselho Nacional de Desenvolvimento Científico e Tecnológico (CNPq) (Brazil), process 406060/2025-8.

Data Availability Statement: The original contributions presented in this study are included in the article. Further inquiries can be directed to the corresponding author.

Acknowledgments: The authors would like to thank São Paulo State University—UNESP—Prope and PROAP/AUXPE for the financial support.

Conflicts of Interest: The authors declare no conflicts of interest.

REFERENCES

ANTHONY, K.; ARUNACHALAM, V. Voltage Stability Monitoring and Improvement in a Renewable Energy Dominated Deregulated Power System: A Review. **e-Prime - Advances in**

Electrical Engineering, Electronics and Energy, v. 11, p. 100893, 2025. DOI: https://doi.org/10.1016/j.prime.2024.100893

BENTO, M. E. C. Load Margin Assessment of Power Systems Using Physics-Informed Neural Network with Optimized Parameters. **Energies**, v. 17, n. 7, p. 1562, 2024. DOI: https://doi.org/10.3390/en17071562

CHRISTIE, R. D. **Power Systems Test Case Archive**. Seattle: Department of Electrical Engineering, University of Washington, 1999. Disponível em: https://labs.ece.uw.edu/pstca/index.html. Acesso em: 8 set. 2026.

KIM, H. *et al.* An Enhanced Continuation Power Flow Method Using Hybrid Parameterization. **Sustainability**, v. 16, n. 17, p. 7595, 2024. DOI: https://doi.org/10.3390/su16177595

LOPEZ, G. J. *et al.* Voltage Stability Control Based on Angular Indexes from Stationary Analysis. **Energies**, v. 15, n. 19, p. 7255, 2022. DOI: https://doi.org/10.3390/en15197255

MALIK, F. H. *et al.* A Comprehensive Review on Voltage Stability in Wind-Integrated Power Systems. **Energies**, v. 17, n. 3, p. 644, 2024. DOI: https://doi.org/10.3390/en17030644

MOLLA, S.; FARROK, O.; ALAM, M. J. Electrical Energy and the Environment: Prospects and Upcoming Challenges of the World's Top Leading Countries. **Renewable and Sustainable Energy Reviews**, v. 191, p. 114177, 2024. DOI: https://doi.org/10.1016/j.rser.2023.114177

RUAN, C. *et al.* Improved Continuation Power Flow Calculation Method Based on Coordinated Combination of Parameterization. *In*: IEEE INTERNATIONAL ELECTRICAL AND ENERGY CONFERENCE (CIEEC), 2., 2018, Beijing. **Proceedings [...]** Beijing: IEEE, 2018. p. 207–211. DOI: https://doi.org/10.1109/CIEEC.2018.8745861

SAFARI, A.; DANESHVAR, M.; ANVARI-MOGHADDAM, A. Energy Intelligence: A Systematic Review of Artificial Intelligence for Energy Management. **Applied Sciences**, v. 14, n. 23, p. 11112, 2024. DOI: https://doi.org/10.3390/app142311112

SANTOS, W. P. L. dos; BONINI NETO, A.; GABRIEL FILHO, L. R. A. Post-Contingency Loading Margin through Plane Change in the Continuation Power Flow. **Energies**, v. 16, n. 22, p. 7583, 2023. DOI: https://doi.org/10.3390/en16227583

SILVA, G. G. da *et al.* Multilayer Perceptron, Radial Basis Function, and Generalized Regression Networks Applied to the Estimation of Total Power Losses in Electrical Systems. **Machine Learning and Knowledge Extraction**, v. 8, n. 1, p. 4, 2026. DOI: https://doi.org/10.3390/make8010004

SIMONIČ, M.; FICKO, M.; KLANČNIK, S. Predicting Corn Moisture Content in Continuous Drying Systems Using LSTM Neural Networks. **Foods**, v. 14, n. 6, p. 1051, 2025. DOI: https://doi.org/10.3390/foods14061051

TOSTADO-VÉLIZ, M.; KAMEL, S.; JURADO, F. Development and Comparison of Efficient Newton-Like Methods for Voltage Stability Assessment. **Electric Power Components and Systems**, v. 48, n. 17-18, p. 1798–1813, 2020. DOI: https://doi.org/10.1080/15325008.2021.1908452

WERKIE, Y. G.; NYAKOE, G. N.; WEKESA, C. W. Power System Voltage Stability Assessment and Control Strategies: State-of-the-Art Review. **Journal of Electrical and Computer Engineering**, v. 2025, p. 6667482, 2025. DOI: https://doi.org/10.1155/jece/6667482

ZHANG, R. *et al.* Voltage Stability Margin Prediction by Ensemble Based Extreme Learning Machine. *In*: IEEE POWER & ENERGY SOCIETY GENERAL MEETING, 2013, Vancouver. **Proceedings [...]** Vancouver: IEEE, 2013. p. 1–5. DOI: https://doi.org/10.1109/PESMG.2013.6672489

AYDIN, F.; GÜMÜŞ, B. Study of Different ANN Algorithms for Voltage Stability Analysis. *In*: INNOVATIONS IN INTELLIGENT SYSTEMS AND APPLICATIONS CONFERENCE (ASYU), 2020, Istanbul. **Proceedings [...]** Istanbul: IEEE, 2020. p. 1–5. DOI: https://doi.org/10.1109/ASYU50717.2020.9259817

CARRERAS, J. *et al.* A Combination of Multilayer Perceptron, Radial Basis Function Artificial Neural Networks and Machine Learning Image Segmentation for the Dimension Reduction and the Prognosis Assessment of Diffuse Large B-Cell Lymphoma. **AI**, v. 2, n. 1, p. 106–134, 2021. DOI: https://doi.org/10.3390/ai2010008

GARSON, G. D. Interpreting neural-network connection weights. **Artificial Intelligence Expert**, v. 6, n. 4, p. 47–51, 1991.

GEVREY, M.; DIMOPOULOS, I.; LEK, S. Review and Comparison of Methods to Study the Contribution of Variables in Artificial Neural Network Models. **Ecological Modelling**, v. 160, n. 3, p. 249–264, 2003. DOI: https://doi.org/10.1016/S0304-3800(02)00257-0

GOH, A. T. C. Back-propagation neural networks for modeling complex systems. **Artificial Intelligence in Engineering**, v. 9, n. 3, p. 143–151, 1995. DOI: https://doi.org/10.1016/0954-1810(94)00011-S

KE, K.-C.; HUANG, M.-S. Quality Prediction for Injection Molding by Using a Multilayer Perceptron Neural Network. **Polymers**, v. 12, n. 8, p. 1812, 2020. DOI: https://doi.org/10.3390/polym12081812

OLDEN, J. D.; JACKSON, D. A. Illuminating the "black box": A randomization approach for understanding variable contributions in artificial neural networks. **Ecological Modelling**, v. 154, n. 1-2, p. 135–150, 2002. DOI: https://doi.org/10.1016/S0304-3800(02)00064-9

OLDEN, J. D.; JOY, M. K.; DEATH, R. G. An accurate comparison of methods for quantifying variable importance in artificial neural networks using simulated data. **Ecological Modelling**, v. 178, n. 3-4, p. 389–397, 2004. DOI: https://doi.org/10.1016/j.ecolmodel.2004.03.013

YOON, Y.; GUIMARAES, T.; SWALES, G. Integrating artificial neural networks with rule-based expert systems. **Decision Support Systems**, v. 11, n. 5, p. 497–507, 1994. DOI: https://doi.org/10.1016/0167-9236(94)90021-3

3 CAPÍTULO III - ADAPTIVE NEURO-FUZZY INFERENCE SYSTEM FOR ACCURATE VOLTAGE ANGLE STATE ESTIMATION IN ELECTRICAL POWER SYSTEMS: A TRAINING, AND VALIDATION ANALYSIS

Neylan Leal Dias[a], Alfredo Bonini Neto[b]

ABSTRACT

Accurate estimation of nodal voltage phase angles is essential for monitoring and analyzing electrical power systems, particularly under highly loaded operating conditions. This study proposes an Adaptive Neuro-Fuzzy Inference System (ANFIS) for estimating nodal voltage angles in the IEEE 14-bus test system and compares its performance with a previously developed Artificial Neural Network (ANN). A dataset comprising 107 operating conditions was generated using Continuation Power Flow, with 96 samples used for training and 11 for validation. Seven operating variables were adopted as inputs, and independent ANFIS models were developed for the 13 non-reference buses using subtractive clustering and hybrid learning. To provide a consistent basis for comparison, ANFIS training was limited to four epochs, matching the training horizon adopted for the ANN. Predictive performance was evaluated using RMSE, MAE, and \(R^2\), together with computational time and perturbation-based sensitivity analysis. Across the 13 non-reference buses, ANFIS achieved mean validation RMSE and MAE values of 3.48×10^{-4} and 2.94×10^{-4}, respectively, with a mean R^2 of 0.99998, compared with 0.032672, 0.026783, and 0.98587 for the ANN. ANFIS also reproduced the nonlinear P-θ trajectories more closely, particularly at higher loading levels. The global CPU time was 3.2721 s for ANFIS and 3.4782 s for ANN, representing a 5.93% reduction. Sensitivity analysis identified Q_g^{slack} (22.73%), P_g^{slack} (21.38%), and the loading parameter λ (17.66%) as the most influential inputs. Overall, ANFIS provided higher predictive accuracy while maintaining computational requirements comparable to those of the ANN benchmark.

Keywords: Adaptive Neuro-Fuzzy Inference System; voltage phase angle; electrical power systems; Continuation Power Flow; sensitivity analysis; artificial neural networks.

[a] School of Engineering, São Paulo State University (Unesp), Bauru 17033-360, Brazil; neylan.dias@unesp.br.
[a] Department of Exact and Technological Sciences, Federal University of Amapá, Macapá 68903-419, Brazil; neylan@unifap.br.
[b] Department of Biosystems Engineering, São Paulo State University (Unesp), School of Sciences and Engineering, Tupa, Brazil.

3.1 INTRODUCTION

The secure and reliable operation of modern electrical power systems depends on the continuous monitoring of variables that describe the network operating state (Anthony and Arunachalam, 2025; Zhao et al., 2025). Among these variables, nodal voltage magnitudes and phase angles are particularly important because they provide information on power-flow distribution, system stability, operational security, and proximity to critical operating conditions (Malik et al., 2024; Anthony and Arunachalam, 2025). The increasing penetration of renewable energy sources, distributed generation, electric vehicles, and nonlinear loads has made electrical networks more dynamic and complex, thereby increasing the need for fast and accurate state-estimation procedures (Molla et al., 2024; Zhao et al., 2025). Ahmed et al. (2023a), for example, demonstrated that data-driven neuro-fuzzy models can effectively represent the nonlinear behavior associated with different electric-vehicle charging scenarios.

Conventional power-system state estimation is generally based on iterative numerical algorithms that process a set of electrical measurements to determine the most probable system state. Although these techniques are well established, their application may require substantial computational effort, particularly in large-scale networks or under real-time operating conditions. Their performance may also be affected by ill-conditioned matrices, measurement uncertainties, missing information, communication failures, and convergence problems. These limitations motivate the development of alternative approaches capable of directly estimating state variables while reducing dependence on repeated numerical iterations (da Silva et al. 2026).

Artificial intelligence and soft-computing techniques have therefore received increasing attention in power-system analysis because of their ability to approximate nonlinear relationships, learn from operational data, and tolerate uncertainties in the input information (Oladipo et al., 2025). Pal and Mitra (1999) demonstrated that neuro-fuzzy approaches are particularly well suited for pattern recognition problems involving uncertainty, imprecision, and noisy data, a capability that has been further confirmed by recent studies (Ouifak and Idri, 2023).

In electrical power systems, artificial neural networks and fuzzy systems have been successfully applied to stability assessment, intelligent control, prediction, and state estimation. One of the pioneering applications of neuro-fuzzy techniques in electrical power systems was reported by Abido and Abdel-Magid (1998), who developed

a hybrid neuro-fuzzy power-system stabilizer for multimachine systems, demonstrating enhanced damping of electromechanical oscillations over a wide range of operating conditions. Since then, advances in artificial intelligence, data-driven methods, and advanced measurement technologies have significantly improved power-system monitoring and state estimation, enabling more accurate and reliable operation of modern power grids (Zhao et al., 2025; Zhu et al., 2024).

Despite their predictive capability, conventional artificial neural networks are often regarded as black-box models because the relationships between their inputs and outputs are not explicitly represented by interpretable rules (Ahmad and Zafar, 2026). This limitation may reduce operator confidence when such models are applied to critical monitoring and control tasks. In contrast, neuro-fuzzy systems integrate adaptive learning with fuzzy rule-based knowledge representation, allowing the acquired knowledge to be expressed through interpretable fuzzy IF–THEN rules while preserving the predictive capability of neural networks. This combination provides a gray-box modeling framework that enhances model interpretability without compromising predictive performance (Ayoubi and Isermann, 1997; Babuška and Verbruggen, 2003). Consequently, among the various neuro-fuzzy approaches, the Adaptive Neuro-Fuzzy Inference System (ANFIS) has become one of the most widely adopted hybrid intelligent models for nonlinear system identification, combining the adaptive learning capability of artificial neural networks with the interpretability of fuzzy inference systems (Jang and Sun, 1995; Babuška and Verbruggen, 2003).

Originally introduced by Jang (1993), ANFIS uses input–output data to adapt the parameters of fuzzy membership functions and inference rules, enabling the model to learn nonlinear relationships while retaining a rule-based structure. According to Walia et al. (2015), the adaptability of ANFIS makes it suitable for a broad range of prediction and system-identification problems. Shihabudheen and Pillai (2018) further highlighted the advances of neuro-fuzzy systems in handling nonlinear, multivariable, and complex modeling problems.

The initial fuzzy inference structure can be generated using clustering methods that identify relevant regions within the input–output space. Subtractive clustering is particularly useful because it determines cluster centers directly from the data and reduces the need to manually define the number and position of membership functions (Chiu, 1994). The resulting fuzzy structure can subsequently be optimized by the ANFIS learning algorithm, which adjusts premise and consequent parameters to minimize

the prediction error. This combination allows the construction of parsimonious models with a reduced number of fuzzy rules and adequate generalization capability. The continuing relevance of this approach is evidenced by its widespread adoption in recent applications, including wave height prediction (Hakimi and Farjami, 2025), soil water retention estimation (Seyedmohammadi and Navidi, 2026), and fault detection systems (Bisker et al., 2025), where the ability to automatically generate interpretable fuzzy rules from data remains a key advantage.

In power engineering, neuro-fuzzy systems have been successfully applied to stability enhancement, power-flow control, energy management, renewable-energy optimization, and frequency regulation. Talaat et al. (2010) developed a genetically optimized neuro-fuzzy power system stabilizer for multimachine power systems, demonstrating improved damping of electromechanical oscillations under a wide range of operating conditions. Jamal and Syahputra (2014) developed an adaptive neuro-fuzzy controller for a Unified Power Flow Controller (UPFC) to regulate power flow in multimachine power systems. Gaber et al. (2021) developed an ANFIS-based energy-management system for an electric ship power system, whereas Siddikov and Porubay (2022) proposed a neuro-fuzzy approach for regulating power-flow processes in electric power facilities. More recent applications include the optimization of photovoltaic power systems under partial shading conditions and adaptive frequency regulation in interconnected power systems with high penetration of renewable energy sources, and ANFIS-assisted state estimation in nonlinear dynamic systems (Mohammed et al., 2025; Elborlsy et al., 2025; Ibrahim et al., 2025).

Recently, Leal Dias et al. (2026) developed an Artificial Neural Network (ANN) approach for the direct estimation of nodal voltage phase angles in IEEE test systems using operating conditions generated by Continuation Power Flow. The proposed ANN demonstrated high predictive accuracy and low computational cost, confirming the feasibility of data-driven approaches for voltage-angle estimation. Nevertheless, the ANN architecture remains essentially a black-box model, and the potential benefits of combining nonlinear learning with fuzzy rule-based representation for this specific application have not yet been systematically investigated.

Although previous studies have demonstrated the successful application of neuro-fuzzy systems to a wide range of power-engineering problems, their use for the direct estimation of nodal voltage phase angles remains comparatively limited. In par-

ticular, there is still a lack of studies evaluating ANFIS models under operating conditions extending from the base case to the vicinity of the voltage-stability limit and directly comparing their predictive performance with previously validated ANN models. Moreover, the influence of the electrical input variables on ANFIS-based voltage-angle estimates has received limited attention. Therefore, a comprehensive assessment combining prediction accuracy, convergence behavior, error distribution, computational performance, and input-variable sensitivity is required to better characterize the applicability of ANFIS to this state-estimation problem.

Accordingly, this study proposes and evaluates an Adaptive Neuro-Fuzzy Inference System (ANFIS) for the direct estimation of nodal voltage phase angles in the IEEE 14-bus test system. The initial fuzzy inference structure is generated using subtractive clustering and subsequently optimized through a hybrid learning algorithm combining least-squares estimation and gradient descent. The ANFIS models are trained using 96 operating conditions and evaluated using an independent validation set comprising 11 previously unseen operating conditions. Detailed analyses are performed for buses 3, 6, 13, and 14, while the overall predictive performance is assessed across the 13 non-reference buses of the IEEE 14-bus system. The performance of the ANFIS models is compared with that of the previously developed ANN using RMSE, MAE, and R^2. In addition, convergence behavior, error distributions, P−θ characteristics, computational performance, and perturbation-based input-variable sensitivity are investigated to provide a comprehensive assessment of the proposed neuro-fuzzy approach.

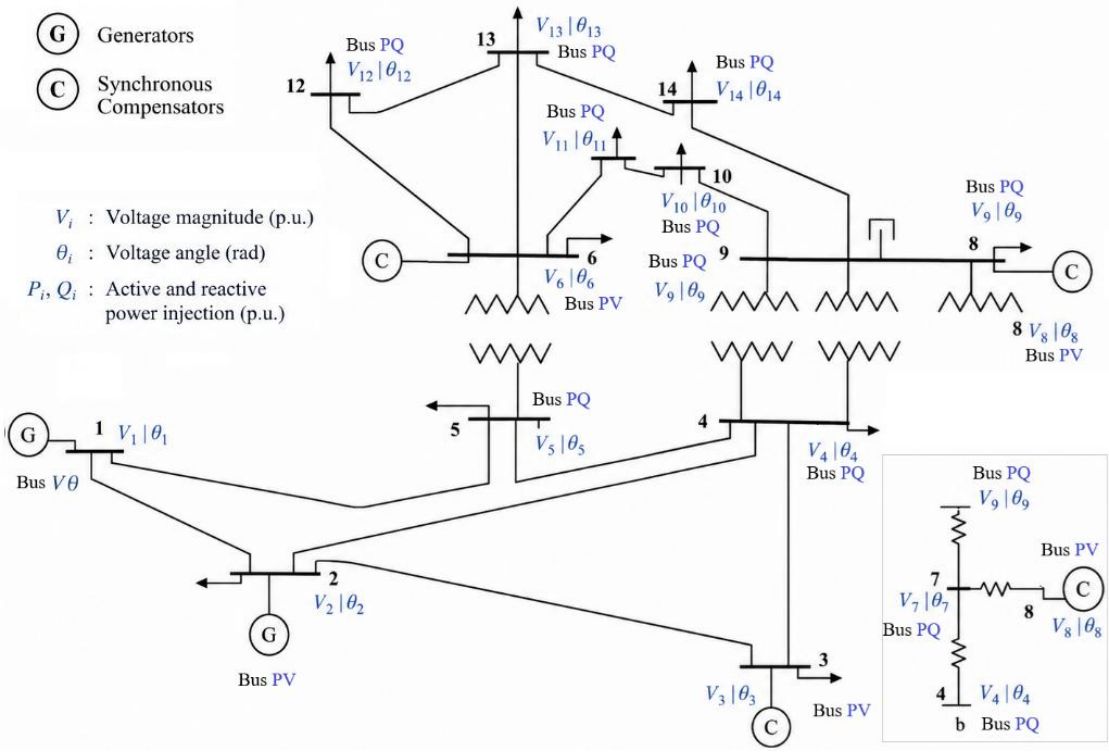
3.2 MATERIALS AND METHODS

3.2.1 Dataset

The dataset used in this study was generated from Continuation Power Flow (CPF) simulations performed on the IEEE 14-bus test system (Figure 1), using the continuation method originally proposed by Ajjarapu and Christy (1992) and subsequently applied in the formulation described by dos Santos et al. (2023). The CPF algorithm enables the system operating point to be continuously traced as the loading level increases, providing a sequence of feasible steady-state operating conditions from the base case to the vicinity of the maximum loading point (voltage stability limit).

This procedure allows the generation of representative operating scenarios covering a wide range of network conditions.

Figure 1. Single-line diagram of the IEEE 14-bus test system, based on data from the Power Systems Test Case Archive.



Source: Christie (1999).

In the CPF formulation, the system loading level is controlled by the loading parameter λ, which proportionally modifies the active and reactive power demands according to equation (1):

$$P_i = P_{i0}(1+\lambda)$$
$$Q_i = Q_{i0}(1+\lambda) \quad (1)$$

where Pi and Qi are the active and reactive power demands at bus i under the loading level defined by λ, whereas Pi0 and Qi0 are the corresponding base-case demands. The parameter λ controls the progressive increase in system loading during the CPF

analysis. As λ increases, successive equilibrium operating points are obtained until the maximum loading point (voltage stability limit) is reached.

Using this procedure, a total of 107 operating scenarios were generated, each corresponding to a distinct loading condition obtained from the continuation power flow analysis. For each operating point, the electrical variables resulting from the power-flow solution were extracted and organized into an input–output dataset for training and evaluating the proposed Adaptive Neuro-Fuzzy Inference System (ANFIS).

Each sample consisted of 21 variables, including seven input variables and fourteen output variables. The input variables comprised the loading factor (λ), the active power generated at the slack bus (P_g^{slack}), the reactive power generated at the slack bus (Q_g^{slack}), and the specified active power injections at the generation buses ($P_{g,k}$). These variables were selected because they characterize the operating condition of the electrical network and directly influence the distribution of voltage phase angles. The output variables corresponded to the voltage phase angles (θ) of the 14 buses in the IEEE 14-bus system, expressed in radians. Consequently, each operating condition was represented by a seven-dimensional input vector associated with a fourteen-dimensional output vector.

Before model development, all input variables were normalized to improve numerical stability during the learning process and prevent variables with larger numerical ranges from dominating the optimization procedure. Subsequently, the complete dataset was divided into two mutually exclusive subsets following a holdout strategy: 90% of the samples (96 operating conditions) were allocated to training, while the remaining 10% (11 operating conditions) were reserved for independent validation. The same training and validation samples were used for all ANFIS models and for comparison with the previously developed ANN (Leal Dias et al. 2026), ensuring a consistent performance assessment between the two approaches.

3.2.2 Architecture of the Adaptive Neuro-Fuzzy Inference System (ANFIS)

The Adaptive Neuro-Fuzzy Inference System (ANFIS), introduced by Jang (1993), is a hybrid intelligent model that combines the learning capability of artificial neural networks with the reasoning mechanism of fuzzy inference systems. It is based on the first-order Takagi–Sugeno fuzzy inference model. Considering the input layer, the proposed ANFIS comprises six sequential processing layers, each responsible for

a specific stage of the fuzzy inference process. The initial fuzzy inference system (FIS) was automatically generated using the subtractive clustering algorithm proposed by Chiu (1994), which identifies representative data clusters and automatically determines the initial fuzzy rules and membership functions.

Figure 2 illustrates the complete ANFIS learning architecture, showing the flow of normalized input data through the six processing layers until the estimation of the nodal voltage angle.

The first layer corresponds to the input layer, where the normalized input variables are introduced into the model. In the present application, the inputs include the loading factor (λ), the slack bus active and reactive powers, and the active power injections at the remaining buses. Data normalization is performed before training to ensure numerical stability and improve the convergence of the learning algorithm.

The second layer performs the fuzzification process, in which each input variable is transformed into fuzzy values through membership functions. These functions quantify the degree to which each input belongs to the predefined fuzzy sets. During the training process, the parameters defining the membership functions are continuously adjusted to minimize the prediction error.

The third layer is the rule layer. Each node represents a fuzzy IF–THEN rule generated from the initial fuzzy inference system created by the subtractive clustering algorithm (Chiu, 1994). The logical AND operator combines the membership degrees of all input variables to compute the firing strength of each fuzzy rule.

The fourth layer performs normalization of the firing strengths. Each firing strength is divided by the sum of all firing strengths, producing normalized weights whose values range between zero and one. Consequently, the contribution of each rule becomes proportional to its relative importance for the current operating condition.

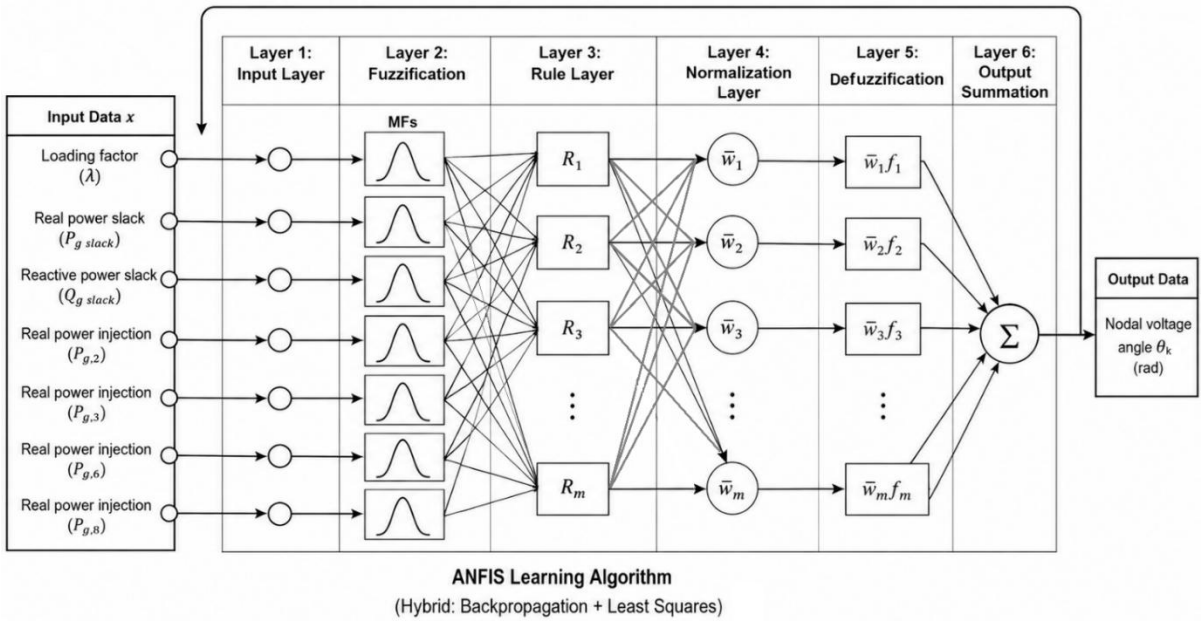
The fifth layer corresponds to the defuzzification (consequent) layer. Each normalized firing strength is multiplied by the corresponding linear consequent function associated with the Takagi-Sugeno rule. The parameters of these linear functions are estimated during training using the hybrid learning algorithm proposed by Jang (1993), which combines the least-squares estimation method with backpropagation (gradient descent) to optimize the consequent and premise parameters, respectively.

Finally, the sixth layer produces the overall output by summing the contributions of all fuzzy rules. In this study, the output corresponds to the estimated nodal voltage angle (θ), expressed in radians.

Unlike the previously developed ANN, which simultaneously estimates the voltage angles of all system buses through a multi-output architecture, the ANFIS framework adopted in this study employs an independent single-output model for each non-reference bus. Thus, each ANFIS model receives the same seven electrical variables as inputs and provides the estimated voltage angle θ_k of a specific bus k as its output. Because the voltage angle of bus 1 is fixed as the reference angle, ANFIS models were developed for the 13 non-reference buses (buses 2–14).

As illustrated in Figure 2, this layered architecture enables nonlinear relationships between electrical variables and voltage angles to be accurately approximated while preserving the interpretability provided by fuzzy rules. The hybrid learning mechanism enables the premise and consequent parameters to be adaptively optimized during model training.

Figure 2. Architecture of the ANFIS model adopted for nodal voltage angle estimation, illustrating the six processing layers, including input normalization, fuzzification, fuzzy inference, firing-strength normalization, defuzzification, and final output generation.



Source: Elaborated by the author

3.2.3 Mathematical formulation of the ANFIS model

For a given input vector x=[*x1, x2, …, x7*], the fuzzification layer determines the membership degree of each input variable according to its corresponding membership function:

$$\mu A_{ij}(x_i) = e^{-\frac{(x_i - c_{ij})^2}{2\sigma_{ij}^2}} \tag{2}$$

where cij and σij represent the center and width of the membership function associated with the j-th fuzzy set of input xi. These premise parameters are adjusted during the ANFIS training process.

The firing strength of each fuzzy rule Rj is obtained by combining the membership degrees of the input variables:

$$w_j = \prod_{i=1}^{7} \mu A_{ij}(x_i) \tag{3}$$

The firing strengths are then normalized as:

$$\overline{w}_j = \frac{w_j}{\sum_{b=1}^{m} w_b} \tag{4}$$

where m is the total number of fuzzy rules generated by subtractive clustering.

For the first-order Takagi–Sugeno model adopted in this study, the consequent of each rule is expressed as a linear function of the seven inputs:

$$f_j = p_{j1}x_1 + p_{j2}x_2 + \cdots + p_{j7}x_7 + r_j \tag{5}$$

Finally, the estimated nodal voltage angle is obtained from the weighted contribution of all fuzzy rules:

$$\widehat{\theta}_k = \sum_{j=1}^{m} \overline{w}_j f_j \tag{6}$$

where $\hat{\theta}_k$ denotes the estimated voltage angle of bus k. The consequent parameters are determined by least-squares estimation, whereas the premise parameters of the membership functions are adjusted by gradient descent during the hybrid ANFIS learning process.

The subtractive-clustering radius was set to 0.6. The ANFIS models were trained using the hybrid optimization method, combining least-squares estimation for the consequent parameters with gradient descent for the premise parameters. To maintain consistency with the ANN benchmark, the maximum number of ANFIS training epochs was set to four, corresponding to the number of training epochs required for convergence of the previously developed ANN. The FIS associated with the minimum validation error was retained as the final model for each bus.

3.2.4 Model Performance Evaluation

The predictive performance of the ANFIS models was evaluated using the root mean square error (RMSE), mean absolute error (MAE), and coefficient of determination (R^2), calculated independently for the training and validation datasets. Lower RMSE and MAE values and R^2 values closer to unity indicate better agreement between the target and estimated voltage angles.

The metrics were calculated for each of the 13 non-reference buses (buses 2–14), excluding bus 1 because its voltage angle is fixed as the reference. Mean values across the 13 buses were used to assess the overall model performance, while buses 3, 6, 13, and 14 were selected for detailed analysis.

The ANFIS results were compared with the previously developed ANN model (Leal Dias et al., 2026) using the same dataset and training-validation partition. Because the ANN simultaneously estimates all nodal voltage angles, whereas ANFIS uses an independent model for each bus, computational performance was assessed under the same computational environment by considering both the individual and cumulative training times of the ANFIS models.

3.2.5 Perturbation-Based Sensitivity Analysis

To assess the relative influence of the input variables on the voltage angles estimated by the ANFIS models, a perturbation-based sensitivity analysis was performed. This approach evaluates the response of a trained model to controlled changes in individual input variables and has been previously applied to assess variable importance in ANFIS models (Ahmed et al., 2023b).

After model training, each of the seven input variables (λ, P_g^{slack}, Q_g^{slack}, $P_{g,2}$, $P_{g,3}$, $P_{g,6}$, and $P_{g,8}$) was individually increased by 10%, while the remaining variables were kept unchanged. The perturbed dataset was then applied to the trained ANFIS model, and the resulting change in the estimated voltage angle was used to calculate the sensitivity index:

$$S_j = \frac{\Delta O_j}{\Delta U_j} \tag{7}$$

where Sj is the sensitivity index associated with input variable j, ΔOj represents the change in the ANFIS-estimated nodal voltage angle resulting from the perturbation, and ΔUj represents the corresponding change in the input variable. The absolute sensitivity indices were subsequently normalized to express the relative importance of each input variable as a percentage. A 10% perturbation level was selected within the perturbation-based sensitivity framework adopted by Ahmed et al. (2023b).

The sensitivity analysis was independently performed for each of the 13 non-reference buses (buses 2–14), since a separate ANFIS model was developed for each bus. The mean relative importance across the 13 buses was used to characterize the overall influence of each input variable on voltage-angle estimation.

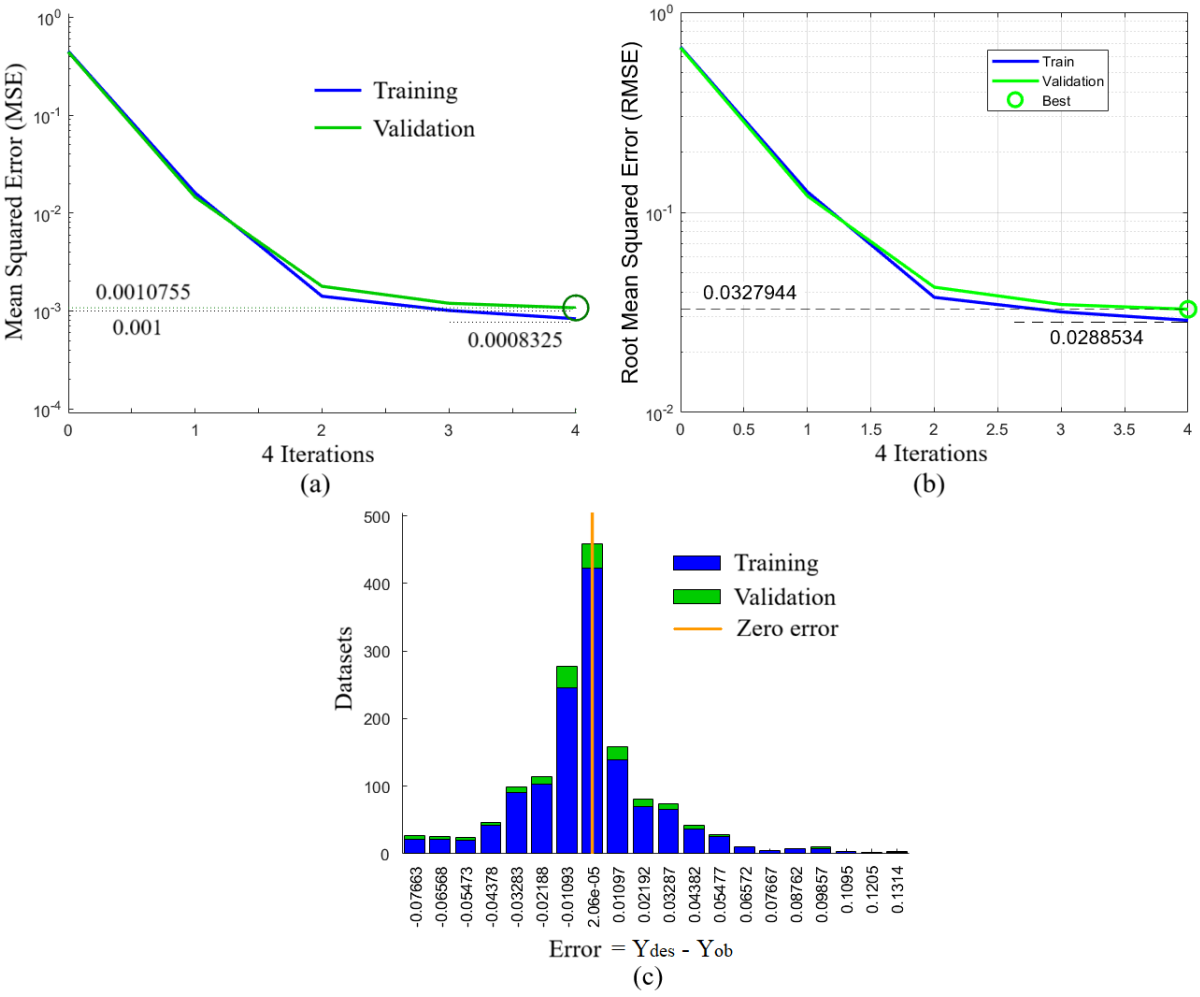
3.3 RESULTS AND DISCUSSION

3.3.1 Training and Convergence Performance

The training and validation behavior of the ANN and ANFIS models is presented in Figures 3 and 4. To provide a consistent basis for comparison, the ANFIS training process was limited to four epochs, matching the number of epochs used by the previously developed ANN (Leal Dias et al., 2026). The same 96 operating conditions were used for training and the same 11 previously unseen conditions were used for validation in both approaches.

For the ANN, the training and validation RMSE decreased progressively over the four epochs. The training RMSE decreased from 0.67049 at the initial stage to 0.02885 at epoch 4, while the validation RMSE decreased from 0.66445 to 0.03279. Thus, the minimum validation error was obtained at the fourth epoch, which was retained as the final ANN model.

Figure 3. Training performance of the ANN model: (a) mean squared error, (b) root mean squared error, and (c) error distribution for the training and validation datasets.

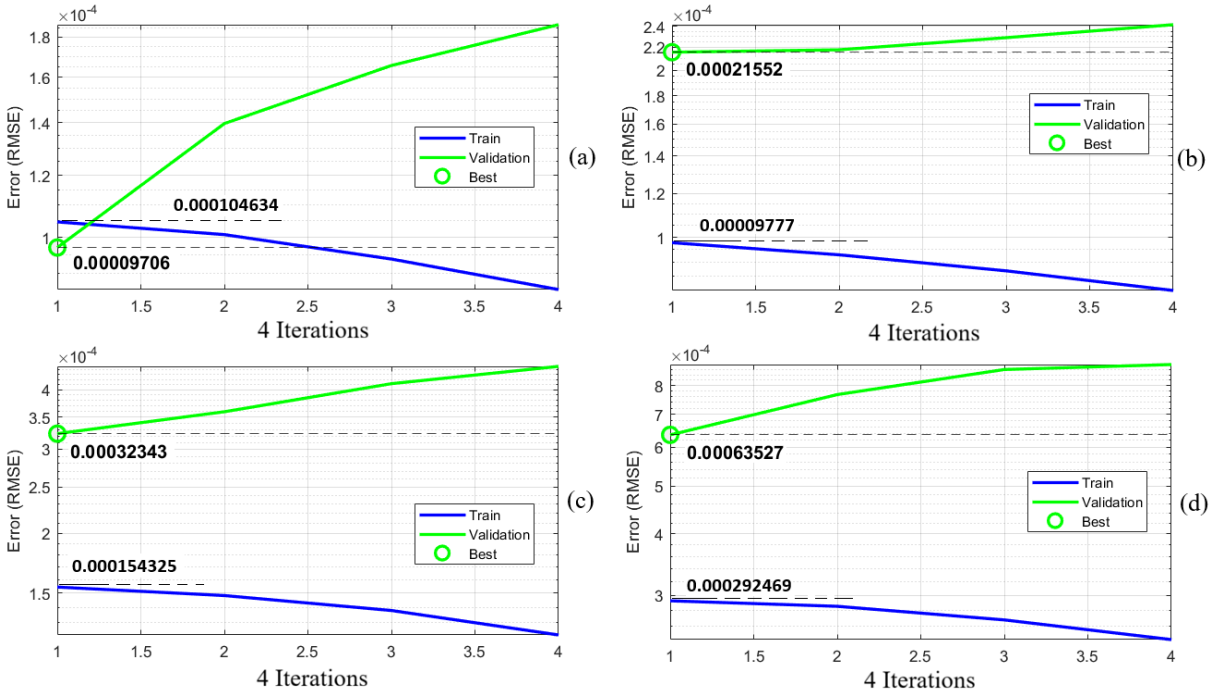


Source: Elaborated by the author

The ANFIS models exhibited a different training behavior (Figure 4). For the representative buses 3, 6, 13, and 14, the training RMSE progressively decreased over the four epochs. However, the minimum validation RMSE was consistently reached at the first epoch. The corresponding minimum validation RMSE values were 9.71×10^{-5}, 2.16×10^{-4}, $.23\times10^{-4}$, and 6.35×10^{-4} for buses 3, 6, 13, and 14, respectively.

Although the ANFIS training RMSE continued to decrease after the first epoch, additional epochs did not improve validation performance. Therefore, the FIS corresponding to the minimum validation error was retained as the final model for each bus. This result indicates that ANFIS was able to capture the nonlinear input–output relationships within the initial stage of the learning process, whereas the ANN required the complete four-epoch training sequence to reach its minimum validation error.

Figure 4. Evolution of the training and validation RMSE for the ANFIS models corresponding to buses (a) 3, (b) 6, (c) 13, and (d) 14. The markers indicate the minimum validation error used to select the final FIS.



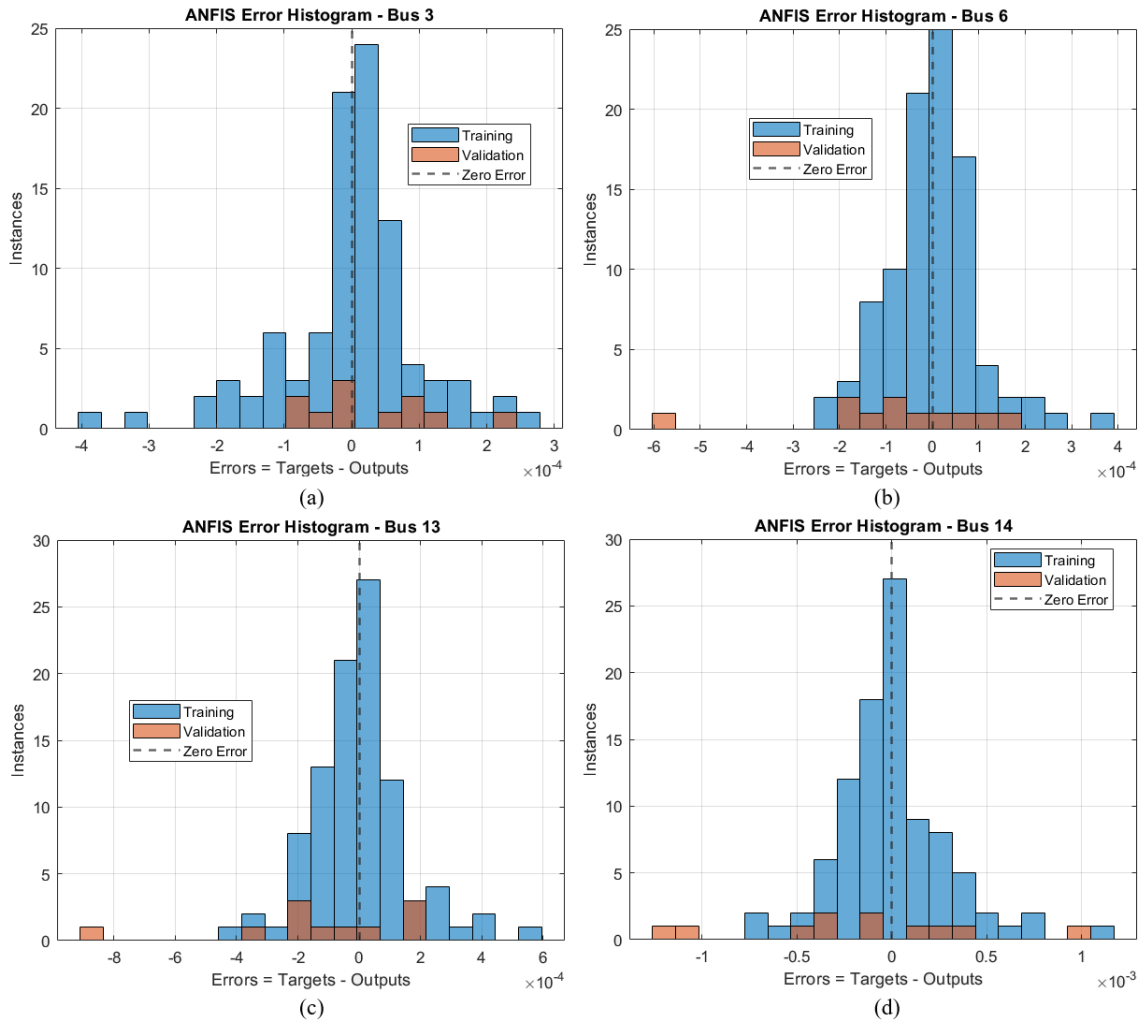
Source: Elaborated by the author

The error distributions provide additional insight into the behavior of the two modeling approaches. As shown in Figure 3(c), the ANN errors were predominantly distributed around zero for both the training and validation datasets, indicating an overall agreement between the target and estimated voltage angles. However, a broader error distribution can be observed for the ANN model.

Figure 5 presents the corresponding ANFIS error histograms for buses 3, 6, 13, and 14. In all cases, the residuals were strongly concentrated around zero, with rela-

tively narrow distributions for both training and validation samples. The dispersion increased slightly for buses 13 and 14, particularly for the validation samples, but the magnitude of the errors remained small. This behavior is consistent with the low validation RMSE values obtained for these buses and indicates that the ANFIS predictions remained close to the CPF reference values across the analyzed operating conditions. Compared with the ANN error distribution shown in Figure 3(c), the ANFIS histograms exhibit a substantially narrower concentration of residuals around zero. This result provides complementary evidence that, for the representative buses, ANFIS achieved greater prediction accuracy than the ANN benchmark.

Figure 5. Error histograms of the ANFIS models for buses (a) 3, (b) 6, (c) 13, and (d) 14, considering the training and validation datasets.



Source: Elaborated by the author

3.3.2 Predictive Performance and Comparison between ANN and ANFIS

The predictive performance of ANN and ANFIS was evaluated using RMSE, MAE, and R^2 for both the training and validation datasets. Because the ANN uses a multi-output architecture, whereas ANFIS employs an independent model for each non-reference bus, the comparison was conducted at two levels. First, the overall performance was assessed considering all 13 non-reference buses (buses 2–14). Subsequently, buses 3, 6, 13, and 14 were examined individually to provide a detailed assessment of the predictive behavior of both models. Table 1 presents the performance metrics for these representative buses, together with the mean values calculated across all 13 non-reference buses to provide an overall assessment of model performance.

In addition to predictive accuracy, the computational performance of both approaches was evaluated, as summarized in Table 2. The individual ANFIS models required approximately 0.25 s of CPU time per bus, with a mean value of 0.2517 s across the 13 non-reference buses. Because ANFIS requires an independently trained model for each bus, the cumulative CPU time was also considered to provide a more consistent comparison with the multi-output ANN. The global CPU time for the 13 ANFIS models was 3.2721 s, whereas the ANN required 3.4782 s to simultaneously estimate the nodal voltage angles. Thus, ANFIS reduced the overall computational time by 5.93% compared with ANN. Although this reduction was relatively modest at the system level, it indicates that the higher predictive accuracy achieved by ANFIS did not result in an increased computational cost.

Table 1. Performance metrics of the ANN and ANFIS models for the representative buses during training and validation.

Bus	Model	Training RMSE	Training MAE	Training (R^2)	Validation RMSE	Validation MAE	Validation (R^2)
3	ANN	0.010171	0.008323	0.992762	0.009506	0.008665	0.993733
3	ANFIS	0.000105	0.000071	0.999999	0.000097	0.000073	0.999999
6	ANN	0.022274	0.016744	0.989391	0.027087	0.021010	0.982412
6	ANFIS	0.000098	0.000070	1.000000	0.000216	0.000149	0.999999
13	ANN	0.034342	0.029248	0.983325	0.040116	0.036770	0.975240
13	ANFIS	0.000154	0.000109	1.000000	0.000323	0.000226	0.999998
14	ANN	0.044170	0.033803	0.989365	0.049980	0.036688	0.984096
14	ANFIS	0.000292	0.000204	1.000000	0.000635	0.000487	0.999997
Mean 13 buses	ANN	0.087394	0.02303	0.98971	0.032672	0.026783	0.98587
	ANFIS	0.00017	0.00012	1.00000	0.000348	0.000294	0.99998

Note: Mean values were calculated considering the 13 non-reference buses (buses 2–14). Bus 1 was excluded because its voltage phase angle is fixed as the reference angle.

Table 2. Computational performance of the ANN and ANFIS models.

Model / Bus	CPU time (s)
ANFIS – Bus 3	0.2538
ANFIS – Bus 6	0.2603
ANFIS – Bus 13	0.2541
ANFIS – Bus 14	0.2614
ANFIS – Mean (13 buses)	0.2517
ANFIS – Global (13 buses)	3.2721
ANN – Global (13 buses)	3.4782

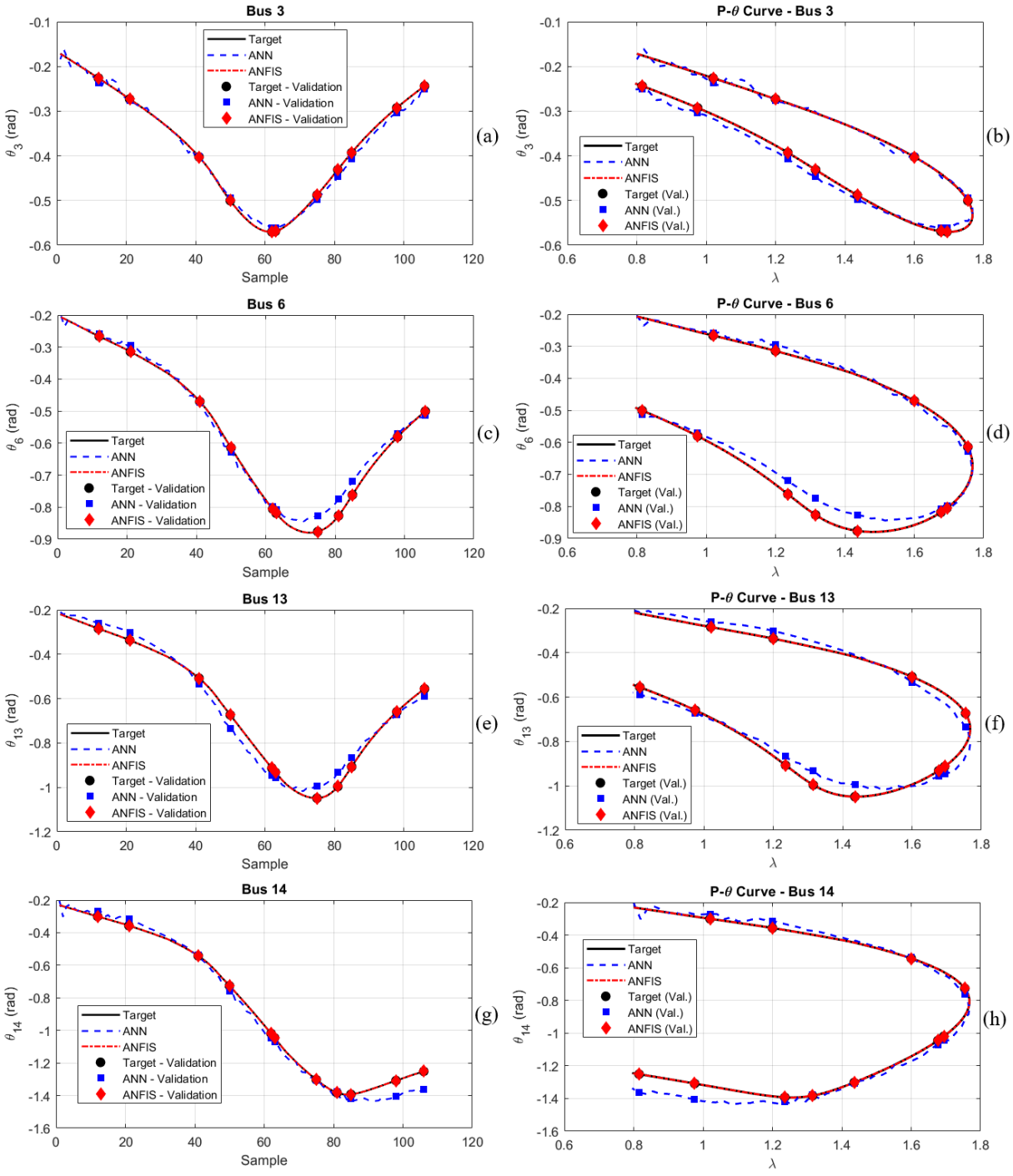
3.3.3 Voltage-Angle Estimation and P−θ Characteristics

The predictive behavior of ANN and ANFIS over the complete set of operating conditions is illustrated in Figure 6 for buses 3, 6, 13, and 14. The left-hand panels compare the voltage-angle values obtained from the CPF simulations (Target) with those estimated by ANN and ANFIS, while the right-hand panels present the corresponding P−θ curves as a function of the loading parameter λ. The validation samples are highlighted to illustrate the performance of both models for operating conditions not used during training.

As shown in Figure 6(a), (c), (e), and (g), both models reproduced the general variation of the nodal voltage angles throughout the loading trajectory. However, the ANFIS estimates remained consistently closer to the target values, whereas the ANN exhibited more noticeable deviations in some portions of the trajectories. These differences became more evident for buses 6, 13, and 14, particularly around the regions where the voltage-angle trajectories showed stronger nonlinear behavior.

The P−θ curves in Figure 6(b), (d), (f), and (h) provide a clearer representation of this behavior. Both approaches were able to reproduce the characteristic nonlinear evolution of the nodal voltage angles as the loading parameter increased. Nevertheless, ANFIS followed the CPF reference curves more closely, including the curved region associated with higher loading levels and the vicinity of the maximum loading point. In contrast, the ANN presented larger deviations from the target curve in these more nonlinear regions, particularly for buses 6 and 13. For bus 3, the differences between the two approaches were less pronounced.

Figure 6. Figure 6. Comparison of target, ANN-estimated, and ANFIS-estimated nodal voltage angles for buses 3, 6, 13, and 14. Left panels show voltage angles as a function of the operating-condition sample: (a) bus 3, (c) bus 6, (e) bus 13, and (g) bus 14. Right panels show the corresponding P−θ curves as a function of the loading parameter λ: (b) bus 3, (d) bus 6, (f) bus 13, and (h) bus 14. Markers identify the validation samples.



Source: Elaborated by the author

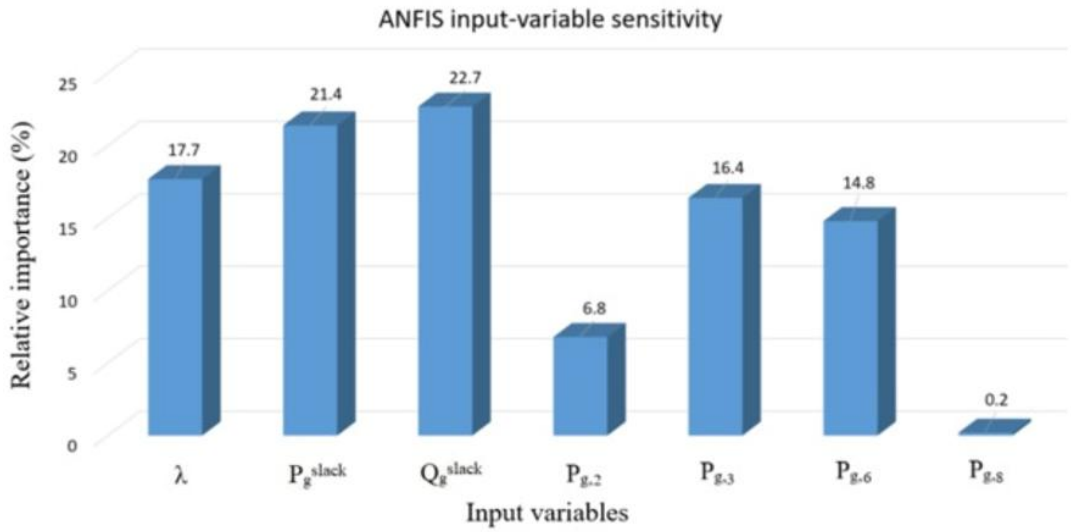
The ability of ANFIS to more closely reproduce the nonlinear P−θ trajectories is consistent with the lower RMSE and MAE and the higher R^2 values reported in Table 1. These results indicate that the neuro-fuzzy structure provided greater flexibility for representing the nonlinear relationship between the selected operating variables and nodal voltage angles, especially as the system approached more highly loaded operating conditions.

3.3.4 Input-Variable Sensitivity Analysis

The perturbation-based sensitivity analysis was performed for all 13 non-reference buses to quantify the influence of each input variable on the ANFIS voltage-angle estimates. Although buses 3, 6, 13, and 14 were selected for detailed graphical representation of the predictive performance, the sensitivity results discussed in this section correspond to the mean relative importance calculated across all 13 buses, providing a system-level assessment of the influence of the seven input variables. Figure 7 presents the mean relative importance obtained across the 13 buses, providing a system-level assessment of the contribution of the seven input variables.

As shown in Figure 7, Q_g^{slack} was the most influential input variable, with a mean relative importance of 22.73%, followed by P_g^{slack} (21.38%), λ (17.66%), $P_{g,3}$ (16.42%), $P_{g,6}$ (14.81%), and $P_{g,2}$ (6.81%). In contrast, $P_{g,8}$ exhibited a markedly lower relative importance of only 0.19%. These results indicate that the ANFIS estimates were particularly sensitive to variations in the active and reactive power supplied by the slack generator, together with the loading parameter λ.

Figure 7. Mean relative importance of the input variables obtained from the perturbation-based sensitivity analysis of the ANFIS models considering all 13 non-reference buses.



Source: Elaborated by the author

The sensitivity pattern obtained with ANFIS can also be compared with that previously reported for the ANN by Leal Dias et al. (2026). In the ANN, Garson's method (Garson, 1991) identified λ as the most influential variable (21.23%), followed by $P_{g,6}$ (19.36%), $P_{g,3}$ (16.97%), P_g^{slack} (14.61%), $P_{g,2}$ (13.25%), and Q_g^{slack} (12.51%), while $P_{g,8}$ again presented the lowest contribution (2.06%). Thus, although the ranking of the most influential variables differed between the two approaches, both analyses consistently identified $P_{g,8}$ as the least influential input.

These differences should be interpreted considering the distinct sensitivity-analysis procedures adopted for each model. Garson's method estimates variable importance from the connection weights of the ANN, whereas the perturbation-based analysis evaluates the change in the ANFIS output resulting from a controlled variation in each input variable. Therefore, the relative-importance percentages obtained by the two methods should not be interpreted as directly equivalent. Rather, they provide complementary perspectives on the contribution of the input variables to nodal voltage-angle estimation.

From a power-system perspective, the prominent contributions of λ, P_g^{slack}, and Q_g^{slack} in the ANFIS analysis are consistent with the evolution of the operating conditions generated by the CPF. As system loading changes, the loading parameter and the active and reactive power supplied by the slack generator reflect important adjustments in the system operating state. The sensitivity analysis therefore complements the predictive results by identifying the variables that most strongly affect the ANFIS voltage-angle estimates.

3.5 CONCLUSION

This study demonstrated the applicability of an Adaptive Neuro-Fuzzy Inference System (ANFIS) for the direct estimation of nodal voltage phase angles in the IEEE 14-bus test system under operating conditions generated by Continuation Power Flow. The proposed approach successfully captured the nonlinear relationships between the selected operating variables and the voltage angles across the 13 non-reference buses.

Compared with the previously developed ANN, ANFIS provided higher predictive accuracy, particularly for the validation dataset. Considering the mean performance across the 13 non-reference buses, ANFIS achieved an RMSE of 3.48×10^{-4}, an MAE of 2.94×10^{-4}, and an R^2 of 0.99998, compared with 0.032672, 0.026783, and 0.98587, respectively, for the ANN. The P-θ curves further showed that ANFIS more closely reproduced the nonlinear behavior of the reference solutions, especially under higher loading conditions.

Despite requiring an independent model for each non-reference bus, the cumulative CPU time of ANFIS was 3.2721 s, compared with 3.4782 s for the multi-output ANN, corresponding to a modest reduction of 5.93%. Thus, the improvement in predictive accuracy was achieved without increasing the overall computational cost.
The perturbation-based sensitivity analysis identified Q_g^{slack}, P_g^{slack}, and the loading parameter λ as the most influential variables, with mean relative importance values of 22.73%, 21.38%, and 17.66%, respectively. In contrast, $P_{g,8}$ exhibited the lowest influence (0.19%). These findings complement the predictive analysis by identifying the operating variables that most strongly affect the ANFIS voltage-angle estimates.

Overall, the results indicate that ANFIS provides an accurate and computationally competitive alternative for nonlinear nodal voltage-angle estimation. Future studies

should evaluate the proposed approach in larger power systems, under a broader range of operating conditions, and using measurement-based or real-world data to assess its scalability and practical applicability.

REFERENCES

ABIDO, M. A.; ABDEL-MAGID, Y. L. A hybrid neuro-fuzzy power system stabilizer for multimachine power systems. **IEEE Transactions on Power Systems**, v. 13, p. 1323–1330, 1998. DOI: https://doi.org/10.1109/59.736272.

AHMAD, A.; ZAFAR, K. Bridging black box and explainability: a complete post-hoc grey-box XAI framework. **Applied Soft Computing**, v. 172, p. 115423, 2026. DOI: https://doi.org/10.1016/j.asoc.2026.115423.

AHMED, I.; REHAN, M.; BASIT, A.; TUFAIL, M.; HONG, K. S. Neuro-fuzzy and networks-based data driven model for multi-charging scenarios of plug-in-electric vehicles. **IEEE Access**, v. 11, p. 87150–87165, 2023a. DOI: https://doi.org/10.1109/ACCESS.2023.3303963.

AHMED, I. E.; MEHDI, R.; MOHAMED, E. A. The role of artificial intelligence in developing a banking risk index: an application of adaptive neural network-based fuzzy inference system (ANFIS). **Artificial Intelligence Review**, v. 56, p. 13873–13895, 2023b. DOI: https://doi.org/10.1007/s10462-023-10473-9.

AJJARAPU, V.; CHRISTY, C. The continuation power flow: a tool for steady-state voltage stability analysis. **IEEE Transactions on Power Systems**, v. 7, p. 416–423, 1992. DOI: https://doi.org/10.1109/59.141737.

ANTHONY, K.; ARUNACHALAM, V. Voltage stability monitoring and improvement in a renewable energy dominated deregulated power system: a review. **e-Prime - Advances in Electrical Engineering, Electronics and Energy**, v. 11, p. 100893, 2025. DOI: https://doi.org/10.1016/j.prime.2024.100893.

AYOUBI, M.; ISERMANN, R. Neuro-fuzzy systems for diagnosis. **Fuzzy Sets and Systems**, v. 89, n. 3, p. 289–307, 1997. DOI: https://doi.org/10.1016/S0165-0114(97)00011-0.

BABUŠKA, R.; VERBRUGGEN, H. Neuro-fuzzy methods for nonlinear system identification. **Annual Reviews in Control**, v. 27, p. 73–85, 2003. DOI: https://doi.org/10.1016/S1367-5788(03)00009-9.

BISKER, T. I.; HADROUG, N.; HAFAIFA, A.; IRATNI, A.; NOURI, A. S.; COLAK, I. Gas turbine fault's detection using neuro-fuzzy adaptive inference system combined with subtractive clustering hybridization. **International Journal of Dynamics and Control**, v. 13, p. 343, 2025. DOI: https://doi.org/10.1007/s40435-025-01853-w.

CHIU, S. L. Fuzzy model identification based on cluster estimation. **Journal of Intelligent & Fuzzy Systems**, v. 2, p. 267–278, 1994. DOI: https://doi.org/10.3233/IFS-1994-2306.

CHRISTIE, R. D. **Power Systems Test Case Archive**. Seattle: Department of Electrical Engineering, University of Washington, 1999. Disponível em: https://labs.ece.uw.edu/pstca/index.html. Acesso em: 8 set. 2026.

DA SILVA, G. G.; ROQUE, R. F. M.; ARREGUÍN SÁMANO, M.; DIAS, N. L.; GOLZIO, A. C. DE J.; BONINI NETO, A. Multilayer perceptron, radial basis function, and generalized regression networks applied to the estimation of total power losses in electrical systems. **Machine Learning and Knowledge Extraction**, v. 8, p. 4, 2026. DOI: https://doi.org/10.3390/make8010004.

DOS SANTOS, W. P. L.; BONINI NETO, A.; GABRIEL FILHO, L. R. A. Post-contingency loading margin through plane change in the continuation power flow. **Energies**, v. 16, p. 7583, 2023. DOI: https://doi.org/10.3390/en16227583.

ELBORLSY, M. S.; HAMAD, S. A.; EL-SOUSY, F. F. M.; MOSTAFA, R. M.; KESHTA, H. E.; GHALIB, M. A. Neuro-fuzzy controller based adaptive control for enhancing the frequency response of two-area power system. **Heliyon**, v. 11, p. e42547, 2025. DOI: https://doi.org/10.1016/j.heliyon.2025.e42547.

GABER, M.; EL-BANNA, S.; EL-DABAH, M.; HAMAD, M. Designing and implementation of an intelligent energy management system for electric ship power system based on adaptive neuro-fuzzy inference system (ANFIS). **Advances in**

Science, Technology and Engineering Systems Journal, v. 6, p. 195–203, 2021. DOI: https://doi.org/10.25046/aj060223.

GARSON, G. D. Interpreting neural-network connection weights. **AI Expert**, v. 6, p. 46–51, 1991.

HAKIMI, A.; FARJAMI, H. Enhanced significant wave height prediction in the Southern Ocean using an ANFIS model optimized with subtractive clustering. **Scientific Reports**, v. 15, p. 35072, 2025. DOI: https://doi.org/10.1038/s41598-025-18140-5.

IBRAHIM, M.; HUSSEIN, M.; ABOZIED, M. A. H.; ASHRY, M. Enhancing four-tank system through model predictive control-based adaptive neuro-fuzzy system. **International Journal of Fuzzy Systems**, 2025. DOI: https://doi.org/10.1007/s40815-025-02085-y.

JAMAL, A.; SYAHPUTRA, R. Power flow control of power systems using UPFC based on adaptive neuro fuzzy. **Journal of Electrical Technology UMY**, v. 1, p. 33–38, 2014. DOI: https://doi.org/10.12962/j23546026.y2014i1.423.

JANG, J.-S. R. ANFIS: adaptive-network-based fuzzy inference system. **IEEE Transactions on Systems, Man, and Cybernetics**, v. 23, n. 3, p. 665–685, 1993. DOI: https://doi.org/10.1109/21.256541.

JANG, J. S. R.; SUN, C. T. Neuro-fuzzy modeling and control. **Proceedings of the IEEE**, v. 83, p. 378–406, 1995. DOI: https://doi.org/10.1109/5.364486.

LEAL DIAS, N.; DE QUEIROZ, A.; GOLZIO, A. C. DE J.; BUZO, R. F.; LEAL, S. D. A. D.; DOI, G. H.; BONINI NETO, A. Estimation of nodal voltage angles in electrical power systems using artificial neural networks and sensitivity analysis of input variables. **Technologies**, v. 14, p. 481, 2026. DOI: https://doi.org/10.3390/technologies14080481.

MALIK, F. H.; KHAN, M. W.; RAHMAN, T. U.; EHTISHAM, M.; FAHEEM, M.; HAIDER, Z. M.; LEHTONEN, M. A comprehensive review on voltage stability in wind-integrated power systems. **Energies**, v. 17, p. 644, 2024. DOI: https://doi.org/10.3390/en17030644.

MOHAMMED, H. A.; MOHD-MOKHTAR, R.; ALI, H. I. An optimal adaptive neuro-fuzzy inference system for photovoltaic power system optimization under partial shading conditions. **Energy Systems**, 2025. DOI: https://doi.org/10.1007/s12667-025-00745-4.

MOLLA, S.; FARROK, O.; ALAM, M. J. Electrical energy and the environment: prospects and upcoming challenges of the world's top leading countries. **Renewable and Sustainable Energy Reviews**, v. 191, p. 114177, 2024. DOI: https://doi.org/10.1016/j.rser.2023.114177.

OLADIPO, S.; SUN, Y.; ADEGOKE, S. A. Application of soft computing techniques to load frequency control system of electric power systems: a brief survey. **Cogent Engineering**, v. 12, p. 2572297, 2025. DOI: https://doi.org/10.1080/23311916.2025.2572297.

OUIFAK, H.; IDRI, A. Application of neuro-fuzzy ensembles across domains: a systematic review of the two last decades (2000–2022). **Engineering Applications of Artificial Intelligence**, v. 124, p. 106582, 2023. DOI: https://doi.org/10.1016/j.engappai.2023.106582.

PAL, S. K.; MITRA, S. **Neuro-Fuzzy Pattern Recognition: Methods in Soft Computing**. New York: John Wiley & Sons, 1999. ISBN 0-471-34844-9.

SEYEDMOHAMMADI, J.; NAVIDI, M. N. Optimizing soil water retention predictions using a subtractive clustering-based ANFIS model. **Cogent Food & Agriculture**, v. 12, p. 2612450, 2026. DOI: https://doi.org/10.1080/23311932.2025.2612450.

SHIHABUDHEEN, K. V.; PILLAI, G. N. Recent advances in neuro-fuzzy system: a survey. **Knowledge-Based Systems**, v. 152, p. 136–162, 2018. DOI: https://doi.org/10.1016/j.knosys.2018.04.014.

SIDDIKOV, I. K.; PORUBAY, O. V. Neuro-fuzzy system for regulating the processes of power flows in electric power facilities. **AIP Conference Proceedings**, v. 2432, p. 020010, 2022. DOI: https://doi.org/10.1063/5.0089473.

TALAAT, H. E. A.; ABDENNOUR, A.; AL-SULAIMAN, A. A. Design and experimental investigation of a decentralized GA-optimized neuro-fuzzy power system stabilizer. **International Journal of Electrical Power & Energy Systems**, v. 32, p. 751–759, 2010. DOI: https://doi.org/10.1016/j.ijepes.2010.01.011.

WALIA, N.; SINGH, H.; SHARMA, A. ANFIS: adaptive neuro-fuzzy inference system-a survey. **International Journal of Computer Applications**, v. 123, p. 32–38, 2015. DOI: https://doi.org/10.5120/ijca2015905635.

ZHAO, J.; SRIVASTAVA, A.; GUO, Y.; CETENOVIC, D.; LIN, Y.; LEVI, V.; YIN, G.; HUANG, M.; ZHANG, T.; LI, Z.; CHEN, Y.; EXPOSITO, A. G.; ZHANG, W.; ZHENG, W.; CHAKRABARTI, S.; LI, Y.; SHARMA, A.; KAMWA, I.; GUO, Q.; TERZIJA, V.; MILI, L. State estimation for integrated energy systems: motivations, advances, and future work. **IEEE Transactions on Power Systems**, v. 40, p. 3057–3073, 2025. DOI: https://doi.org/10.1109/TPWRS.2024.3524323.

ZHU, J.; GAO, W.; LI, Y.; GUO, X.; ZHANG, G.; SUN, W. Power system state estimation based on fusion of PMU and SCADA data. **Energies**, v. 17, p. 2609, 2024. DOI: https://doi.org/10.3390/en17112609

4 CONCLUSÃO GERAL

A presente tese de doutorado investigou o desenvolvimento e a aplicação de técnicas avançadas de inteligência computacional para a estimativa direta dos ângulos de fase da tensão nodal (θ) e a construção de curvas de carregamento P-θ em Sistemas Elétricos de Potência (SEP). O objetivo central do trabalho focou na superação dos gargalos computacionais associados aos métodos numéricos iterativos tradicionais, como o Fluxo de Potência Continuado (CPF), oferecendo ferramentas precisas, eficientes e interpretáveis para o monitoramento da estabilidade de tensão estática.

No Capítulo II, demonstrou-se a viabilidade do uso de Redes Neurais Artificiais (RNA) do tipo Multilayer Perceptron (MLP), treinadas via algoritmo *backpropagation*, para realizar a estimativa direta dos ângulos de tensão nos sistemas de teste IEEE de 14, 30 e 57 barras. A abordagem baseada em RNA eliminou a necessidade de resolver repetidamente as equações de fluxo de potência na etapa de aplicação, alcançando uma redução drástica de aproximadamente 88% no tempo de processamento computacional em relação ao CPF, mantendo elevada precisão preditiva (R^2 > 0,985 e erro quadrático médio na ordem de 10^{-3}) e mapeando com sucesso o ponto crítico de carregamento. Além disso, o Capítulo II trouxe uma contribuição metodológica para a análise de sensibilidade das variáveis de entrada pelos métodos de Garson e Olden onde identificou-se que variáveis de entrada com magnitudes numéricas extremamente pequenas (próximas de zero) provocavam distorções nos pesos sinápticos, concentrando artificialmente a relevância do modelo. A aplicação da estratégia de normalização proposta corrigiu essa limitação, restabelecendo a coerência física dos índices de importância (destacando o fator de carregamento λ e a potência ativa do gerador *slack* $P_{\{g,slack\}}$ como os principais fatores operacionais) sem comprometer a acurácia da rede.

No Capítulo III, a pesquisa avançou para solucionar o caráter de "caixa-preta" inerente às RNAs convencionais e aprimorar a precisão preditiva em regiões de forte comportamento não-linear, próximas ao limite de estabilidade de tensão. Para isso, propôs-se um Sistema de Inferência Neuro-Fuzzy Adaptativo (ANFIS) baseado no modelo Takagi–Sugeno de primeira ordem, utilizando agrupamento subtrativo e aprendizado híbrido para criar modelos independentes por barra de não-referência. Os resultados do ANFIS superaram significativamente o modelo de RNA de referência

no sistema IEEE de 14 barras: atingiu-se um coeficiente de determinação (R^2) médio de 0,99998, um RMSE de $3{,}48\times10^{-4}$ rad e um MAE de $2{,}94\times10^{-4}$ rad no conjunto de validação. O modelo ANFIS acompanhou com alta fidelidade a trajetória não-linear das curvas P-θ na vizinhança do ponto de colapso de tensão e alcançou a convergência ideal de validação logo na primeira época de treinamento. Em termos computacionais, o ANFIS obteve uma redução adicional de 5,93% no tempo global de CPU em comparação com a RNA multi-saída (3,2721 s contra 3,4782 s). Por meio da análise de sensibilidade por perturbação de 10%, identificou-se que a potência reativa da barra *slack* ($Q_{\{g,slack\}}$, 22,73%), a potência ativa da barra *slack* ($P_{\{g,slack\}}$, 21,38%) e o fator de carregamento (λ, 17,66%) foram os fatores mais determinantes na estimativa dos ângulos.

Em síntese, a trajetória desenvolvida nesta tese demonstra que:

1. As técnicas aprendidas a partir de dados operacionais reduzem drasticamente o tempo computacional para estimativa de estado em comparação aos métodos numéricos tradicionais, viabilizando análises de estabilidade em tempo real.
2. A transição de um modelo essencialmente preditivo de "caixa-preta" (RNA) para uma estrutura "caixa-cinza" (ANFIS) preserva e amplia o desempenho computacional, garantindo a transparência das regras fuzzy SE–ENTÃO (*if-then*) para os operadores do sistema.
3. O modelo ANFIS estabeleceu um patamar superior de precisão na modelagem do comportamento não-linear perto do limite de estabilidade de tensão, consolidando-se como uma alternativa robusta para o monitoramento de redes elétricas modernas.

APÊNDICE A - PRODUÇÃO ACADÊMICA DESENVOLVIDA DURANTE O DOUTORADO

ARTIGOS CIENTÍFICOS EM PERIÓDICOS

Publicados:

LEAL DIAS, N.; DE QUEIROZ, A.; GOLZIO, A.C.D.J.; BUZO, R.F.; LEAL, S.D.A.D.; DOI, G.H.; BONINI NETO, A. Estimation of Nodal Voltage Angles in Electrical Power Systems Using Artificial Neural Networks and Sensitivity Analysis of Input Variables. **Technologies** 2026, 14, 481. https://doi.org/10.3390/technologies14080481

SILVA, G. G. da; ROQUE, R. F. M.; ARREGUÍN SÁMANO, M.; **DIAS, N. L.**; GOLZIO, A. C. de J.; BONINI NETO, A. Multilayer Perceptron, Radial Basis Function, and Generalized Regression Networks Applied to the Estimation of Total Power Losses in Electrical Systems. **Machine Learning and Knowledge Extraction**, v. 8, n. 1, art. 4, 2026. DOI: https://doi.org/10.3390/make8010004

ARTIGOS CIENTÍFICOS EM CONGRESSOS

Publicados:

DA SILVA, G.G.; **DIAS, N.L.**; DE QUEIROZ, A.; BONINI NETO, A. Redes Neurais Percéptron Multicamadas e Função de Base Radial na Estimativa das Perdas Totais de Potência dos Sistemas Elétricos. In: **XI Simpósio Brasileiro de Sistemas Elétricos (SBSE 2025)**, São João del-Rei, MG, Brasil, 2025.

Submetidos:

Congresso Nacional de Matemática aplicada e Computacional – CNMAC 2026
Presidente Prudente - SP – 14 a 18 de Setembro de 2026. Artigo Completo aceito, intitulado: “Estimativa dos Ângulos das Tensões Nodais em Sistemas Elétricos de Potência Utilizando Redes Neurais Artificiais.”

Encontro Nacional de Modelagem Computacional – ENMC 2026
Bento Gonçalves, Rio Grande do Sul, Brasil – 06 a 09 de outubro de 2026. Artigo Completo aceito, intitulado: “ANFIS-BASED RECONSTRUCTION OF P-θ CURVES FOR VOLTAGE STABILITY ASSESSMENT IN THE IEEE 14-BUS SYSTEM.”

technologies

MDPI

Article

Estimation of Nodal Voltage Angles in Electrical Power Systems Using Artificial Neural Networks and Sensitivity Analysis of Input Variables

Neylan Leal Dias [1,2], Alexandre de Queiroz [1], Ana Claudia de Jesus Golzio [3], Ricardo Fonseca Buzo [3], Simone de Almeida Delphin Leal [2], Gabriel Henrique Doi [3] and Alfredo Bonini Neto [3,*]

[1] School of Engineering, São Paulo State University (Unesp), Bauru 17033-360, Brazil
[2] Department of Exact and Technological Sciences, Federal University of Amapá (Unifap), Macapá 68903-419, Brazil
[3] School of Sciences and Engineering, São Paulo State University (Unesp), Tupã 17602-496, Brazil
* Correspondence: alfredo.bonini@unesp.br

Abstract

The estimation of nodal voltage angles is essential for the efficient and secure operation of electrical power systems. Traditionally, this estimation depends on the prior solution of the power flow problem, a procedure that may become computationally expensive in studies involving multiple operating scenarios. The present research demonstrates relevant potential impact by employing artificial neural networks for the direct estimation of nodal voltage angles. Although the power flow is used during the database generation stage, it is no longer required during the model application phase, resulting in a significant reduction in computational effort of approximately 80%. The proposed model was trained using the error backpropagation algorithm, achieving a mean squared error (MSE) on the order of 10^{-3} in only four iterations, with a training time of approximately 3 s and a correlation coefficient (R) of 0.99. Validation using unseen samples (10% of the samples) also demonstrated high accuracy, with an error on the order of 10^{-3} between the estimated and expected values. Furthermore, the P–θ curves were successfully obtained for the IEEE 14-, 30-, and 57-bus systems, enabling the identification of the maximum loading point with low estimation error. These results confirm the neural network's ability to generalize and operate as a reliable estimator under different system loading conditions. Another relevant aspect of this work was the sensitivity analysis of the input variables, which made it possible to identify the variables that exerted the greatest influence on the neural network response. In addition, a normalization step was proposed to overcome distortions associated with the magnitudes of the input data, demonstrating the efficiency and robustness of the proposed method.

Keywords: artificial neural networks; nodal voltage angles; electrical power systems; state estimation; power flow

Check for updates

Academic Editors: Yong Li, Gang Lin, Weiyu Wang, Junjie Ma and Manoj Gupta

Received: 12 June 2026
Revised: 18 July 2026
Accepted: 24 July 2026
Published: 3 August 2026

Copyright: © 2026 by the authors. Licensee MDPI, Basel, Switzerland. This article is an open access article distributed under the terms and conditions of the Creative Commons Attribution (CC BY) license.

1. Introduction

The dispatch of electrical energy has become increasingly complex in recent years, mainly due to the expansion of electrical networks, the integration of intermittent renewable energy sources, and long-distance power transmission [1]. These developments have intensified the challenges associated with power system stability, resulting in a higher risk of voltage instability and voltage collapse events. In particular, the increasing penetration

machine learning & knowledge extraction

MDPI

Article

Multilayer Perceptron, Radial Basis Function, and Generalized Regression Networks Applied to the Estimation of Total Power Losses in Electrical Systems

Giovana Gonçalves da Silva [1], Ronald Felipe Marca Roque [2], Moisés Arreguín Sámano [3], Neylan Leal Dias [1], Ana Claudia de Jesus Golzio [4] and Alfredo Bonini Neto [4,*]

[1] School of Engineering, São Paulo State University (UNESP), Bauru 17033-360, SP, Brazil; giovana.goncalves@unesp.br (G.G.d.S.); neylan.dias@unesp.br (N.L.D.)
[2] School of Biomedical Engineering, Valparaíso University (UV), Valparaiso 2362552, Chile; ronald.marca@postgrado.uv.cl
[3] Faculty of Agricultural Sciences, Bolívar State University (UEB), Guaranda 020150, Ecuador; marreguin@ueb.edu.ec
[4] School of Sciences and Engineering, São Paulo State University (UNESP), Tupã 17602-496, SP, Brazil; a.golzio@unesp.br
* Correspondence: alfredo.bonini@unesp.br

Abstract

This paper presents an Artificial Neural Network (ANN) approach for estimating total real and reactive power losses in electrical power systems. Three network architectures were explored: the Multilayer Perceptron (MLP), the Radial Basis Function (RBF) network, and the Generalized Regression Neural Network (GRNN). The main advantage of the proposed methodology lies in its ability to rapidly compute power loss values throughout the system. ANN models are especially effective due to their capacity to capture the nonlinear characteristics of power systems, thus eliminating the need for iterative procedures. The applicability and effectiveness of the approach were evaluated using the IEEE 14-bus test system and compared with the continuation power flow method, which estimates losses using conventional numerical techniques. The results indicate that the ANN-based models performed well, achieving mean squared error (MSE) values below the predefined threshold during both training and validation (0.001). Notably, the networks accurately estimated the total power losses within the expected range, with residuals on the order of 10^{-4}. Among the models tested, the RBF network showed slightly superior performance in terms of error metrics, requiring fewer centers to meet the established criteria compared to the MLP and GRNN models (11 centers). However, the GRNN achieved the shortest processing time; even so, all three networks produced satisfactory and consistent results, particularly in identifying the critical points of electrical power systems, which is of fundamental importance for ensuring system stability and operational reliability.

Keywords: artificial intelligence; power losses; forecasting; electric power systems; artificial neural networks

Check for updates

Academic Editor: Marek Sikora

Received: 4 November 2025
Revised: 9 December 2025
Accepted: 23 December 2025
Published: 26 December 2025

Copyright: © 2025 by the authors. Licensee MDPI, Basel, Switzerland. This article is an open access article distributed under the terms and conditions of the Creative Commons Attribution (CC BY) license.

1. Introduction

In the supply of electrical energy to consumers, a significant portion is dissipated in transmission and distribution systems, resulting in both technical and non-technical losses. Technical losses, caused by inefficiencies in equipment and infrastructure, generate considerable economic and environmental impacts [1]. For this reason, mitigating such

Redes Neurais Percéptron Multicamadas e Função de Base Radial na Estimativa das Perdas Totais de Potência dos Sistemas Elétricos

G. G. da Silva*, N. L. Dias, A. de Queiroz***, A. Bonini Neto******

**Faculdade de Engenharia de Bauru (FEB), Universidade Estadual Paulista (UNESP), Bauru, SP, Brasil, (e-mail: giovana.goncalves@unesp.br)*
*** Faculdade de Engenharia de Bauru (FEB), Universidade Estadual Paulista (UNESP), Bauru, SP, Brasil, (e-mail: neylan@unifap.br)*
**** Faculdade de Engenharia de Bauru (FEB), Universidade Estadual Paulista (UNESP), Bauru, SP, Brasil, (e-mail: alexandre.queiroz@unesp.br)*
***** Faculdade de Ciências e Engenharia (FCE), Universidade Estadual Paulista (UNESP), Tupã, SP, Brasil, (e-mail: alfredo.bonini@unesp.br)*

Abstract: This paper presents the ANN (Artificial Neural Networks) approach to estimating total real and reactive power losses in electrical power systems. Two networks were presented: the MLP (multilayer perceptron) and the RBF (radial basis function) networks. The key advantage of our methodology is the speed of obtaining power loss values across the system. ANN models are particularly beneficial as they capture the nonlinear characteristics of the system, eliminating the need for iterative procedures. The applicability and effectiveness of the proposed methodology have been investigated on IEEE test systems (14 buses) and compared with the continuation power flow method, which calculates power losses based on conventional numerical techniques. The results show that the ANN approach performed well, achieving a mean squared error (MSE) in training below the specified threshold. The network successfully estimated 98.5% of the total power loss values within the expected range, with residuals around 10^{-4} and an accuracy of approximately 98%. The RBF (radial basis function) network demonstrated superior performance compared to the MLP (multilayer perceptron) network.

Resumo: Este artigo apresenta a abordagem baseada em Redes Neurais Artificiais (RNA) para a estimativa das perdas totais de potência ativa e reativa em sistemas elétricos de potência. Foram utilizadas duas arquiteturas de rede: Perceptron Multicamadas (MLP) e Função de Base Radial (RBF). A principal vantagem da metodologia proposta é a rapidez na obtenção dos valores de perda de potência ao longo do sistema. Os modelos de RNA são particularmente vantajosos, pois capturam as características não lineares do sistema, eliminando a necessidade de procedimentos iterativos. A aplicabilidade e a eficácia da metodologia foram investigadas no sistema teste IEEE de 14 barras e comparadas com o fluxo de potência continuado, que calcula as perdas de potência por meio de técnicas numéricas convencionais. Os resultados demonstram que a abordagem baseada em RNA apresentou um desempenho satisfatório, com erro quadrático médio (MSE) no treinamento abaixo do limite especificado. A rede conseguiu estimar 98.5% dos valores de perda total de potência dentro da faixa esperada, com resíduos em torno de 10^{-4} e uma precisão aproximada de 98%. A rede RBF (Função de Base Radial) apresentou um desempenho superior em comparação com a rede MLP (Perceptron Multicamadas).

Keywords: Artificial intelligence; power losses; forecasting; electric power systems; artificial neural networks.

Palavras-chaves: Inteligência artificial; perdas de potência; previsão; sistemas elétricos de potência; redes neurais artificiais.

1. INTRODUÇÃO

No processo de entrega de energia aos consumidores finais, uma parcela significativa da energia é dissipada nos sistemas de transmissão e distribuição, resultando em perdas técnicas e não técnicas. As perdas técnicas, que decorrem de ineficiências nos equipamentos e na infraestrutura, causam impactos econômicos e ambientais em escala nacional [1]. Por essa razão, a otimização dessas perdas deve ser tratada de maneira abrangente, independentemente da estrutura institucional do setor elétrico ou da propriedade das concessionárias. O volume de perdas nos sistemas de transmissão e distribuição varia entre 3% e 13%, evidenciando sua relevância para a eficiência do sistema como um todo (Moldoveanu et al. 2021).